HIGHWAY EMBANKMENT CONSTRUCTION USING FLY ASH AND SNOW IN COLD REGIONS

by

Altuğ SAYGILI

B.S., Civil Engineering, Yıldız Technical University, 1998

Submitted to the Institute for Graduate Studies in
Science and Engineering in partial fullfilment of
the requirements for the degree of
Doctor of Philosophy

Graduate Program in Civil Engineering

Boğaziçi University

2008

ACKNOWLEDGEMENTS

I would like to express my sincere gratitude to Professor Gökhan Baykal for submission of the subject, for his suggestions in the development of this study and for his invaluable guidance and help during the preparation of this dissertation.

I would like to thank Professor Erol Güler and Professor Feyza Çinicioğlu for their suggestions in the development of this study.

I would like to thank Professor Gökhan Baykal, Professor Erol Güler, Professor Ayşe Edinçliler, Professor Mahmut Savaş and Professor Ismail Hakkı Aksoy for their precious suggestions for the final editions of this thesis.

Thanks to our technicians İlhan Dilmen and Kadir Gündoğdu for providing valuable technical assistance during the labotarory work.

This thesis has been supported by Boğaziçi University Scientific Research Fund BAP Projects 03 A 403 & 06 A 402 D.

ABSTRACT

HIGHWAY EMBANKMENT CONSTRUCTION USING FLY ASH AND SNOW IN COLD REGIONS

During winter season, due to workability problems, it is very hard to continue construction. Water needed for compaction will be very hard to handle. However, snow is readily available on site. With Type C fly ash, snow may be mixed with fly ash and compacted. Due to its silt size one or two per cent wet of optimum water content makes the compaction of fly ash impractical. An excess amount of water is needed to enhance reactions leading to formation of cementitious products, which increases strength. A new technology has been developed to add more water into fly ash samples to enhance the pozzolanic reactions, leading to cementitious mineral formation. Fly ash at optimum water content and fly ash with additional 10 per cent by weight of snow were compacted, sealed and cured for one, seven, 14, 28, and 90 days at 21^0C. Unconfined compression, splitting tensile and hydraulic conductivity tests were conducted. The initial hydration process has been investigated using infrared thermography. Gamma-spectroscopic analysis techniques were used to determine 238U, 235U, 226Ra, 232Th. The dosimetric calculations are reported. The addition of snow into fly ash increased the unconfined compressive strength and splitting tensile strength noticeably beginning from 14 days of curing reaching up to two times that of control samples at the end of 90 days of curing. The hydraulic conductivity increased two to three orders of magnitude for snow-added samples. Gamma radiation has decreased 30 to 40 per cent of that of control samples. XRD and ESEM examinations provided detailed information about the microstructural development of the tested specimens. Snow addition had a remarkable effect on improving the freeze-thaw and thermal conductivity properties of the compacted fly ash specimens. The leaching fluid quality data indicated that the leachate from the control fly ash and snow added fly ash had no discernable impact on ground water quality. With its higher void ratio, lighter weight, higher strength, higher hydraulic conductivity, lower gamma radiation and higher freeze-thaw performance, the proposed technique may be beneficial for highway agencies exposed

to rough winter conditions in two ways; construction activities will not be ceased during snow, a higher performance road construction material will be obtained.

ÖZET

Kış koşullarında yol inşa faaliyetleri çalışılabilirlik açısından karşılaşılan sorunlar yüzünden aksamakta, sıkıştırma için gerekli olan suyun temininde ve bulundurulmasında sorunlar yaşanmaktadır. Ancak, arazide bulunan doğal kar ve C tipi uçucu kül kullanılarak sıkıştırma işlemi gerçekleştirilebilmektedir. Uçucu kül sıkıştırma su muhtevası açısından çok hassastır, bu husus uçucu külün yol inşaatlarında kullanımını kompleks hale getirmektedir. Sıkıştırma su muhtevası optimum su muhtevasının bir-iki derece üzerinde olması halinde sıkıştırma işlemi imkansız olmakta, uçucu kül sıvı gibi davranış göstermektedir. Daha fazla çimentolaşma minerallerinin oluşması, dolayısıyla yüksek dayanımlı bir yapı malzemesi elde etmek için ortamda daha fazla su olması gerekmektedir. Üniversitemizde yapılan çalışmalarda geliştirilen yeni bir yöntemde uçucu külün hidratasyonu numunelere doğal kar eklenerek yavaşlatılmakta, ihtiyaç duyulan ekstra su yapıya katı fazda katılmaktadır. Optimum su muhtevasında ve %10 doğal kar ilavesi ile sıkıştırılan numuneler hava sızdırmazlığı sağlanıp bir, yedi, 14, 28 ve 90 gün süresince 21^0C sabit sıcaklıktaki kür odasında bekletilmiştir. Serbest basınç, yarılma gerilmesi ve hidrolik geçirimlilik testleri gerçekleştirilmiştir. Hidratasyon başlangıç süreci infrared termografi ile incelenmiştir. 238U, 235U, 226Ra, 232Th elementlerinin tayini için gamma spektrometrik analiz tekniği kullanılmış, dozimetrik hesaplamalar raporlanmıştır. Uçucu kül numunelerine %10 oranında doğal kar katılması ile serbest basınç ve yarılma kesme dayanımı değerlerinde 14 günlük kür edilmiş numunelerden itibaren fark edilir artış gözlenmiş, 90 günlük kür edilmiş numunelerde artış miktarının kontrol numunelere göre iki misline yaklaştığı görülmüştür. Hidrolik geçirimlilik değerleri doğal kar eklenmiş numunelerde kontrol numunelere göre iki-üç büyüklük mertebesinde daha fazladır. Kontrol numunelerine göre gamma radyoaktivite değerleri %30-%40 oranlarında daha düşük saptanmıştır. XRD ve ESEM analizleri test edilen numunelerdeki mikroyapı değişiklikleri hakkında detaylı bilgi vermiştir. Doğal kar eklenmesi numunelerin donma çözünme ve termal geçirgenlik test sonuçlarını kayda değer oranda iyileştirmiştir. Test numunelerinden elde edilen sızıntı suyu analizleri sonucunda numunelerde yeraltı suyunu fark edilebilir derecede kirletecek ağır metallere rastlanmamıştır. Yüksek boşluk oranı, düşük birim hacim ağırlığı, yüksek mukavemeti, yüksek hidrolik geçirimliliği, düşük gamma radyasyon değerleri ve daha iyi donma-çözünme performansı ile geliştirilen yöntem kış koşullarında

çalışan yol inşa ekipleri için iki yönden faydalı olacaktır; soğuk hava şartları nedeniyle inşa faaliyetleri duraklamayacak ve doğal kar eklenerek daha yüksek performanslı bir yol inşa malzemesi elde edilmiş olacaktır.

TABLE OF CONTENTS

ACKNOWLEDGEMENTS..... iii
ABSTRACT..... iv
ÖZET..... vi
LIST OF FIGURES..... xii
LIST OF TABLES..... xvii
LIST OF SYMBOLS / ABBREVIATIONS..... xix
1.INTRODUCTION..... 1
2.LITERATURE REVIEW..... 7
2.1.Fly Ash..... 7
2.1.1. General Description..... 7
2.1.2. The Origin of Coal..... 7
2.1.3. Coal Types..... 9
2.1.4. Coal Composition..... 10
2.1.5. Fly Ash Formation..... 13
2.1.6. Classification of Fly Ash 13
2.1.6.1. Classification in Terms of Lime and Silica..... 14
2.1.6.2. ASTM Classification..... 14
2.1.6.3. ENV Classification..... 14
2.1.6.4. TSE Classification..... 15
2.1.7. Chemical Properties of Fly Ash..... 15
2.1.8. Mineralogical Properties of Fly Ash..... 17
2.1.9. Physical Properties of Fly Ash..... 18
2.1.10.Hydration of Fly Ash..... 18
2.2. Environmental Risks of Fly Ash Utilization..... 19
2.2.1. Radioactivity……..... 19
2.2.2. Leaching from Fly Ash..... 22
2.3. Utilization Areas of Fly Ash..... 23
2.3.1. Fills,Embankments and Backfills..... 23
2.3.2. Pavement Base and Subbase Courses..... 24
2.3.3. Subgrade Stabilization..... 25

2.3.4. Landfill Cover..... 25
2.3.5. Soil Improvement..... 26
2.3.6. Flowable Fill..... 27
2.4. Highway Uses and Processing Requirements..... 29
2.4.1. Portland Cement Concrete..... 29
2.4.2. Asphalt Concrete..... 29
2.4.3. Stabilized Base 29
2.4.4. Flowable Fill..... 30
2.4.5. Embankment and Fill Material..... 30
2.5. Properties of Ice 31
2.5.1. General Description..... 31
2.5.2. Structure..... 32
2.5.3. Physical Properties..... 32
2.5.4. The Classification of Solid Precipitation..... 33
2.5.5. Aggregation of Ice Crystals to Form Snowflakes..... 34
2.5.6. Properties of Frozen Ground..... 35
2.5.7. Natural Snow Added Samples-A Four Phase Material..... 36
2.6. Cold Regions..... 37
2.6.1. Seasonal and Perennially Frozen Ground..... 39
2.6.1.1. Seasonally Frozen Ground..... 39
2.6.1.2. Frost Heave..... 40
2.6.1.3. Perennially Frozen Ground..... 40
2.6.2. Engineering Considerations..... 41
2.6.2.1. The Freezing Process..... 42
2.6.2.2. Thawing..... 44
2.6.3. Construction in Cold Weather Regions..... 45
2.6.3.1. Thermal Design of Roads..... 47
2.6.4. Pavement Structures For Cold Regions..... 48
2.6.4.1. Pavement Design Under Seasonal Frost Action..... 49
2.7. Background..... 50
3.EXPERIMENTAL STUDY..... 57
3.1. Soma Thermal Power Plant..... 57
3.2. Materials Used 59

3.2.1. Fly Ash..... 59
3.2.2. Snow..... 60
3.3. Samples..... 60
3.3.1. Sample Preparation..... 60
3.3.2. Sample Curing..... 61
3.4. Sample Testing..... 61
3.4.1. Unconfined Compression Testing..... 62
3.4.2. Splitting Tensile Strength Testing..... 63
3.4.3. Hydraulic Conductivity Testing..... 64
3.4.4. pH Measurements..... 65
3.4.5. Temparature Measurement of Fresh Specimens..... 66
3.4.6. Radioisotope Activity Comparison..... 67
3.4.7. Thermographic Measurements..... 68
3.4.8. X-Ray Diffraction Analysis..... 69
3.4.9. Environmental Scanning Electron Microscope Analysis..... 70
3.4.10. Resistance of Samples to Rapid Freezing and Thawing..... 71
3.4.11. Thermal Conductivity Analysis..... 73
3.4.12. Erosion Analysis (Pinhole Test)..... 74
3.4.13. Leachate Analysis..... 77
3.4.14. Length Change Determination 79
4. MICROCHEMICAL AND MICROFABRIC INVESTIGATION..... 80
4.1. X-Ray Diffraction Analysis..... 80
4.2. Environmental Scanning Electron Microscope Analysis..... 83
5. TEST RESULTS AND EVALUATION..... 90
5.1. Physical Properties of the Compacted Samples..... 90
5.2. Settlement and Stress Increase In Soil From Embankment Construction.... 91
5.3. Unconfined Compression Testing..... 94
5.4. Splitting Tensile Strength Testing..... 97
5.5. Hydraulic Conductivity Testing..... 98
5.6. pH Measurements..... 100
5.7. Temperature Measurement of Fresh Specimens..... 102
5.8. Radioisotope Activity Comparison..... 106

5.9. Resistance of Samples to Rapid Freezing and Thawing..... 109
5.10. Thermal Conductivity Analysis..... 119
5.11. Erosion Analysis (Pinhole Test)..... 125
5.12. Leachate Analysis..... 126
5.13. Length Change Determination 131
5.14. Summary of the Test Results..... 132
6. CONCLUSIONS..... 138
REFERENCES..... 140
APPENDIX A: STRESS-STRAIN CURVES FOR SAMPLES CURED AT DIFFERENT TIME PERIODS..... 159

LIST OF FIGURES

Figure 1.1. Fly ash utilization statistics for UK, 1999..... 5

Figure 2.1. Distribution of uranium concentration in coal from two areas of the United States..... 20

Figure 2.2. Typical range of uranium concentration in coal, fly ash, and a variety of common rocks..... 21

Figure 2.3. The four phases of natural snow added fly ash samples..... 36

Figure 2.4. Cold regions of the northern hemisphere..... 38

Figure 3.1. Miniature harvard compaction apparatus……..…….... 62

Figure 3.2. pH meter..... 66

Figure 3.3. Gamma spectrometer..... 68

Figure 3.4. Thermal imager..... 69

Figure 3.5. X-ray diffractometer..... 70

Figure 3.6. Environmental scanning electron microscope..... 71

Figure 3.7. Freeze-thaw cabinet..... 72

Figure 3.8. Freeze-thaw apparatus refrigerating and heating equipment and controls. 73

Figure 3.9. Schematic drawing of the pinhole test equipment..... 74

Figure 3.10. Schematic drawing of pinhole test specimen..... 75

Figure 3.11. Pinhole test setup..... 76

Figure 3.12. Pinhole test mold, screens, nipple and needle..... 77

Figure 3.13. Atomic absorption spectrophotometer……... 78

Figure 3.14. Shrinkage mold……..…….…….. 79

Figure 4.1. X-ray diffraction patterns of raw fly ash (FA), fly ash cured for one day at optimum moisture content (FA1), fly ash cured for 28 days at optimum moisture content (FA28), fly ash cured for 90 days at optimum moisture content (FA90), fly ash cured for five years at optimum moisture content (FA5Y)..... 81

Figure 4.2. X-ray diffraction patterns of fly ash (FA), snow-added fly ash cured for one day (FI1), snow-added fly ash cured for 28 days (FI28), snow added fly ash cured for 90 days (FI90), snow-added fly ash cured for five years (FI5Y)..... 82

Figure 4.3. The environmental scanning electron microscope (ESEM) micrographs after one day curing (350x)..... 84

Figure 4.4. The environmental scanning electron microscope (ESEM) micrographs after one day curing (2000x)..... 84

Figure 4.5. The environmental scanning electron microscope (ESEM) micrographs after one day curing (4000x)..... 85

Figure 4.6. The environmental scanning electron microscope (ESEM) micrographs after 28 days curing (350x)..... 86

Figure 4.7. The environmental scanning electron microscope (ESEM) micrographs after 28 days curing (2000x)..... 86

Figure 4.8. The environmental scanning electron microscope (ESEM) micrographs after 90 days curing (350x)..... 87

Figure 4.9. The environmental scanning electron microscope (ESEM) micrographs after 90 days curing (2000x) 87

Figure 4.10. The environmental scanning electron microscope (ESEM) micrographs after five years curing (350x) 88

Figure 4.11. The environmental scanning electron microscope (ESEM) micrographs after five years curing (2000x) 88

Figure 5.1. Compacted dry unit weight-moisture content relationship of control fly ash and natural snow added fly ash samples..... 91

Figure 5.2. Typical fly ash embankment section in the I-495 and Edgemoor road interchange, Delaware..... 92

Figure 5.3. Influence factor for calculating the vertical stress increase under the corner of a rectangle..... 93

Figure 5.4. Typical fly ash embankment section resting on a clay layer..... 93

Figure 5.5. Variation of the unconfined compressive strength values of fly ash (FA) and snow-added fly ash (FI) with time..... 95

Figure 5.6. Stress-strain curves for samples cured at different time periods (FA1, FA28, FA90, fly ash cured for one, 28, and 90 days at optimum moisture content; FI1, FI28, FI90, snow-added fly ash cured for one, 28, and 90 days)..... 96

Figure 5.7. The temperature variation of the outdoor curing conditions..... 97

Figure 5.8. Variation of the splitting tensile strength values of fly ash (FA) and snow-added fly ash (FI) with time..... 98

Figure 5.9. Comparison of the hydraulic conductivity values of 28 and 90 days cured compacted fly ash and compacted fly ash & snow..... 99

Figure 5.10. pH values of fly ash (FA) and snow-added fly ash (FI) with time..... 102

Figure 5.11. Temperature variation of fly ash(FA) and snow-added fly ash(FI) with time..... 103

Figure 5.12. The Thermal imager images after 5, 60 and 240 minutes curing at 21^0C. 104

Figure 5.13. The Thermal imager images after 5, 60 and 240 minutes curing at 2^0C.. 105

Figure 5.14. Automatic environmental cabinet used to carry out the accelerated freeze-thaw test..... 110

Figure 5.15. Resonant frequency test setup..... 111

Figure 5.16. Freeze-thaw cycle of the specimens (ASTM C666 Procedure A)..... 112

Figure 5.17. 90 days cured samples after 33 freeze thaw cycles..... 114

Figure 5.18. 90 days cured samples after 65 freeze thaw cycles..... 115

Figure 5.19. 90 days cured samples after 91 freeze thaw cycles..... 115

Figure 5.20. 180 days cured samples after 33 freeze thaw cycles..... 116

Figure 5.21. 180 days cured samples after 65 freeze thaw cycles..... 116

Figure 5.22. 180 days cured samples after 91 freeze thaw cycles..... 117

Figure 5.23. Deterioration pattern due to ASTM C666 test. 117

Figure 5.24. Durability factors of control compacted fly ash and snow added fly ash samples..... 118

Figure 5.25. The thermal imager images taken at different time periods on the surface of the hotbox apparatus.(FA, FI10, FI20, FI30) 122

Figure 5.26. The surface temperatures of the specimens recorded at different time periods on the surface of the hotbox apparatus. (FA, FI10, FI20, FI30).. 123

Figure 5.27. Cross sections of the control and snow added fly ash specimens (FA, FI10, FI20, FI30) 124

Figure 5.28. Heavy metal content from leachate of 28 days cured fly ash and snow added fly ash samples..... 128

Figure 5.29. Heavy metal content from leachate of 90 days cured fly ash and snow added fly ash samples..... 129

Figure 5.30. Average length change of the cured fly ash and fly ash and snow specimens..... 131

LIST OF TABLES

Table 2.1. Typical proximate and ultimate analysis of coals from the United States. 11

Table 2.2. Proximate and ultimate analysis of lignites from Manisa, Soma..... 12

Table 2.3. Limits of ASTM C 618 for fly ash classification..... 14

Table 2.4. Limits of ENV 187-1 for fly ash classification 15

Table 2.5. Normal range of chemical composition for fly ash produced from different coal types (expressed as per cent by weight)…….... 16

Table 2.6. Frost heave susceptibility of various soil types..... 46

Table 2.7. Hydraulic conductivity values of compacted fly ashes..... 56

Table 3.1. The statistical figures related with the coal combustion, calorific value and fly ash production of the Soma thermal power plant..... 58

Table 3.2. The chemical analysis results on samples obtained from some of the thermal power plants commissioned in Turkey..... 59

Table 3.3. Physical and chemical characteristics of fly ash..... 60

Table 5.1. Comparison of the properties of compacted fly ash and compacted fly ash and snow..... 90

Table 5.2. Comparison of the hydraulic conductivity values of 28 and 90 days cured compacted fly ash and compacted fly ash & snow..... 100

Table 5.3. Comparison of the leaching fluid pH values of 28 days cured compacted fly ash and compacted fly ash & snow..... 101

Table 5.4. Comparison of the radioisotope activities of 28 days cured compacted fly ash and compacted fly ash & snow..... 107

Table 5.5. Radioactivity in fly ash in Bq/kg (UNIPEDE)..... 108

Table 5.6. Visual rating 113

Table 5.7. Development of deterioration of the test specimens..... 113

Table 5.8. Properties of fly ash and snow added compacted fly ash samples used for thermal insulation (cured for 90 days)..... 121

Table 5.9. The surface temperatures of the specimens recorded at different time periods on the surface of the hotbox apparatus. (FA, FI10, FI20, FI30). 124

Table 5.10. Evaluation of the pinhole test results for the cured fly ash and fly ash & snow specimens (method A)..... 126

Table 5.11. Atomic absorption spectrometer test results of the leaching fluids..... 127

LIST OF SYMBOLS/ABBREVIATIONS

t	Thickness
D	Diameter
k	Coefficient of Permeability
A	Area
R	Resistance
Q	Net Heat Flow
Δt	Temperature Differences
e	Void Ratio
L	Thickness of the Specimen
h_i	Initial Head Loss
h_t	Head Loss at t

CCP	Coal Combustion Product
ASTM	American Society for Testing and Materials
TSE	Turkish Standards Institution
EU	European Union
US	United States
EN	European Norm
LOI	Loss on ignition
USGS	United States Geological Survey
PPM	Part Per Million
USEPA	United States Environmental Protection Agency
PPB	Part Per Billion
PSM	Pozzolanic Stabilized Mixture
PSB	Pozzolanic Stabilized Base
RCRA	Resource Conservation and Recovery Act
PCC	Portland Cement Concrete
EÜAŞ	Electricity Generation Co.Inc.
XRD	X-Ray Diffractometer
ESEM	Environmental Scanning Electron Microscope

CBR	California Bearing Ratio
ÇNAEM	Çekmece Nuclear Research and Training Center
HPGe	High Purity Germanium
FPA	Focal Plane Array
JCPDS	Joint Committee on Powder Diffraction Standards
GSE	Gaseous Secondary Electron
FA	Fly Ash
FI	Natural Snow-Added Fly Ash
CSH	Calcium Silicate Hydrate
CCBs	Coal Combustion By-Products
Bq	Becquerel
UNIPEDE	International Union of Producers and Distributors of Electrical Energy
ND	Non-dispersive
MCL	Max Contaminant Level

1. INTRODUCTION

Fly ash is the byproduct of coal burning thermal power plants and has been successfully used as a structural fill or embankment material for highway construction projects throughout the world. Compared with conventional soils used to build embankments, fly ash is somewhat of a unique engineering material. When dry, fly ash is cohesionless and considered by many as a dusty nuisance. When saturated, fly ash becomes an unmanageable mess. But, as with most fine-grained soils, fly ash can be easily handled and compacted at more intermediate moisture contents, and does exhibit some cohesion.

Handling, control and disposal of fly ash produced by coal fired power plants remain a major problem in many parts of the world. Although significant quantities are being used in a range of applications and particularly as a substitute for cement in concrete, large amounts are not used and have to be disposed in waste containment sites at a high cost.

Effective utilization of waste materials decreases the need for large disposal areas, while providing a cheap mineral resource for construction applications. Geotechnical engineering became a key profession in evaluation of the engineering performance of by-product materials, and in finding new applications. The demand on road construction is increasing due to rapid increase in population, and the lack of mineral resources makes the solution of the road construction problem very hard and costly. Utilization of wastes in highway applications is feasible due to the fact that large volumes of material are needed. However, utilization of fly ash may lead to long-term adverse environmental effects in the long run such as heavy metal leaching and gamma radiation[1].

Depending on the source of coal and combustion conditions, the fly ash may contain various levels of trace metals such as arsenic, cadmium, chromium, copper, lead, mercury, nickel, selenium, and zinc. These metals can potentially be released to the soil, surface water, and groundwater by leaching processes. Any improvement in strength generally has a positive effect on decreasing the leaching of heavy metals from fly ash. pH is one of the most important factors affecting metal leaching from fly ash[1].

Chemical constituents of fly ash mainly depend on the chemical composition of the coal. However, fly ash that are produced from the same source and which have very similar chemical composition, can have significantly different ash mineralogies depending on the coal combustion technology used. Because of this, the ash hydration properties can vary significantly between generating facilities.

Radioactivity is also another important environmental concern in fly ash utilization. Depending on the source of coal burned in the power plant, the gamma radiation may become critical for human health[2]. Gamma radiation is more harmful to living organisms than alpha or beta radiation. High levels of gamma rays can produce dangerous ionization of the tissue and cause skin cancer. Any technique that will cause a reduction in the amount of gamma radiation will promote the utilization of more fly ash in a wider range of applications.

Cold weather affects embankment construction when temperatures dip below freezing. Concrete and soil are affected by cold weather because they both contain water. Cold weather regions are defined as those that typically experience subfreezing temperatures for periods of several weeks to several months each year.

Some soils are susceptible to frost heave during prolonged periods of subfreezing temperatures. Frost heave may occur if there is a continual supply of moisture being drawn up by capillary action from the groundwater table. The forces created from the continued growth of ice lenses in the soil can be large enough to give damage to the pavement. This can lead to differential movements if the heave is not uniform and it can develop cracks in the pavement. Additional damage may occur when the ice lenses begin to thaw. The soil typically thaws from the ground surface down. As the ice in the soil melts, the water can not drain into the underlying ground that is still frozen. The soil may then settle owing to the increase in the water content and the loss of support of the now nonexisting ice lenses. This settlement typically is nonuniform and leads to differential settlements and damage the pavement.

Soils consisting primarily of silt-sized particles are the most susceptible to frost action. It is actually the size of the pore spaces in the soil that controls the susceptibility to

frost heave[3]. Soil deposits that consist of up to 25% clay particles can exhibit a strong susceptibility to frost action if their porosity, and thus permeability, are relatively high[4]. Although clay soils can exhibit high capillary rises, their permeability is relatively low and, therefore, they do not allow water to move fast enough to create significant ice lenses during a single freezing event. Conversely, silty soils can generate relatively high capillary rises in a relatively short time. This combination can lead to the formation of large ice lenses.

Concrete is also affected by cold weather during construction. As temperatures decrease, the rate at which concrete gains strength also decreases. The cement in the concrete must react with the water in the concrete for strength development. For this reason, concrete should never be placed directly on frozen ground. All snow, ice and frost should be removed from the underlying strata. If necessary, the subbase should be covered and heated until all of the frost is melted.

It is common to add air-entraining admixtures to the concrete mix to increase its durability against both frost action and the application of deicers on the concrete. Air-entraining admixtures cause small air bubbles to form inside the cementitious matrix. This procedure is known as air-entrainment. For air-entrained concrete to be effective, it is recommended that 30 days of air drying take place after the concrete has cured for a minimum of 3 to 5 days before the use of deicers. The curing period consists of maintaining the moisture content in the concrete and keeping the temperature of the concrete between 4.4^0C and 32.2^0C[5].

If temperatures are below freezing, both the subbase and the concrete need to be insulated to prevent freezing. Common insulating materials include fiberglass-filled blankets or straw. The insulation material should not be removed from the subbase until the concrete is on-site and ready to be placed.

Another construction constraint during subfreezing temperatures is achieving proper compaction with frozen clayey and silty soils. Soils in this condition are difficult to work with and will lose strength once they thaw. Fills consisting of sand and gravel mixtures are

not as difficult to compact when they are frozen and although importing soil adds to the cost of the project, they become a reliable substitute to frozen clayey and silty soils[6].

When used in structural fills or embankments, fly ash offers several advantages over natural soil or rock. Its relatively low unit weight makes it well suited for placement over soft or low bearing strength soils, and its high shear strength, compared with its unit weight, results in good bearing support and minimal settlement. The ease with which fly ash can be placed and compacted, especially when placed at the proper moisture content, can reduce construction time and equipment costs. In areas where fly ash is readily available in bulk quantities, costs for the purchase, permitting and operation of a borrow pit can be reduced or eliminated.

Fly ash is very sensitive to the compaction water content because of the silt sized fly ash spheres. When the optimum water content is exceeded only one or two per cent, the compaction of fly ash becomes nearly impossible. On the other hand, an excess amount of water is needed for the development of stronger and larger cementitious minerals. The increase in water content can be achieved by adding natural snow in solid form, which will not affect the compaction process, but later upon melting, will provide extra water for cementation reactions[7,8,9]. Another contribution of adding natural snow is related to the hydration temperature. The temperature of the sample is decreased, resulting in longer hydration time that will in turn lead to development of stronger cementitious minerals.

During winter season, due to workability problems, it is very hard to continue construction. Water needed for compaction will be very hard to handle. However snow is readily available on site. With Type C fly ash, snow may be mixed with fly ash and compacted. When Type F fly ash is available, lime must be added to fly ash to initiate cementation reactions. In extreme cold regions the cementation reactions will start in the thaw season and strength improvement will be achieved.

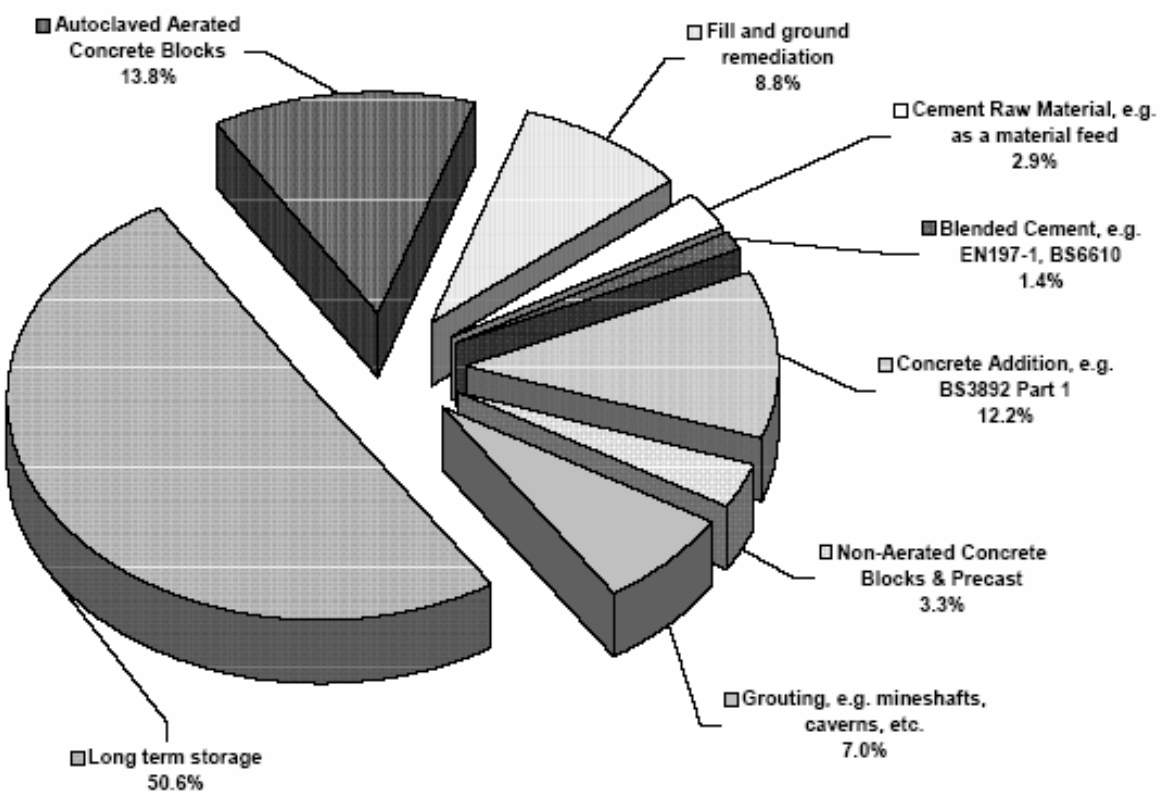

Figure 1.1. Fly ash utilization statistics for UK, 1999.

Fly ash from coal fired power stations has been around for a considerable number of years. There is a wealth of knowledge resulting from both research and the practical use of fly ash. It can be used in, the cement manufacture process as a pozzolanic addition, embankments and structural fills, waste stabilization and solidification, stabilization of soft soils, road subbases, flowable fills, replacement for aggregates and in asphaltic concrete as a mineral filler. However, huge amount of the fly ash produced is not utilized, and therefore stockpiled every year as can be seen in Figure 1.1[10]. In addition, there are many hundred millions of tonnes of fly ash in stockpiles that could be utilised. There are significant environmental benefits to be enjoyed by fully exploiting this by-product material.

The objective of this dissertation is to investigate the usage of snow to aid in embankment construction and see the effects on the microfabric and microstructure of the tested specimens and also to achieve a higher performance and environment friendly road construction material, which leads to lower radiation, less leaching, and higher strength. The extra water can be introduced into the samples with a very simple technique, which

improves the performance of the fly ash used in road construction. More important than the higher performance obtained using natural snow, the new technology will allow construction of highway embankments, bases and subbases during winter time at cold regions, where construction activities are ceased normally due to snow and low temperatures. The hydration heat released from fly ash will melt the snow, and cementitious minerals will grow at a slower pace, allowing formation of stronger and larger minerals resulting in higher performance.

2. LITERATURE REVIEW

2.1. Fly Ash

2.1.1. General Description

Fly ash, also known as a coal combustion product, or CCP, is the finely divided mineral residue resulting from the combustion of powdered coal in electric generating plants. It is also called pulverized fuel ash. Fly ash consists of inorganic, incombustible matter present in the coal that has been fused during combustion into a glassy, amorphous structure. Coal can range in ash content from two to 30 per cent, and of this around 85 per cent becomes fly ash. The remaining 15 per cent is called bottom ash and isn't lifted up by the flue gases [11].

Fly ash material is solidified while suspended in the exhaust gases and is collected by electrostatic precipitators or filter bags. Since the particles solidify while suspended in the exhaust gases, fly ash particles are generally spherical in shape and range in size from 0.5 μm to 100 μm. They consist mostly of silicon dioxide (SiO_2), aluminium oxide (Al_2O_3) and iron oxide (Fe_2O_3), and are hence a suitable source of aluminum and silicon for geopolymers. They are also pozzolanic in nature and react with calcium hydroxide and alkali to form cementitious compounds. Fly ash also contains some heavy metals.

2.1.2. The Origin of Coal

Coal is formed from plant remains that have been compacted, hardened, chemically altered, and metamorphosed by heat and pressure over geologic time.

Coal was formed in swamp ecosystems which persisted in lowland sedimentary basins similar to the peat swamps. These swamp environments were formed during slow subsidence of passive continental margins, and most seem to have formed adjacent to estuarine and marine sediments suggesting that they may have been in tidal delta environments. They are often called the coal forests[12].

When plants die in these peat swamp environments, their biomass is deposited in anaerobic aquatic environments where low oxygen levels prevent their complete decay by bacteria and oxidation. For masses of undecayed organic matter to be preserved and to form economically valuable coal the environment must remain steady for prolonged periods of time, and the waters feeding these peat swamps must remain essentially free of sediment. This requires minimal erosion in the uplands of the rivers which feed the coal swamps, and efficient trapping of the sediments.

Eventually, and usually due to the initial onset of orogeny or other tectonic events, the coal forming environment ceases. In the majority of cases this is abrupt, with the majority of coal seams having a knife-sharp upper contact with the overlying sediments. This suggests that the onset of further sedimentation quickly destroys the peat swamp ecosystem and replaces it with meandering stream and river environments during ongoing subsidence.

Burial by sedimentary loading on top of the peat swamp converts the organic matter to coal by the following processes;

- compaction, due to loading of the sediments on the coal which flattens the organic matter
- removal of the water held within the peat in between the plant fragments
- with ongoing compaction, removal of water from the inter-cellular structure of fossilised plants
- with heat and compaction, removal of molecular water
- methanogenesis; similar to treating wood in a pressure cooker, methane is produced, which removes hydrogen and some carbon, and some further oxygen (as water)
- dehydrogenation, which removes hydroxyl groups from the cellulose and other plant molecules, resulting in the production of hydrogen-reduced coals

Generally, to form a coal seam one meter thick, between 10 and 30 meters of peat is required. Peat has a moisture content of up to 90 per cent, so loss of water is of prime importance in the conversion of peat into lignite, the lowest rank of coal. Lignite is then converted by dehydrogenation and methanogenesis to sub-bituminous coal. Further dehydrogenation reactions, removing progressively more methane and higher hydrocarbon

gases such as ethane, propane, etcetera, create bituminous coal and, when this process is complete at sub-metamorphic conditions, anthracite and graphite are formed[13].

2.1.3. Coal Types

Increasing overburden pressure and rising temperature due to the increased depth of burial are the driving forces for the rank change from peat to lignite, sub-bituminous, bituminous and anthracitic coals. The process of conversion of plant materials, such as peat, to coal is called “coalification”. The basic coal types can be described as below:

- Lignite coal, the softest of the four types of coal. It is a brownish black in color, very crumbly and primarily used for the generation of electricity. Because of its color, it is often referred to as "brown coal." Lignite is the result of millions of tons of plants and trees that decayed in a swampy atmosphere about 50-70 million years ago. The heating content of lignite is approximately 4,000-8,000 Btu's per pound. The carbon content of lignite is 25 to 35 per cent and it has a very high water content about 35 per cent.
- Sub-bituminous coal is a medium soft coal that contains much less moisture than that of lignite and is not nearly as crumbly. It is dull and black in color and is banded. It displays cleavage and usually splits parallel to bedding planes[14]. Like lignite, its primary use is in the generation of electricity. The carbon content of sub-bituminous coal runs from 35 to 45 per cent and its heat value generally ranges from 8,000-13,000 Btu's per pound.
- Bituminous coal contains even less moisture than the sub-bituminous type. It is dense, compacted, banded, brittle, dark black in color and displays columnar clevage. The carbon content of bituminous coal is generally from 45 to 85 per cent. Its heat value ranges from 10,500-15,000 Btu's per pound - greater than either lignite or the sub-bituminous types. In addition to being used for electrical generation, it is also used in making coke or coking coal, an essential ingredient in making steel.
- Anthracite coal is the hardest of the four types. It is the highly metamorphosed coal, is jet black in color, is hard and brittle, breaks with a conchoidal fracture and displays a high luster[14]. It averages 85 to 95 per cent carbon content and has the highest heating value of the four types of coal. It is not uncommon to find anthracite that

produces well in excess of 15,000 Btu's per pound. To put that in perspective, that is roughly one and one-half times as much heat as the same volume of oil and four times as much as seasoned hard-maple firewood. Anthracite makes excellent home heating fuel because it burns cleanly, does not produce volatile gases and does not deteriorate. It can be stored on the ground for long periods of time without creating environmental problems. It is used extensively in municipal water purification and treatment plants and for home heating.

2.1.4. Coal Composition

The composition of coal is determined by ASTM proximate and ASTM ultimate analysis. Proximate analysis determines the moisture content and per cent volatiles, ash and fixed carbon. Ultimate analysis gives elemental analysis for carbon, hydrogen, nitrogen, sulfur and oxygen. The residual mineral matter is shown as ash. Proximate and ultimate analysis for a selected variety of coals from the United States is shown in Table 2.1. In Table 2.2 proximate and ultimate analysis of some Turkish lignites from Manisa, Soma are given.

Typical compositions (mass percentages) of coal include 65 to 95 per cent carbon, two to seven per cent hydrogen, up to 25 per cent oxygen, 10 per cent sulfur and one to two per cent nitrogen[14]. Inorganic mineral matter (ash) as high as 50 per cent has been observed, but five to 15 per cent is more typical [14].

Mineral matter enters the coal deposit at various times of its formation history. Some minerals (mostly detrital clay minerals and quartz) are brought by moving water (e.g. rivers); others (pyrite) are precipitated from waters circulating through the peat with or without the help of specialized bacteria. The most common mineral impurities deposited in, coal are clay minerals, namely silicates of aluminum, iron and magnesium. Pyrite, kaolinite, calcite and cleat fillings of carbonates and sulfides are also found in coal. Quartz, garnets, shale and feldspars are common too.

Table 2.1. Typical proximate and ultimate analysis of coals from the United States

Coal I.D. rank	Utah Church Mine bit.	Pittsburgh bit. (high volatile)	Pittsburgh bituminous	Sewell bit. (medium volatile)	Pocahantas bit. (low volatile)
MOIST.(%)	2.5-2.7	2.0	1.0	—	1.9
PROX.(%)					
Volatiles	44.1-45.5	36.6	28.9	29.2	16.3
Fixed Carbon	42.6-44.2	55.4	63.2	63.9	75.6
Ash	9.2-9.5	6.0	6.9	6.9	6.2
ULT. (%)					
Carbon	69.8-71.5	77.5	80.6	81.4	84.2
Hydrogen	5.5-5.6	5.3	4.9	4.8	4.3
Nitrogen	1.4-1.5	1.5	1.5	1.6	1.2
Sulfur	0.4-0.7	1.2	0.7	0.7	0.7
Oxygen	11.2-13.2	8.5	5.4	4.6	3.4
Ash	9.2-9.5	6.0	6.9	6.9	6.2

Coal I.D. rank	Anthracite (low volatile)	Illinois coal bit.,	Illinois coal char	North Dakota lignite	Wyoming sub-bit.	Kentucky bit.
MOIST. (%)	1.3	10.1	0.9	29.9	27.8	8.6
PROX.(%)						
Volatiles	8.8	35.9	2.4	29.5	32.9	35.2
Fixed carbon	71.8	46.7	76.1	33.4	34.3	41.5
Ash	18.1	7.3	20.6	7.2	5.0	23.3
ULT. (%)						
Carbon	73.2	68.3	74.0	69.7	76.3	61.0
Hydrogen	3.1	5.0	0.7	3.8	4.4	4.4
Nitrogen	0.9	1.3	1.0	1.9	1.1	1.4
Sulfur	0.9	3.5	3.3	1.1	0.5	4.3
Oxygen	3.8	13.8	*0.2*	13.2	10.8	5.6
Ash	18.1	8.1	20.8	10.3	6.9	23. 3

Table 2.2. Proximate and ultimate analysis of lignites from Manisa, Soma

Coal I.D. rank	Sample Number				
	-	2	70	71	72
Moisture (%)	12.14	23.65	14.57	10.11	11.57
Proximate (%)					
Volatiles	32.81	37.47	31.55	35.28	30.80
Fixed Carbon	27.77	32.33	38.20	35.78	29.59
Ash	27.28	6.55	15.68	18.83	28.04
Ultimate {%)					
Carbon	43.44	-	-	-	-
Hydrogen	3.25	-	-	-	-
Sul-fur	1.46	-	-	-	-
ASTM values(%)					
Volatiles	56.59	54.59	46.21	50.90	53.21
Fixed Carbon	43.41	45.41	53.79	49.10	46.79

Coal I.D. rank	Sample Number			
	73	74	75	108
Moisture (%)	12.46	14.68	11.49	12.14
Proximate (%)				
Volatiles	29.36	29.28	35.62	29.22
Fixed Carbon	37.69	35.08	39.05	31.79
Ash	20.49	20.96	13.84	26.85
Ultimate (%)				
Carbon	-	-	-	43.43
Hydrogen	-	-	-	3.24
Sulfur	-	-	-	1.46
ASTM values(%)				
Volatiles	45.02	46.87	48.57	49.95
Fixed Carbon	54.98	53.13	51.43	50.05

The concentration of ash forming elements (excluding O, S and N) in whole coal may range arbitrarily between greater than 0.5 per cent for major elements such as Al, Ca, Fe and Si; 0.02 per cent to 0.5 per cent for minor elements such as PC, Mg, Na, Ti and others; and less than 0.02 per cent for trace elements which include such elements as As, Be, Hg, Cd and the remaining majority of elements in the periodic table[13].

2.1.5. Fly Ash Formation

Most of the coal presently being consumed is by direct combustion of finely pulverized coal in large scale utility furnaces for generation of electric power[14]. As coal passes through the high temperature zone in the furnace, the volatile matter and carbon are burned off whereas most of the mineral impurities deposited in coal during its formation, such as clays, shale, quartz and feldspar generally fuse and remain in suspension in the flue gas[15]. The fused matter is quickly transported to lower temperature zones where it solidifies as spherical particles. Some of the mineral matter agglomerates to form bottom ash, but most of it flies out with the flue gas stream and hence is called fly ash. This ash is subsequently removed from the flue gas by mechanical separators, electrostatic precipitators or bag filters[15].

Pulverized coal combusters, which burn coal crushed and ground to a fineness of 70 to 80 per cent passing the No. 200 (75 μm) sieve, produce the smallest fly ash particles. Fluidized bed combusters generate medium sized, and fixed bed (stokers) combusters generate coarser sized fly ash.

2.1.6. Classification of Fly Ash

There are different classifications of fly ash in terms of different standards of countries and amounts of lime and silica. In classification according to lime and silica, ASTM classification for US, ENV classification for EU and TSE classification for Turkey has been given in this study.

2.1.6.1. Classification in Terms of Lime and Silica. According to this classification, fly ash is mainly divided into three categories [70]:

- Silicate-aluminate fly ash that ash is generally generated from hard coal and is formed by silicate-aluminates.
- Sulphate-calcium fly ash that is generally generated from lignite and contains more silicate and lime compare to other types of fly ashes.
- Silicate-calcium fly ash that is usually generated from lignite and contains higher amounts of lime and silicate.

2.1.6.2. ASTM Classification. Fly ash, which is used in cement production, is classified according to ASTM C 618 standard as class F or class C, depending on the parent coal source in US. Class F fly ash is generally generated from hard coal. Fly ash, which is generated from lignite, can be classified as class F or C depending on the amount of silicate and lime. Limits of class C and F type of fly ash are given in Table 2.3.

Table 2.3. Limits of ASTM C 618 for fly ash classification

Chemical Properties (%)	F Class	C Class
Max. $S0_3$	5	5
Max. MgO	5	5
$Si0_2$	-	-
Al_20_3	-	-
Fe_20_3	-	-
Minimum S+A+F	70	50
Reactive CaO (%)	-	-
Reactive SiO_2 (%)	-	-
Heating Loss (%)	12	6

2.1.6.3. ENV Classification. Fly ash, which can be used in cement production, is classified by ENV 197-1 standards as class V and class W in EU. Class V fly ash is named as silicate fly ash and class W fly ash is named as calcareous fly ash. Limits of class W and V type of fly ashes are given in Table 2.4.

Table 2.4. Limits of ENV 197-1 for fly ash classification

Chemical Properties (%)	W Class	V Class
Max. $S0_3$	-	-
Max. MgO	-	-
SiO_2	-	-
Al_20_3	-	-
Fe_2O_3	-	-
Minimum S+A+F	-	-
Reactive CaO (%)	<5	>5
Reactive SiO_2 (%)	>25	>25
Heating Loss (%)	<5	<5

2.1.6.4. TSE Classification. In Turkey, fly ash that can be used in cement production, had been classified according to TSE 640 standards until March 2002. However, in the process of adaptation of Turkish laws, regulations and standards to EU laws, regulations and standards, EU fly ash standard ENV 197-1 has been adapted in Turkey, named as TS EN 197-1. This standard has the same limits and regulations with ENV 197-1 and it classifies fly ash as class V and class W in Turkey. Limits of class W and V type of fly ash in terms of TS EN 197-1 standards are the same, which are given in Table 2.4. (TSE, 2002).

2.1.7. Chemical Properties of Fly Ash

The chemical properties of fly ash are influenced to a great extent by those of the coal burned and the techniques used for handling and storage. There are basically four types, or ranks of coal, each of which varies in terms of its heating value, its chemical composition, ash content, and geological origin. The four types, or ranks of coal are anthracite, bituminous, sub-bituminous, and lignite. In addition to being handled in a dry, conditioned, or wet form, fly ash is also sometimes classified according to the type of coal from which the ash was derived.

The principal components of bituminous coal fly ash are silica, alumina, iron oxide, and calcium, with varying amounts of carbon, as measured by the loss on ignition (LOI). Lignite and sub-bituminous coal fly ashes are characterized by higher concentrations of calcium and magnesium oxide and reduced percentages of silica and iron oxide, as well as

a lower carbon content, compared with bituminous coal fly ash[20]. Very little anthracite coal is burned in utility boilers, so there are only small amounts of anthracite coal fly ash.

Table 2.5 compares the normal range of the chemical constituents of bituminous coal fly ash with those of lignite coal fly ash and sub-bituminous coal fly ash. From the table, it is evident that lignite and sub-bituminous coal fly ashes have a higher calcium oxide content and lower loss on ignition than fly ashes from bituminous coals. Lignite and sub-bituminous coal fly ashes may have a higher concentration of sulfate compounds than bituminous coal fly ashes.

The chief difference between Class F and Class C fly ash is in the amount of calcium and the silica, alumina, and iron content in the ash [21]. In Class F fly ash, total calcium typically ranges from one to 12 per cent, mostly in the form of calcium hydroxide, calcium sulfate, and glassy components in combination with silica and alumina. In contrast, Class C fly ash may have reported calcium oxide contents as high as 30 to 40 per cent [22]. Another difference between Class F and Class C is that the amount of alkalis (combined sodium and potassium) and sulfates (SO_4) are generally higher in the Class C fly ashes than in the Class F fly ashes.

Table 2.5. Normal range of chemical composition for fly ash produced from different coal types (expressed as per cent by weight).

Component	Bituminous	Sub-bituminous	Lignite
SiO_2	20-60	40-60	15-45
Al_2O_3	5-35	20-30	10-25
Fe_2O_3	10-40	4-10	4-15
CaO	1-12	5-30	15-40
MgO	0-5	1-6	3-10
SO_3	0-4	0-2	0-10
Na_2O	0-4	0-2	0-6
K_2O	0-3	0-4	0-4
LOI	0-15	0-3	0-5

Although the Class F and Class C designations strictly apply only to fly ash meeting the ASTM C618 specification, these terms are often used more generally to apply to fly ash on the basis of its original coal type or CaO content. It is important to recognize that not all fly ashes are able to meet ASTM C618 requirements and that, for applications other than concrete, it may not be necessary for them to do so.

The loss on ignition (LOI), which is a measurement of the amount of unburned carbon remaining in the fly ash, is one of the most significant chemical properties of fly ash, especially as an indicator of suitability for use as a cement replacement in concrete.

2.1.8. Mineralogical Properties of Fly Ash

Fly ash is a heterogeneous mixture of particles differing in shape, size, and composition. These particles can be classified as carbon from unburned coal, fire-polished sand, thin-walled hollow spheres and their fragments, magnetic iron containing spherical particles, and spherical glassy particles. The majority of mineral matter consists of clays, pyrite and calcite. More than 85 per cent of most fly ash consist of glassy and crystalline compounds formed by the thermal treatment of minerals [41,42,43].

The chemical and mineralogical composition of fly ash depends upon the characteristics and composition of the coal burned in the power plant. Depending on the rate of cooling, fly ash is composed mainly (50 - 90 per cent) of mineral matter in the form of glassy particles, whereas a small amount occurs in the form of crystals. Infrared, Mössbauer Spectroscopy, X-Ray diffractometry etc. techniques may be used to examine the crystalline phases in fly ash. The most important minerals found in fly ash obtained from bituminous coal are [44,45,38,46];

- Magnetite 0.8-6,5 %
- Hematite 1.1-2.7 %
- Quartz 2.2-8.5 %
- Mullite 6.5-9.0 %
- Free CaO up to 3.5 %

The minerals like wustite, goethite, pyrite, calcite, anhydrite and periclase range within trace amounts to 2.5 per cent [26].

2.1.9. Physical Properties of Fly Ash

Fly ash consists of fine, powdery particles that are predominantly spherical in shape, either solid or hollow, and mostly glassy (amorphous) in nature. The carbonaceous material in fly ash is composed of angular particles. The particle size distribution of most bituminous coal fly ashes is generally similar to that of silt (less than a 0.075 mm or No. 200 sieve). Although sub-bituminous coal fly ashes are also silt-sized, they are generally slightly coarser than bituminous coal fly ashes[25].

The specific gravity of fly ash usually ranges from 2.1 to 3.0, while its specific surface area (measured by the Blaine air permeability method[29] may range from 170 to 1000 m^2/kg).

The color of fly ash can vary from tan to gray to black, depending on the amount of unburned carbon in the ash. The lighter the color, the lower the carbon content, lignite or sub-bituminous fly ashes are usually light tan to buff in color, indicating relatively low amounts of carbon as well as the presence of some lime or calcium. Bituminous fly ashes are usually some shade of gray, with the lighter shades of gray generally indicating a higher quality of ash.

2.1.10. Hydration of Fly Ash

Formation of cementitious material by the reaction of free lime (CaO) with the pozzolans (Al_2O_3, SiO_2, Fe_2O_3) in the presence of water is known as hydration. The hydrated calcium silicate gel or calcium aluminate gel (cementitious material) can bind inert material together. For class C fly ash, the calcium oxide (lime) of the fly ash can react with the siliceous and aluminous materials (pozzolans) of the fly ash itself. Since the lime content of class F fly ash is relatively low, addition of lime is necessary for hydration reaction with the pozzolans of the fly ash. For lime stabilization of soils, pozzolanic reactions depend on the siliceous and aluminous materials provided by the soil.

The pozzolanic reactions are as follows:

$$Ca(OH)_2 \Rightarrow Ca^{++} + 2[OH]^- \quad (2.1)$$

$$Ca^{++} + 2[OH]^- + SiO_2 \Rightarrow CSH \quad (2.2)$$

(silica) (gel)

$$Ca^{++} + 2[OH]^- + Al_2O_3 \Rightarrow CAH \quad (2.3)$$

(alumina) (gel)

Hydration of tricalcium aluminate in the ash provides one of the primary cementitious products in many ashes. The rapid rate at which hydration of the tricalcium aluminate occurs results in the rapid set of these materials, and is the reason why delays in compaction result in lower strengths of the stabilized materials[30].

The hydration chemistry of fly ash is very complex in nature. So the stabilization application must be based on the physical properties of the ash treated stabilized soil and cannot be predicted based on the chemical composition of the fly ash.

2.2. Environmental Risks of Fly Ash Utilization

2.2.1. Radioactivity

Coal is largely composed of organic matter, but it is the inorganic matter in coal (minerals and trace elements) that have been cited as possible causes of health, environmental, and technological problems associated with the use of coal. Some trace elements in coal are naturally radioactive. These radioactive elements include uranium (U), thorium (Th), and their numerous decay products, including radium (Ra) and radon (Rn). Although these elements are less chemically toxic than other coal constituents such as arsenic, selenium, or mercury, questions have been raised concerning possible risk from radiation. In order to accurately address these questions and to predict the mobility of radioactive elements during the coal fuel-cycle, it is important to determine the concentration, distribution, and form of radioactive elements in coal and fly ash[2].

Assessment of the radiation exposure from coal burning is critically dependent on the concentration of radioactive elements in coal and in the fly ash that remains after combustion. Data for uranium and thorium content in coal is available from the U.S. Geological Survey (USGS), which maintains the largest database of information on the chemical composition of U.S. coal.

Figure 2.1 displays the frequency distribution of uranium concentration for approximately 2.000 coal samples from the western United States. In the majority of samples, concentrations of uranium fall in the range from slightly below one to four parts per million (ppm). Similar uranium concentrations are found in a variety of common rocks and soils, as indicated in Figure 2.2. Coals with more than 20 ppm uranium are rare in the United States. Thorium concentrations in coal fall within a similar one–four ppm range, compared to an average crustal abundance of approximately 10 ppm. Coals with more than 20 ppm thorium are extremely rare[31].

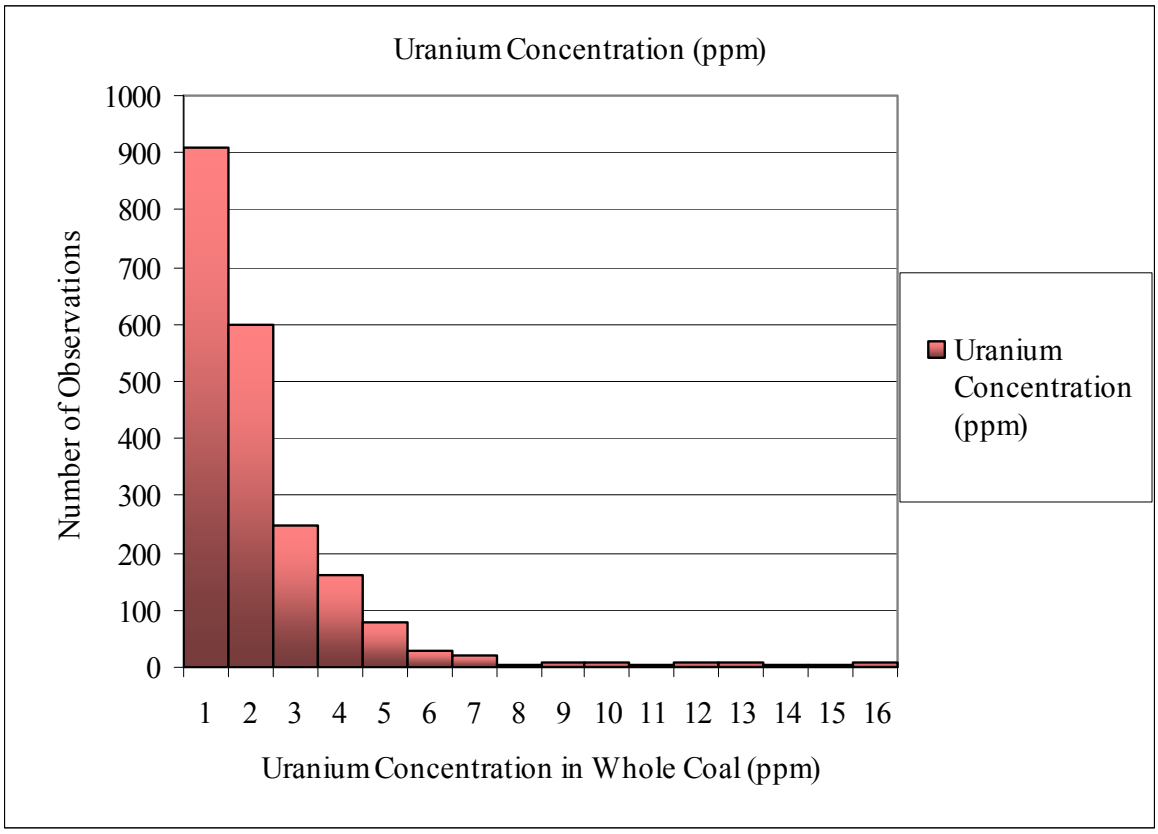

Figure 2.1. Distribution of uranium concentration in coal from two areas of the western United States .

During coal combustion most of the uranium, thorium, and their decay products are released from the original coal matrix and are distributed between the gas phase and solid combustion products.

Fly ash is commonly used as an additive to concrete building products, but the radioactivity of typical fly ash is not significantly different from that of more conventional concrete additives or other building materials such as granite or red brick. One extreme calculation that assumed high proportions of fly ash rich concrete in a residence suggested a dose enhancement, compared to normal concrete, of three per cent of the natural environmental radiation.

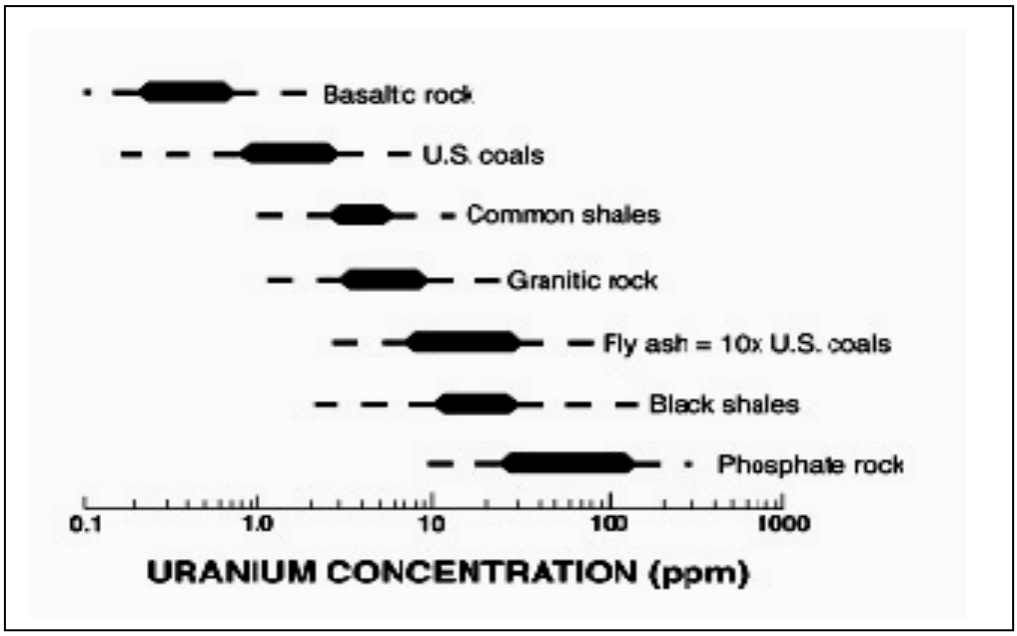

Figure 2.2. Typical range of uranium concentration in coal, fly ash, and a variety of common rocks.

Another consideration is that low density, fly ash rich concrete products may be a source of radon gas. Direct measurement of this contribution to indoor radon is complicated by the much larger contribution from underlying soil and rock. The emanation of radon gas from fly ash is less than from natural soil of similar uranium content. Present calculations indicate that concrete building products of all types contribute less than 10 per cent of the total indoor radon.

Radioactive elements in coal and fly ash should not be sources of alarm. The vast majority of coal and the majority of fly ash are not significantly enriched in radioactive elements, or in associated radioactivity, compared to common soils or rocks. This observation provides a useful geologic perspective for addressing societal concerns regarding possible radiation and radon hazard[49,2].

2.2.2. Leaching from Fly Ash

The leachability of radioactive elements from fly ash has relevance in view of the U.S. Environmental Protection Agency (USEPA) drinking water standard for dissolved radium (five picocuries per liter) and the proposed addition of drinking water standards for uranium and radon by the year 2000. Previous studies of radioelement mobility in the enviroment, and in particular, in the vicinity of uranium mines and mills, provide a basis for predicting which chemical conditions are likely to influence leachability of uranium, barium (a chemical analog for radium), and thorium from fly ash. For example, leachability of radioactive elements is critically influenced by the pH that results from reaction of water with fly ash. Extremes of either acidity (pH<4) or alkalinity (pH>8) can enhance solubility of radioactive elements[1]. Acidic solutions attack a variety of mineral phases that are found in fly ash. However, neutralization of acid solutions by subsequent reaction with natural rock or soil promotes precipitation or sorption of many dissolved elements including uranium, thorium, and many of their decay products. Highly alkaline solutions promote dissolution of the glassy components of fly ash that are an identified host of uranium; this can, in particular, increase uranium solubility as uranium-carbonate species. Fortunately, most leachates of fly ash are rich in dissolved sulfate, and this minimizes the solubility of barium (and radium), which form highly insoluble sulfates.

Direct measurements of dissolved uranium and radium in water that has contacted fly ash are limited to a small number of laboratory leaching studies, including some by USGS researchers, and sparse data for natural water near some ash disposal sites. These preliminary results indicate that concentrations are typically below the current drinking water standard for radium (five picocuries per liter) or the initially proposed drinking water standard for uranium of 20 parts per billion (ppb)[31].

2.3. Utilization Areas of Fly Ash

Due to the development in industry and changes in people's life styles, demand for electricity generation has increased, and it leads to increase in production of electricity generation and the number of power plants. Coal-burning power plants have been preferred due to use of inappropriate local resources (lignite that has lower heating calorie) for dwelling use. Moreover, environmental problems, especially wide area requirements, of fly ash have become preventing items for coal-burning power plants. As environmental consciousness increases, utilization of fly ash like other waste materials have become important in order to decrease the fly ash deposit amount that leads to lower area requirements, lower construction and operational cost with lower environmental pollution risks.

2.3.1. Fills, Embankments and Backfills

Coal fly ash has been successfully used as a structural fill or embankment material for highway construction projects throughout the world. Compared with conventional soils used to build embankments, fly ash is somewhat of a unique engineering material. When dry, fly ash is cohesionless and considered by many as a dusty nuisance. When saturated, fly ash becomes an unmanageable mess. But, as with most fine-grained soils, fly ash can be easily handled and compacted at more intermediate moisture contents, and does exhibit some cohesion[32].

When used in structural fills or embankments, fly ash offers several advantages over natural soil or rock. Its relatively low unit weight makes it well suited for placement over soft or low bearing strength soils, and its high shear strength, compared with its unit weight, results in good bearing support and minimal settlement. The ease with which fly ash can be placed and compacted, especially when placed at the proper moisture content, can reduce construction time and equipment costs. In areas where fly ash is readily available in bulk quantities, costs for the purchase, permitting, and operation of a borrow pit can be reduced or eliminated[33].

There are some disadvantages of using fly ash in structural fills or embankments. Unless delivered to the project site within the proper moisture range, dust control measures may be needed. Also, since fly ash is a predominantly silt-size material, it is subject to erosion and, as a result erosion control procedures may be needed.

2.3.2. Pavement Base and Subbase Courses

Fly ash stabilized base courses are proportioned mixtures of fly ash, aggregate, and an activator (cement or lime) that, when properly placed and compacted, produce a strong and durable pavement base course. Fly ash stabilized base courses are cost effective substitutes for properly engineered full depth asphalt, cement treated, and crushed stone base courses. Fly ash stabilized base course is suitable for both flexible and rigid pavements[33].

The stabilization of aggregate road bases with fly ash has a long and successful history. This application, termed pozzolanic-stabilized mixture (PSM) uses several materials and material combinations to construct stabilized bases. Class C fly ash can be used as a stand alone material.

The successful performance of pozzolanic stabilized base (PSB) mixtures depends on the development of strength within the cementitious matrix formed by the pozzolanic reaction between the fly ash and the activator. This cementitious matrix acts as a binder that holds the aggregate particles together, similar in many respects to a low-strength concrete. However, unlike concrete, PSB mixtures are produced at a compactable consistency, not a plastic consistency, for placement at or near optimum moisture content and densification by roller compaction.

PSB pavements have provided good to excellent performance over many years in numerous locations. In general, these mixtures have also been more economical than alternative base materials in many areas[32].

2.3.3. Subgrade Stabilization

A subgrade is a surface, which acts as a foundation for pavements, floor slabs, embankments, or other structures. The soil cement methodology has been used as a massive fill to provide foundation strength and uniform support under large structures. Fly ash alone or in combination with lime, is used to stabilize the subgrade in order to reduce plasticity, enhance strength, and improve workability of weak soils. Pozzolanic reactions between fly ash, lime and water give rise to cementitious products, which bind the soil particles. In sandy or muddy soils, the fine particles of soil act as fillers and cementation due to the pozzolanic reactions bind the soil. There appears no optimum proportion of lime and fly ash to stabilize soil, but soils containing clays need a greater lime/fly ash and lime/soil proportion to ensure an adequate subsoil strength due reactions between lime, fly ash, and soil. Studies show that for clayey soils, the lime content should range between five to nine per cent and fly ash content between 10 to 25 per cent by weight. For granular soils the ranges may vary between three to six per cent and 10 to 25 per cent respectively. Fly ash having self hardening property may be used to stabilize soils without any additives. The subgrade stabilization is needed in the construction of roadways, parking areas, railroad beds, building foundations, airport runways, etc[42,51].

2.3.4. Landfill Cover

Landfill capping is a containment technology that forms a barrier between the contaminated media and the surface, thereby shielding humans and the environment from the harmful effects of its contents and perhaps limiting the migration of the contents. A cap must restrict surface water infiltration into the contaminated subsurface to reduce the potential for contaminants to leach from the site.

The use of fly ash as landfill cover is mostly used to cover inorganic wastes. Toxic waste materials, which are released from industrial processes, are encapsulated by solidification and immobilization. Fly ash, when mixed with lime and/or cement is an excellent solidification material to be used in such applications due to its several favorable properties such as compactability, shrinkage and cementing behaviour, and the rate of leaching from the toxic substances are reduced. The fly ash and lime/cement mixture may

be used to cover ordinary waste disposal sites as well. It can be used in place of silts or clays for daily, intermediate, and final covers. The use of fly ash cover becomes economically attractive where other soils are scarce.

The use of fly ash as landfill cover or liner material provides advantages due to its practicality in applications, better engineering performance than natural soils for stability, suitable hydraulic conductivity values less than 10^{-6} cm/sec. The Resource Conservation and Recovery Act (RCRA) Subtitle D specifies the maximum hydraulic conductivity value as $1.0x10^{-7}$ cm/sec. Recent studies indicate that mixing of fly ash with native soils consisting clays decreases the hydraulic conductivity below 10^{-7} cm/sec[34].

2.3.5. Soil Improvement

Soil stabilization is the alteration of soil properties to improve the engineering performance of soils. The properties most often altered are density, water content, plasticity and strength. Modification of soil properties is the temporary enhancement of subgrade stability to expedite construction.

Class C fly ash and Class F-lime product blends can be used in numerous geotechnical applications common with highway construction to enhance strength properties, to stabilize embankments, to control shrink swell properties of expansive soils and as a drying agent to reduce soil moisture contents to permit compaction[35].

Fly ash has been used successfully in many projects to improve the strength characteristics of soils. Fly ash can be used to stabilize bases or subgrades, to stabilize backfill, to reduce lateral earth pressures and to stabilize embankments to improve slope stability. Typical stabilized soil depths are 15 to 46 centimeters. The primary reason fly ash is used in soil stabilization applications is to improve the compressive and shearing strength of soils. The compressive strength of fly ash treated soils is dependent on in-place soil properties, delay time, moisture content at time of compaction and fly ash addition ratio.

Fly ash reduces the potential of a plastic soil to undergo volumetric expansion by a physical cementing mechanism, which cannot be evaluated by the plasticity index. Fly ash

controls shrink-swell by cementing the soil grains together much like a portland cement bonds aggregates together to make concrete. By bonding the soil grains together, soil particle movements are restricted. Typical addition rates based on dry weight of soil are 12 to 15 per cent.

Soils must be compacted to their maximum practical density to provide a firm base for overlying structures. For soils to be compacted the moisture content must be controlled because of the relationship between soil density and moisture content. If the soil to be compacted is either to wet or too dry, the moisture content must be adjusted to near optimum to achieve maximum density. If a soil is too dry, moisture is simply added. If a soil is too wet, the moisture content of the soil must be lowered. Class C fly ash and other high lime fly ash have been found to be very effective drying agents, capable of reducing soil moisture content by 30 per cent or more[36].

The fly ash dries the soil by two basic mechanisms, chemical reactions that consume moisture in the soil and by simple dilution. Class C fly ashes contain tricalcium aluminate (C_3A), which is highly reactive with water. C_3A is the chemical compound present in ordinary portland cement which is responsible for early strength. The C_3A present in fly ash reacts with the water, lowering the overall moisture content of the soil. The drying effect of fly ash in wet soil is very rapid and immediate, permitting the contractor to quickly proceed with construction. In addition to the speeding up of the construction process the use of fly ash provides several other benefits, such as making the soil more resistant to additional water infiltration, provides additional support for traffic, creates a more stable work platform and reduces dusting from construction traffic.

The use of fly ash in soil stabilization and soil modification may be subject to local environmental requirements pertaining to leaching and potential interaction with ground water and adjacent water courses[37].

2.3.6. Flowable Fill

Flowable fill is a mixture of coal fly ash, water, and portland cement that flows like a liquid, sets up like a solid, is self-leveling, and requires no compaction or vibration to

achieve maximum density. In addition to these benefits, a properly designed flowable fill may be excavated later. For some mixes, an optional filler material such as sand, bottom ash, or quarry fines is added. Flowable fill is also referred to as controlled low-strength material, flowable mortar, or controlled density fill. It is designed to function in the place of conventional backfill materials such as soil, sand, or gravel and to alleviate problems and restrictions generally associated with the placement of these materials[38].

Coal fly ash can be used as a component in the production of flowable fill, which is used as self-leveling, self-compacting backfill material in lieu of compacted earth or granular fill. Flowable fill includes mixtures of Portland cement and filler material and can contain mineral admixtures, such as fly ash. Filler material usually consists of fine aggregate (in most cases sand), but some flowable fill mixes may contain approximately equal portions of coarse and fine aggregates. Fly ash has also been used as filler material.

Flowable fill is mainly used as a trench backfill for storm drainage and utility lines on street and highway projects. Flowable fill has also been used to backfill abutments and retaining walls, fill abandoned pipelines and utility vaults, fill cavities and settled areas, and help to convert abandoned bridges into culverts[40].

There are two basic types of flowable fill mixes that contain fly ash: high fly ash content mixes and low fly ash content mixes. The high fly ash content mixes typically contain nearly all fly ash, with a small percentage of Portland cement and enough water to make the mix flowable. Low fly ash content mixes typically contain a high percentage of fine aggregate or filler material (usually sand), a low percentage of fly ash and Portland cement, and enough water to also make the mix flowable[38].

There are no specific requirements for the types of fly ash that may be used in flowable fill mixtures. Low lime or Class F fly ash is well suited for use in high fly ash content mixes, but can also be used in low fly ash content mixes. High lime or Class C fly ash, because it is usually self-cementing, is almost always used only in low fly ash content flowable fill mixes. There is also a flowable fill product in which both Class F and Class C fly ash are used in varying mix proportions[39].

2.4. Highway Uses and Processing Requirements

2.4.1. Portland Cement Concrete

Fly ash has been successfully used as a mineral admixture in PCC for nearly 60 years. This is the largest single use of fly ash. It can also be used as a feed material for producing Portland cement and as a component of a Portland-pozzolan blended cement.

Fly ash must be in a dry form when used as a mineral admixture. Fly ash quality must be closely monitored when the material is used in PCC. Fineness, loss on ignition, and chemical content are the most important characteristics of fly ash affecting its use in concrete. Fly ash used in concrete must also have sufficient pozzolanic reactivity and must be of consistent quality[19].

2.4.2. Asphalt Concrete

Fly ash has been used as substitute mineral filler in asphalt paving mixtures for many years. Mineral filler in asphalt paving mixtures consists of particles, less than 0.075 mm (No. 200 sieve) in size, that fill the voids in a paving mix and serve to improve the cohesion of the binder (asphalt cement) and the stability of the mixture. Most fly ash sources are capable of meeting the gradation (minus 0.075 mm) requirements and other pertinent physical (nonplastic) and chemical (organic content) requirements of mineral filler specifications.

Fly ash must be in a dry form for use as mineral filler. Fly ash that is collected dry and stored in silos requires no additional processing. It is possible that some sources of fly ash that have a high lime (CaO) content may also be useful as an antistripping agent in asphalt paving mixes[20].

2.4.3. Stabilized Base

Stabilized bases or subbases are mixtures of aggregates and binders, such as Portland cement, which increase the strength, bearing capacity, and durability of a pavement

substructure. Because fly ash may exhibit pozzolanic properties, or self-cementing properties, or both, it can and has been successfully used as part of the binder in stabilized base construction applications. When pozzolanic-type fly ash is used, an activator must be added to initiate the pozzolanic reaction. Self-cementing fly ash does not require an activator. The most commonly used activators or chemical binders in pozzolan-stabilized base (PSB) mixtures are lime and Portland cement, although cement kiln dusts and lime kiln dusts have also been used with varying degrees of success. Sometimes, combinations of lime, Portland cement, or kiln dusts have also been used in PSB mixtures.

The successful performance of PSB mixtures depends on the development of strength within the matrix formed by the pozzolanic reaction between the fly ash and the activator. This cementitious matrix acts as a binder that holds the aggregate particles together, similar in many respects to a low-strength concrete[20].

2.4.4. Flowable Fill

Flowable fill is a slurry mixture consisting of sand or other fine aggregate material and a cementitious binder that is normally used as substitute for a compacted earth backfill. Fly ash has been used in flowable fill applications as a fine aggregate and (because of its pozzolanic properties) as a supplement to or replacement for the cement. Either pozzolanic or self-cementing fly ash can be used in flowable fill. When large quantities of pozzolanic fly ash are added, the fly ash can act as both fine aggregate and part of the cementitious matrix. Self-cementing fly ash is used in smaller quantities as part of the binder in place of cement.

The quality of fly ash used in flowable fill applications need not be as strictly controlled as in other cementitious applications. Both dry and reclaimed ash from settling ponds can be used. No special processing of fly ash is required prior to use[33].

2.4.5. Embankment and Fill Material

Fly ash has been used for several decades as an embankment or structural fill material, particularly in Europe. There has been relatively limited use of fly ash as an

embankment material in Turkey, although its use in this application is becoming more widely accepted.

As an embankment or fill material, fly ash is used as a substitute for natural soils. Fly ash in this application must be stockpiled and conditioned to its optimum moisture content to ensure that the material is not too dry and dusty or too wet and unmanageable. When fly ash is at or near its optimum moisture content, it can be compacted to its maximum density and will perform in an equivalent manner to well compacted soil[20].

2.5. Properties of Ice

2.5.1. General Description

Ice is the frozen state of water, it has crystals and all the physical properties of a mineral. Ice has several important attributes and uses that helps make the living earth what it is today. The different types of ice such as glaciers, ice caps, and snowflakes have a definite affect on the climate of all the geographic regions around the world. Some of them are huge masses that cover the ground for many miles and others are small chunks that fall from the sky. Naturally, the more natural ice there is in a given region, the colder it will be. With the current technology ice is also very important in climates that are relatively warm all year round or at least part of the year.

Ice is considered a mineral because it is a natural, inorganic, homogeneous solid with definite chemical composition and crystalline structure. It has a white color but can appear blue or colorless. It is a part of the hexagonal crystal system. It can occur as a dihexagonal dipyramidal. Ice has a hardness of about 1.5, a specific gravity of 0.9 (just lower than water at 1.0), and a density of 0.99 grams per cubic centimeter (just lower than water at 1.0). The luster of ice is vitreous to dull. It has a white or no streak and no cleavage. It has a brittle or conchoidal fracture and it mostly has a massive habit. However, individual crystals have a dendritic habit with many complex tree-like branchs.

2.5.2. Structure

Ice is defined as any of the solid states of pure water. Water also exists in solid forms that are not usually referred to as ice. There are a number of clathrate compounds involving water as a solid, like natural gas hydrate. Normally water tends to crystallize as ice I. It belongs to the hexagonal system and finds expression in the myriad forms and shapes of snow and ice crystals and frost figures. Other forms of ice known to exist at higher pressure are ice II, III and IV to VIII. Phase diagrams showing their temperature-pressure stability fields are widely available. A cubic and amorphous ice have been described as forming by vapor condensation at very low temperatures (-120 to -140^{0}C). There seems little doubt that these two forms can occur, but to date neither has been found in naturally occurring frozen soil or rock; the only pure solid phase so far unambiguously reported is hexagonal ice I.

Two structural features are common to all the ice polymorphs:

- The water molecule is intact in each with bond angles and lengths not greatly different from those of the free molecule, H_2O.
- Each water molecule is hydrogen-bonded to four other molecules in an approximately tetrahedral coordination.

In the high-pressure forms some additional non-hydrogen-bonded molecules are found, and the crystal lattices tend to interpenetrate. At low temperatures, the hydrogen atoms tend to become localized.

2.5.3. Physical Properties

Extensive tabulations of thermodynamic, electrical, and other physical properties of ice are readily available. In general it is found that all vary significantly with temperature and pressure. Empirical formulas from which a desired property can be computed are generally included.

A number of properties of interest in the physics and chemistry of frozen ground are insufficiently known. Interfacial phenomena are of great importance in frost heaving and

the development and sustenance of heaving pressures. Considerably more information on the surface energies of ice is needed. Data on the specific free energy (the work required to create a unit area) of the various interfaces present would advance and facilitate the development of a quantitative theory for the frost-heaving pressures. Energies for the vapor-liquid interface, the vapor-solid interface, the liquid-solid interface, the grain-boundary interface and the unfrozen adsorbed water-ice interface are needed. Hobbs gives value for the vapor-liquid interface as 75.7 mJ/m^2 at 0^0 C[41]. Values for the liquid-solid interface range from 7.7 to 14.5 mJ/m^2 at -40^0C. The variation of the liquid-solid interface with temperature is given as 0.1 to 0.35 mJ/m^2 K. At 0^0C, the liquid-solid interface is given as 33 ± 3 mJ/m^2; the vapor-liquid interface is given as 109 ± 3 mJ/m^2, and the grain-boundary interface is given as 65 ± 3 mJ/m^2. No values have yet been determined for the unfrozen adsorbed water-ice interface. Data on the partial specific volumes and partial specific enthalpies of the unfrozen water-ice phase change also are needed. Additional data are also needed on the thermal conductivity of ice at low temperatures. At present, sufficient data for computations and for testing the theory of heat conduction rigorously are not available.

2.5.4. The Classification of Solid Precipitation

The ice elements formed in natural clouds are of four main types: individual ice crystals (or groups of crystals having a common nucleus), snowflakes, ice pellets, and hailstones. The ice crystals grow in an ice-supersaturated atmosphere by the diffusion of water vapour to their growing surfaces, and may exist as individual units of simple geometrical shape, for example hexagonal prismatic columns (prisms) and hexagonal plates or, under suitable conditions, may grow into complex, richly-branched forms. Several of these snow crystals may coagulate to form a snowflake. Graupel (or soft hail) pellets and true hailstones may originate from ice crystals or from frozen drops, but their subsequent growth proceeds predominantly by collision with supercooled cloud droplets. Snow crystals and snowflakes may also collect super-cooled droplets that freeze on impact and endow the crystal surface with a rimed appearance[42].

2.5.5. Aggregation of Ice Crystals to Form Snowflakes

Snowflakes are agglomerates of individual crystals in which the star-shaped dendrites are generally prominent, but in which needle and plate forms may also be found. The growth of these aggregates is governed by the collision and aggregation efficiencies of the crystals and by their relative motions which, because of the aerodynamic problems posed by the complexity and variability of the ice-crystal geometry, are not amenable to quantitative computation.

Clusters composed of a few individual crystals of the same shape may arise as the result of collision and aggregation of the component crystals, or alternatively, several crystals may grow from a single nucleus, frozen droplet, or host crystal. Thus spatial dendrites, which usually grow only at temperatures between -12 and -16°C in mixed clouds, probably develop as the result of the primary crystals collecting supercooled droplets, some of which freeze and grow into crystals. These crystals will not usually grow in the same orientation as the host crystal because freezing droplets tend not to take the same orientation as the substrate if the temperature of the latter is below -10°C. On the other hand, rimed needles may grow as bundles of parallel rods at temperatures above-5°C. At temperatures below -25°C, spatial clusters of prisms arise in convective cirrus clouds from single frozen drops, but only single prisms appear in cirrostratus because of the absence of supercooled droplets.

In natural snowflakes, adhesion is affected partly by interlocking of the crystals and by sintering of the ice at the points of contact, although deposition of water vapour and the freezing of collected supercooled droplets may act as a cement[42].

When two ice particles come into contact, adhesion occurs as the bridge between them grows in order to minimize the surface free energy of the system. When two ice spheres were pushed together to touch at a point, the area of contact grew with time, even when the original force of contact was removed. By measuring the growth rate of the neck between the two spheres, the material was transferred from the convex surfaces of the spheres into the concave neck by surface diffusion. With pure ice, the growth rate of the neck was quite slow; typically it took some hours for the radius of the neck to grow to one-

quarter of the radius of the sphere. Under these conditions, there was no evidence for a liquid-like layer on the ice surfaces, but if the ice contained dissolved salts, or if the surfaces of the spheres became otherwise contaminated, the neck grew much more rapidly by the flow into it of a film of contaminated liquid.

In a layer cloud releasing persistent snow, only the first kilometre or so above the 0°C level may be appreciably supersaturated and contain supercooled droplets, and this may explain why aggregation of snow crystals to form large flakes occurs most readily at temperatures just below 0°C. Accordingly, it would appear that vapour deposition and riming are more effective than sintering in causing the adhesion of crystals, especially in mixed clouds[42].

2.5.6. Properties of Frozen Ground

Much is known about the properties of frozen soils and ice, mainly because of the efforts of engineers working in permafrost areas and in arctic regions, where in many instances the properties of naturally frozen ground can be taken advantage of. In contrast, a road or foundation engineer may have to deal with the problem of seasonal freezing and thawing causing damage by frost heave, collapse upon thawing, and loss of durability; this has resulted in greatly detailed studies of moisture migration during freezing and of other phenomena. The experience gained from dealing with naturally frozen soils is, however, not necessarily transferable to artificially frozen ground; distinct differences in behavior are caused by the following aspects:

The temperature maintained during artificial freezing is lower (-20°C to -160°C) than that commonly found in a natural ground environment (seldom < -15°C). Ice structure and lense formation and orientation depend on the direction of heat flow, the rate of freezing, and other factors. In permafrost, ice lenses are parallel to the ground surface and diminish with depth; in artificially frozen ground, they are parallel to the freezing pipes.

Laboratory freezing may produce an ice structure which is neither equivalent to that found in the same soil for permafrost conditions nor that induced by artificial freezing in the field.

In this study, natural snow is added in the fly ash samples and a uniform distribution is achieved.

2.5.7. Natural Snow Added Samples-A Four Phase Material

Natural snow added fly ash samples, because it contains both unfrozen water and natural snow, becomes a four-phase material. Therefore new definitions must be introduced as follows:

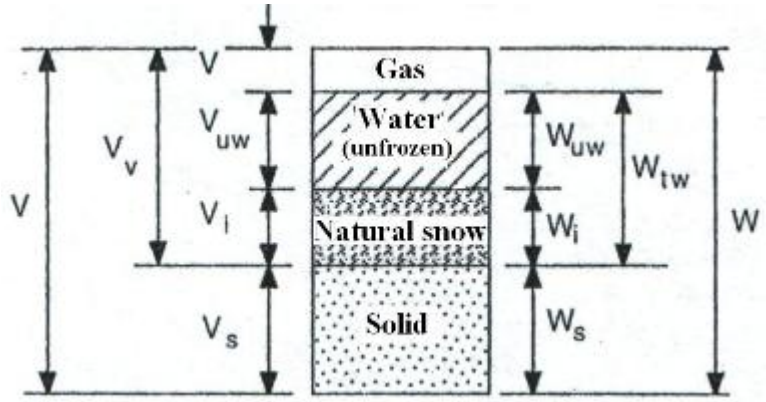

Figure 2.3. The four phases of natural snow added fly ash samples

W_{uw} = weight of unfrozen water

W_i = weight of ice

$$W_{tw} = W_{uw} + W_i \tag{2.4}$$

V_{uw} = volume of unfrozen water

V_i = volume of natural snow

$$w_{uw} = \frac{W_{uw}}{W_s} = \text{unfrozen water content} \tag{2.5}$$

$$w_i = \frac{W_i}{W_s} = \text{natural snow water content} \tag{2.6}$$

$$W_{tw} = w_i + w_{uw} = \text{total water content} \tag{2.7}$$

$$i_{ice} = \frac{W_i}{W_t} = \text{relative iciness} = 1 - \frac{W_{uw}}{w_t} \tag{2.8}$$

Water contents may be expressed in per cent by multiplying the above ratios by 100[43].

2.6. Cold Regions

The cold regions of the world, with a few mountain-top exceptions, are centered around the poles. In the Northern Hemisphere the southern limit of the cold regions extends to about the 40th parallel. Exceptions include the northwest coast of both North America and Europe, where ocean currents such as the Japan current and the Gulf Stream moderate the climate of adjacent land areas. Identification of the cold regions requires both climatological and geographical delineation. Climatologists often use the isotherm based upon the average temperature for the warmest month of the year being above 0^0C but not above 10°C to identify the southern boundary of the cold regions. The 150-mm. and 300-mm. depth of frost penetration or soil freezing has been used by engineers to identify the southern limits of cold regions in the United States. The southern limit of substantial frost penetration is shown in Figure 2.4[44]. A practical definition of cold regions is one based on the design and operation requirements essential to the maintenance of the industrial and social economy. A city or state geographically located in the mid-temperate zone which spends large sums of money to maintain a program of snow removal for operational purposes is located in the cold regions.

Altitude has a marked effect on climate. Vertical temperature gradients up mountain slopes vary from 3°C per 100 m. for dry air to 1.6°C per 100 m. for saturated air. An average value of 1.8°C is commonly used by climatologists when transferring temperature information from low elevations to higher elevations[45]. The extension of the cold regions into the mountain areas of North America and southeast Eurasia is due to the high elevation in these areas.

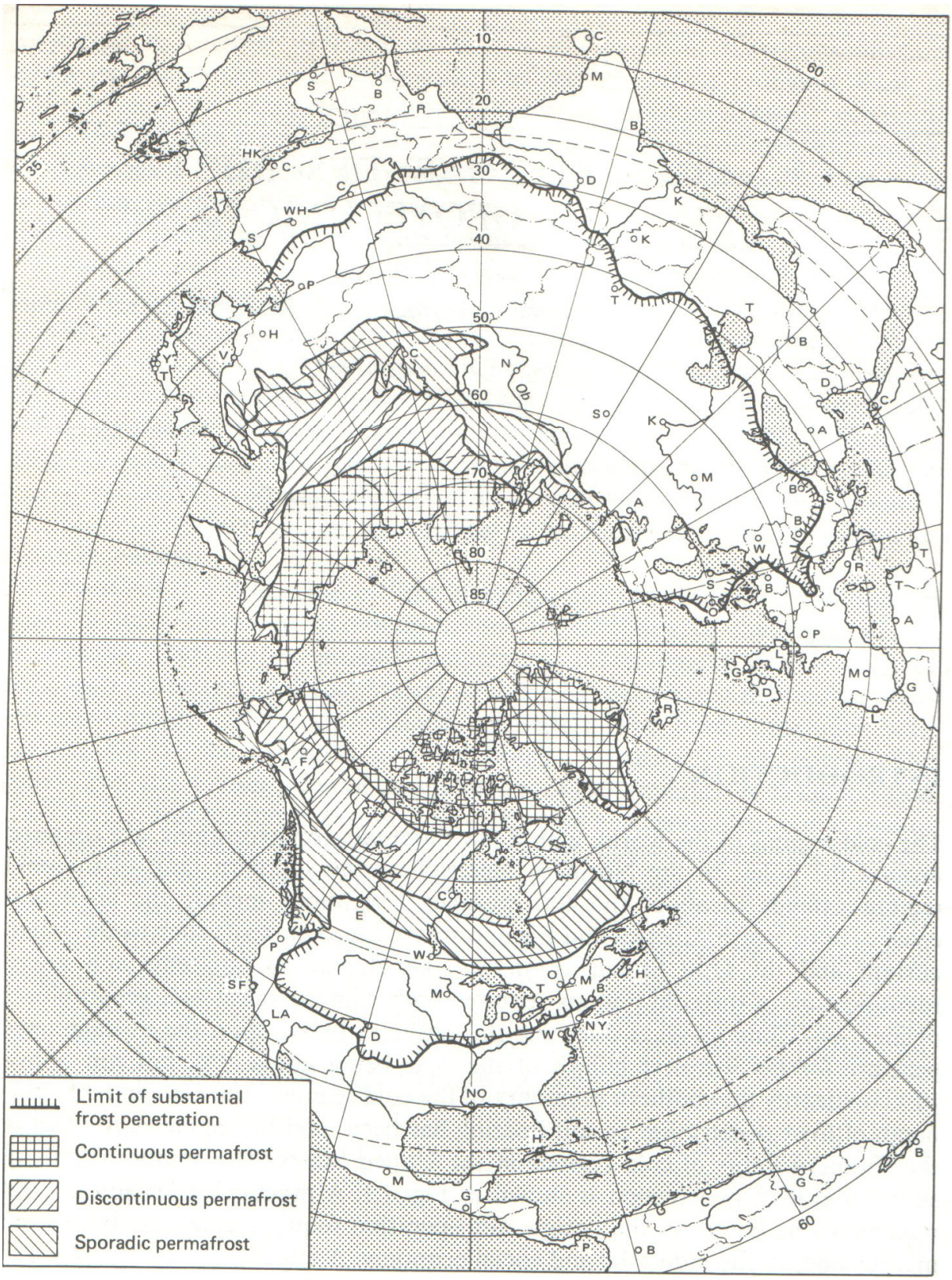

Figure 2.4. Cold regions of the northern hemisphere

Net yearly solar radiation in the polar regions is minimal because of the glancing angle of even the summer sun and further because of atmospheric attenuation: a low sun angle means, that its rays travel an unusually long distance through the atmosphere allowing opportunity for increased diffusion and reflection of the sun's energy back into space. For cold regions in the temperate zone the effect of reduced radiation is primarily a winter phenomenon which decreases in intensity with distance from the poles.

Seasonal and permanently frozen ground are characteristics of cold regions which require special attention from the geotechnical engineer. In areas of seasonal frost, structure loads are taken to depths below the active zone, and use of non-frost susceptible soils minimizes possible trouble from heave and lateral thrust. In permafrost areas structure loads are often transferred to frozen ground with special care taken to maintain the frozen state. It is essential that the engineer have an understanding of the freezing process, thawing, and permafrost. In permafrost regions, knowledge of polygons, wedges, lakes, and pingos gives an understanding of the ground features which may be encountered. The cold environment may create special problems such as buildup of successive ice layers adjacent to a small stream, which requires consideration when it occurs near roads or buildings[44].

2.6.1. Seasonally and Perennially Frozen Ground

2.6.1.1. Seasonally Frozen Ground. Where ice in lakes, rivers, and harbors interferes with navigation, where frost heaving affects roadways and the possible snow load on structures must be considered in design, the engineer is dealing with a cold region environment. Snow and ice control in the United States costs more than 100 million dollars each winter. Regions where frost penetrates the ground to a depth of about 0.3 m. or more at least once in 10 years are part of the cold regions of the world. Because the depth of frost penetration is not regularly reported or easy to measure, the annual freezing index is used as a measure of potential frost penetration. The freezing index is the area above the curve of mean daily temperatures and below the 0°C line, that is the accumulated negative degree-days during a single freezing season. If the mean freezing index is 50 degree-days or more, the criterion for about 0.3 m. of frost penetration is considered to be met. This makes the assessment of the boundary of cold regions independent of the complexities of other factors, such as the

variation of thermal diffusivity among differing soils, the variations of freezing temperature among soils, the water contents, the surface cover, and so forth.

The seasonal frost layer may be described as the top layer of the ground in which the temperature fluctuates above and below 0°C during the year. It corresponds to the active layer above perennially frozen ground (permafrost). In the far north the active layer is as shallow as 150 mm. Farther south, near the discontinuous permafrost zone, the active layer or frost penetration can be as much as 3 m thick[44].

2.6.1.2. Frost Heave. When damp ground of silty texture freezes, there is a migration of moisture to the freezing surface. Masses of ice begin to form along the freezing front, supplied with water by vapor transfer and by liquid migration. If water is available from a lower layer and if the soil has capillarity, ice layers of considerable thickness (1 to 100 mm are common) may develop, displacing the soil to make room for the ice. This is the familiar frost heave that bedevils engineers and others. The accumulation of ice under such circumstances has been known to double the volume of the frozen soil. More commonly, the total amount of heave amounts to anything from 0 to about 150 mm in a season.

2.6.1.3. Perennially Frozen Ground. Ground of any kind which stays colder than the freezing temperature of water throughout several years qualifies as permafrost. If the ground is dry sand, it is permafrost no less than if it were a conglomerate of soil particles cemented by ice. From an engineering standpoint, frozen soil with no ice in it is nearly as tractable as similar soil in temperate or tropic regions. Much frozen ground tends not only to be cemented by ice but also interbedded with large ice masses whose melting could bring about subsidence, erosion, and structural distress.

In general, permafrost is associated with the polar regions as shown in Figure 2.4 and lies as a thick layer (under a thin "active" layer of seasonally melting soil) in the very high latitudes, thinning gradually toward the lower latitudes, until the layer becomes discontinuous, then fragmented, at its southern boundary. On mountain peaks, it is possible to find permafrost near the equator, but permafrost south of the bush country of Alaska, Canada, and Siberia is rare. Even Scandinavia, despite its high latitude (to 72^0N), has permafrost only in isolated areas of high altitude. Yet the continuous layer of frozen subsoil

extends far southward in continental parts of Canada and Siberia (down to 53^0N). Trees can and do grow over frozen soils, but the tree line marks fairly well the southern boundary of the continuous layer of permafrost. It is not far wrong to say that the treeless tundra overlies continuous permafrost and that the forested taiga covers the frayed margins of the permafrost blanket. In the interior of Alaska, in the taiga of the Yukon, Kuskokwim, and Copper River valleys, for instance, the permafrost is marginal. Almost at the melting point, permafrost exists or not in these areas depending on such apparently minor influences as whether the land slopes to the north or to the south, whether the forest cover has remained intact in recent years, or whether the land is swampy.

The point is that if the climate is cold enough for a long period, there will be permafrost. One could even create it by keeping the ground surface cold for a long time, and the resulting frozen soil would be indistinguishable from naturally occurring permafrost[44].

2.6.2. Engineering Considerations

The effects of frozen ground on engineering considerations can be grouped into various categories according to cause or end results. In moderate climates foundations and watermains are protected against the effects of frost by placing them deep enough to avoid frost heave or freezing. The solution for the construction of ice rinks, cold-storage facilities, and liquid-natural-gas storage facilities where continuous subfreezing temperatures may cause deep frost penetration into the soil is usually found by placement of adequate insulation between the cooling system and the subsoil. Pewe has classified the problems of permafrost as those involving thawing of ice-rich permafrost and subsequent subsidence of the surface under unheated structures such as roads and airfields; those involving subsidence under heated structures; those resulting from frost action, generally intensified by poor drainage caused by permafrost; and those involved only with the temperature of permafrost, causing buried sewer, water, and soil lines to freeze[46].

For many years permafrost was a geological curiosity, and the early literature on the subject was dominated by reports of geologists who provided a great deal of information in

these early studies. Today engineers dealing with frozen ground owe a debt to these first investigators, who often pursued their studies with little financial support.

When people from the outside began to enter the arctic and subarctic regions to harvest their natural resources or occupy their strategic locations, they were immediately engaged in reproducing the buildings, communication routes and utilities that had become necessities in their civilization. At this time the properties of frozen ground became an engineering consideration.

Early developers coped with frozen ground as best they could. Their solutions to the problems encountered, while often ingenious, were also often expensive in money and effort, and sometimes the success was very temporary. However, solutions of some sort were found and many of their accomplishments, especially those in the early mining operations are impressive even by today's standards. Unfortunately, exchange of information was limited and many of the mistakes and unsound approaches discovered in one operation were repeated by each succeeding group of engineers. Probably in no other field has so much effort been spent in reinventing the wheel. This problem, while much improved, is still not completely solved. Until quite recently, political considerations have limited exchange of information between some of the major countries working in the arctic. Also, the highly competitive petroleum industry, currently one of the largest sponsors of arctic operations, has historically tended to classify much of the information it discovers as proprietary. It is to be hoped that as more investigators enter the field, the interchange of information will improve.

The approach is to divide the engineering problems related to frozen ground into those caused primarily by the freezing process, thawing and the steady-state frozen condition[44].

2.6.2.1. The Freezing Process. While many of the geotechnical engineering problems of cold regions are mainly associated with the arctic and subarctic, the occurrence of most difficulties caused by the freezing of soil depends only upon sufficient degree-days, below 0^0C to freeze approximately the top meter of the soil. This condition, of course, occurs over a large portion of the temperate zone, as shown in Fig. 2.4.

The most troubling aspect of soil freezing is the phenomenon of frost heaving which has especially plagued highway engineers.

Three conditions are required for frost heaving to occur:

- There must be a cold surface to propagate freezing;
- There must be a source of water to feed the ice growth;
- The physical composition of the soil must promote the migration of the moisture to the freezing front.

When the air temperature drops below freezing, the moisture in the upper soil layer will freeze in place, well distributed through the layer. If the conditions described above exist, the free moisture from below will migrate along the thermal gradient toward the colder surface. When it reaches the frost line it will freeze preferentially to existing ice grains forming small ice lenses. As these lenses grow and expand, the ground surface moves upward. If conditions are uniform, the movement is uniform and for many engineering projects, such as roads and runways, this can be tolerated. However, if the soil profile, drainage pattern, surface cover, or the soil conductivity varies, differential movement will occur producing undesirable effects. The frost-heave problem is most noticeable in the transportation area, where such linear works as highways, railroad beds, and airport runways designed for high-speed traffic are sensitive to differential displacements.

While frost heave is usually thought of as vertical movement, it can produce displacement in any direction. A vertical face exposed to the freezing temperatures by the retaining wall creates a horizontal thermal gradient, resulting in the lateral bulge and a forward rotation of the wall. Non-frost-susceptible soils are usually placed behind retaining walls to avoid this problem.

Structures with exposed foundations are also subject to frost heaving. The differential effects are particularly severe where part of the foundation is heated and part is not. Normally footings are placed below the level of frost penetration. Insulation can be used to prevent this frost heave.

Pole jacking is another frost-heave phenomenon. When poles or pilings are installed in frost-susceptible soil, a bond is developed between the pile and frozen earth at the ground surface, transferring uplift forces to the pole.

Another problem produced by the freezing of soil is a result of shrinkage caused by thermal contraction and desiccation. The polygonal cracking of the ground is reflected through surface pavements and creates additional maintenance difficulties. The movement of water through these cracks tends to increase the rate of stripping in asphalt pavements and can result in the formation of an ice lens below the crack which produces an upward lipping of both edges. In some cases localized thawing of the base occurs when deicing solution enters the cracks[44].

2.6.2.2. Thawing. For convenience, the engineering considerations pertaining to the thawing of soil can be divided into those relating to seasonal frost, or the active layer, and those relating to permafrost.

In the active layer, when the previously described ice lenses that caused the heaving melt and the resulting water escapes, voids are left in the soil. When loads are applied to pavements, which depend on support from the soil, the pavements sag into the depressions and begin to crack and fail. Even when there is no significant ice segregation, pavement distress may develop. As the 0°C thawing isotherm progresses downward below the plowed roadway surface, the meltwater produced cannot penetrate the frozen soil and often it cannot dissipate laterally as snow berms keep the sides of the roadway from thawing quickly. The trapped water induces a high moisture content directly under the pavement reducing the bearing capacity. Until a drainage path is restored, loads must be restricted to prevent disintegration of the road surface.

When seasonal ice melts under piles, poles, or spread footings, it is rare for the member to settle back to its original elevation. Instead the surrounding soil may tend to fill (at least partially) the space formerly occupied by the ice; this, combined with skin friction, will restrict downward movement. This cycle of heaving and blocked restoration can be repeated yearly until failure results.

When ice is well distributed and its volume is less than the pore volume of the soil, the consolidation and resultant settlement are negligible. As the ice content increases, so does the potential for settlement. Buildings which introduce a concentrated heat source, like a dwelling are particularly vulnerable to settlement.

Thermal equilibrium can be changed by changing the existing ground cover. Unless the new construction provides a heat balance that matches that of the original surface, the permafrost level will change. In high-arctic roadway embankments, gravel 1 to 2 m. thick will approximate the natural cover. In the subarctic, where the permafrost temperature approaches 0^0C, the height of fill required to maintain equilibrium becomes prohibitive. Roadway settlements can be expected when normal fills are placed over ice-rich permafrost. Vigorous maintenance can keep a gravel surface serviceable while a new thermal equilibrium is reached.

In addition to settlement, the general stability of soil can be lowered by thawing. Not only is the binding force of the ice removed, but the released moisture may act both as a "lubricant" and under some conditions as a transport agent in promoting soil flow. Slope stability should be investigated whenever an engineering project changes the thermal regime of a permafrost region. Thawing permafrost can have effects on drainage patterns which must be considered. Water which cannot penetrate the frozen ground will follow porous paths thawed in the permafrost. Buried pipes transporting warm liquids can create new drainage channels below ground, and vehicle traffic can thaw out surface channels. That these changes can direct water to new locations must be recognized. In addition to allowing the passage of water, thawing also permits the movement of the soil particles, and the combination of these two conditions may produce serious erosion with its resultant problems.

2.6.3. Construction in Cold Weather Regions

Cold weather can affect embankment construction when temperatures dip below freezing. Concrete and soil are affected by cold weather because they both contain water. Cold weather regions are defined as those that typically experience subfreezing temperatures for periods of several weeks to several months each year.

Some soils are susceptible to frost heave during prolonged periods of subfreezing temperatures. Frost heave may occur if there is a continual supply of moisture being drawn up by capillary action from the groundwater table. The forces created from the continued growth of ice lenses in the soil can be large enough to give damage to the pavement. This can lead to differential movements if the heave is not uniform and it can develop cracks in the pavement. Additional damage may occur when the ice lenses begin to thaw. The soil typically thaws from the ground surface down. As the ice in the soil melts, the water can not drain into the underlying ground that is still frozen. The soil may then settle owing to the increase in the water content and the loss of support of the now nonexistence ice lenses. This settlement typically is nonuniform and leads to differential settlements and damage the pavement.

Soils consisting primarily of silt-sized particles are the most susceptible to frost action. It is actually the size of the pore spaces in the soil that controls the susceptibility to frost heave[3]. Soil deposits that consist of up to 25% clay particles can exhibit a strong susceptibility to frost action if their porosity, and thus permeability, are relatively high[4]. Although clay soils can exhibit high capillary rises, their permeability is relatively low and, therefore, they may not move the water fast enough to create significant ice lenses during a single freezing event. Conversely, silty soils can generate relatively high capillary rises in a relatively short time. This combination can lead to the formation of large ice lenses. Table 2.6 is a ranking of the susceptibility of different soils to frost heave[4].

Table 2.6. Frost heave susceptibility of various soil types

Frost heave susceptibility	Soil type
None	Gravel and Sand
Moderate	“Fine” Clay (>40% Clay)
Strong	Silt and “Coarse” Clay (clay content = 15-25%)

Concrete is also affected by cold weather during construction. As temperatures decrease, the rate at which concrete gains strength also decreases. The cement in the concrete must react with the water in the concrete in order to build strength. For this reason, concrete should never be placed directly on frozen ground. All snow, ice and frost

should be removed from the underlying strata. If necessary, the subbase should be covered and heated until all of the frost is melted.

It is common to add air-entraining admixtures to the concrete mix to increase its durability against both frost action and the application of deicers on the rigid pavement. Air-entraining admixtures cause small air bubbles to form inside the cementitious matrix. This procedure is known as air-entrainment. For air-entrained concrete to be effective, it is recommended that 30 days of air drying take place after the concrete has cured for a minimum of 3 to 5 days before the use of deicers. The curing period consists of maintaining the moisture content in the concrete and keeping the temperature of the concrete between 4.4^0C and 32.2^0C[5].

If temperatures are below freezing, both the subbase and the concrete need to be insulated to prevent freezing in rigid pavements. Common insulating materials include fiberglass-filled blankets or straw. The insulation material should not be removed from the subbase until the concrete is on-site and ready to be placed.

Another construction constraint during subfreezing temperatures is achieving proper compaction with frozen clayey and silty soils. Soils in this condition are difficult to work with and will lose strength once they thaw. Fills consisting of sand and gravel mixtures are not as difficult to compact when they are frozen and although importing soil adds to the cost of the project, they become a reliable substitute to frozen clayey and silty soils[6].

2.6.3.1. Thermal Design of Roads

Thermal design of roads refer to thaw-related effects in initially frozen ground, but the same relations developed are valid for frost effects in unfrozen ground provided the thermal properties are interchanged.

For many engineering applications, allowing deep thaw penetration during summer (or frost penetration in winter) into subgrade soils beneath roads may prove intolerable because of the excessive settlement or heaving that may occur. The resulting damage and

subsequent maintenance may prove considerably more costly than providing some measure of thermal protection for the subgrade.
This is often done in one of three ways:

- An increased thickness of granular fill is used to limit thaw penetration and dissipate stresses resulting from wheel loads in the thawing subgrade.
- A layer of organic insulation such as wood chips, brush, or sawdust is introduced within the fill pad.
- A layer of synthetic insulation, e.g., rigid polystyrene board, is installed at some elevation within the granular pad.

Increasing granular fill may prove very expensive in many cases and often does not prevent thaw penetration into the native soils. Organic or natural insulating layers suffer from the disadvantage that they are likely to become waterlogged in time, with consequent deterioration in thermal properties. Synthetic insulations such as polystyrene are water-resistant and relatively inexpensive. These materials have been used successfully on many projects in both temperate and arctic latitudes.

The design of roads involving insulation must satisfy several criteria, including structural protection of the insulation, the prevention of excessive settlements or shear failure within any thawed subgrade layer, the suitability of the granular fill material for base and surface courses, and the overall thermal design. Attention must be confined to the last of these criteria, concerning the geothermal aspects. The configuration of interest involves three materials of different thermal properties, i.e., granular fill, insulation, and the underlying permafrost[44].

2.6.4. Pavement Structures For Cold Regions

Pavement design in seasonal frost as well as in permafrost areas depends on the types of subgrade soil. The main concern is the limitation of the surface deformation resulting from frost action during the freezing period or the adequacy of bearing capacity during the seasonal thawing period. In permafrost areas, additional consideration must be given to the

influence of construction on the existing ground thermal balance. Changes in the ground thermal regime may cause degradation of the permafrost, resulting in total or differential settlement and reduction in the bearing capacity of the pavement structure. Thus when pavement design is considered for permafrost areas, it is of utmost importance to recognize the significant influence of thermal variations on the soil and pavement properties. In addition, identification of frozen-ground features and susceptibility of the soil to thermal disturbances are critical design factors.

2.6.4.1. Pavement Design Under Seasonal Frost Action. Pavement structures located in cold regions are subjected to frost heaving of subgrade soils as a result of ice segregation during freezing, a reduction in bearing capacity during the melting periods and cracking resulting from shrinkage of the pavement and base under the extreme low temperatures. Other related detrimental effects include development of surface roughness, restriction of drainage by the frozen substrata, and the influence of fatigue damage under repetitive stressing as a result of changes in stiffness characteristics of the subgrade soil, base course, and pavement surface. The potential for frost damage to the pavement structure depends on the presence of frost-susceptible soils, freezing and thawing temperatures in the soil, and the availability of water to the freezing soil. For uniform conditions, heaving will be uniform, and the pavement surface will remain relatively smooth with no effect on pavement serviceability as long as the frozen and heaved condition lasts. For irregular conditions, differential heaving will occur, causing surface roughness and possible cracking at points of severe distortion. Permanent roughness will develop from the cumulative effects of traffic loads during the period of frost heave.

Thawing and reduction in pavement bearing capacity may occur during relatively mild winters and during the spring. The spring thaw, proceeding almost entirely from the surface downward, leads to extremely poor drainage conditions. Frozen soil below blocks downward drainage. Lateral drainage may be restricted due to still frozen shoulders resulting from the insulating effect of snow and or different thermal conductivity and surface reflectivity characteristics. Lack of drainage combined with excess water in the base course and thawed subgrade will greatly reduce the bearing capacity. Thaw-consolidation theory helps to explain the phenomenon occurring in the base course and

subgrade soils. The magnitude of the reduced subgrade strength becomes a major part of the design process.

Several methods available for reducing thaw penetration beneath highway pavements in permafrost areas include the placement of non-frost-susceptible base materials, use of insulating layers as part of the subbase materials, and/or painting the pavement surface white. The required thickness of non-frost-susceptible materials is based on the seasonal thaw penetration. This approach is effective when sufficient non-frost-susceptible materials are available. It is often used in combination with the other alternatives. The insulation may include foamed-in-place polyurethane or factory-produced polystyrene boards. White painted pavement surfaces have a high reflectivity, which reduces the amount of shortwave radiation absorbed at the pavement surface, giving lower surface temperatures. Experimental data indicated that the total thickness required for confinement of thaw penetration within a non-frost-susceptible base course can be reduced by as much as 35 per cent[47]. The effects of traffic and maintenance procedures govern the loss in effectiveness of the painted surface in reducing thaw penetration. About 26 per cent loss in reflectivity was observed for one season at the Thule Air Force Base[47].

Two types of pavement cracking are associated with frost or low temperatures. The first, with random orientation and spacing, is caused by differential frost heaving and develops at points of severe distortion. It occurs in both flexible and rigid pavements. The second form of cracking results from thermal contraction and appears as transverse cracks penetrating the entire pavement structure and extending into the shoulders of the road. This type of crack occurs at freezing temperatures when the entire pavement structure contracts as the temperature drops. When the tensile strength is exceeded, the crack develops. Problems arise when water enters the cracks, forming an ice lens, which produces an upward lip at the crack edges, or when deicing solution enters the cracks and causes localized thawing of the base, resulting in a pavement depression adjacent to the crack.

2.7. Background

Previous studies conducted by the researchers related to fly ash hydration, microfabric examinations, resistance of samples to rapid freezing and thawing, hydraulic

conductivity testing, radioisotope activity comparison and leachate analysis of cementitious products are presented in this section.

Ezzaine et al. prepared set of specimens made with 0%, 10%, 20%, 30% and 40% of natural pozzolan replacement and cured under constant curing temperature of 20, 40 and 60^0C with saturated humidity and a second set incorporating only 20% of natural pozzolan exposed to elevated temperatures for 1, 3 and 7 days and cured in saturated environment under a temperature of 20^0C. The introduction of the pozzolan enhanced the ultimate compressive strengths and increased the activation energy which indicated the slow reactivity. By using the equivalent time method, the strength at 28 and 90 days of the second set mortar is estimated. This method satisfactorily predicted the strength of concrete cured at any temperature history[48].

Ghrici et al. prepared mortar prisms in which portland cement was replaced by up to 20% limestone filler and 30% natural pozzolana were tested in flexure and compressive strength at 2, 7, 28 and 90 days. Some samples were tested under sulfate and acid solutions and for chloride ions permeability. Results showed that the use of ternary blended cement improved the early age and the longterm compressive and flexural strengths. Durability was also enhanced as better sulfate, acid and chloride ions penetration resistances were proved[49].

Mouli et al. tested six concrete mixtures: one specimen with portland cement (control) and five mixtures with 10%, 20%, 30%, 40%, and 50% of replacement of cement by pozzolan were tested in order to gain more knowledge on the efficiency of pozzolan concrete. Crushed pozzolan was used as lightweight aggregate and natural sand was used in all mixes to produce a lightweight aggregate concrete. Fresh concrete mixtures were tested for workability and density. While for the hardened concrete specimens, compressive strength, splitting tensile strength, and flexural strength were determined after 3, 7, 28, 90 and 365 days. The results of this study suggested that the use of pozzolan at 20% of the weight of cement produced the highest strength increase of the mixtures that were tested[50].

Sahu et al. collected samples extracted from coal combustion by-product storage yards and analyzed using X-ray diffraction and scanning electron microscopy. The analytical results showed the formation of thaumasite, ettringite and an intermediate phase with varying chemical composition of calcium, aluminum, silicon and sulfur. Also most of the thaumasite formed in the system is growing directly from the gypsum matrix and growing in the void space. Thaumasite grown in the system occur as short stubby crystals. Ettringite crystals, on the other hand, grow in isolated pockets when the conditions of a saturated lime environment are available[51].

Nisnevich et al. reported the results of experiments to develop environmentally and economically friendly structural lightweight concretes utilizing coal ashes and other waste materials. The products complied with national and international regulations setting limits on the activity concentration of natural radioisotopes in building products. The utilization reduced the potential damage to the environment caused by the radioactivity in the coal combustion by-products stored in piles and ponds near the power stations prior to their disposal. The study dealed with the radiological characteristics of coal ashes and lightweight concretes based on these ashes[52].

Yu et al. monitored radon emanation rates from 48 concrete blocks throughout a period in excess of 1 year. The blocks had been produced for three distinct mixes of materials, mix A with 25% by weight substitution of type A pulverized fuel ash, mix B with 25% by weight substitution of type B pulverized fuel ash and mix C without pulverized fuel ash. Each mix was represented by four sets of concrete blocks with curing periods of 1, 3, 7 and 28 days. Every set consisted of four blocks each with the same composition and curing period. From the results, rates of change of radon emanation had been identified for the first month following curing and for the period following the first month. The different emanation rates have been linked to the role of the superficial and inner pores of the concrete. The radon emanation rate decreased with the age of the blocks for curing periods of 1, 3 and 7 days, but increased for a curing period of 28 days. The results are rationalized in terms of the gradual dehydration of concrete as it ages. The patterns were similar for the different mixes, although the exact effect of pulverized fuel ash upon radon emanation rates remained unresolved[53].

Kovler et al. focused on studying the influence of fly ash on radon exhalation rate from cementitious materials. The tests were carried out on cement paste specimens with different fly ash contents. It was found that despite the higher 226Ra content in fly ash (more than 3 times, compared with Portland cement) the radon emanation is significantly lower in fly ash (7.65% for cement vs. 0.52% only for FA)[54].

Wang et al. conducted a set of experiments on concrete from pure cement and cement with fly ash to assess the effects of several fly ashes on the performances of freezing and thawing test. The freeze-thaw tests indicated that all fly ash concrete has statistically equal or less weight loss than the pure cement concrete[55].

Liu et al. tested various methods designed to improve the freeze-thaw property of the compacted fly ash bricks, including using higher compaction pressure and optimum fly ash to water ratio, adding a small amount of fiber to the fly ash before compaction, adding some cement or lime to the fly ash before compaction, using certain liquid sealents to coat the bricks, using a higher compaction pressure to make stronger bricks, lengthening the curing time in order to make stronger bricks, use of a split mold to make better bricks and use of an air-entrainment agent to improve the freeze thaw property of the bricks. The tests showed that some of the methods that further improve the compressive strength of the brick do not result in an improvement in the freeze-thaw property. The air entrainment method appeared to be the most effective and practical in all the methods tested. It enabled the bricks to pass the 50 cycle freeze-thaw test without damage[56].

Yazıcı replaced cement with fly ash in various proportions from 30% to 60% with the incorporation of 10% silica fume and investigated the freeze-thaw properties of self compacting concrete mixtures. Test results indicated that fly ash replacement and silica fume addition to the system positively affected both the fresh and hardened properties of the high performance high volume fly ash self compacting concrete. Although there is a little cement content, these mixtures had good mechanical properties and freeze-thaw resistance[57].

Heebink et al. collected fly ash stabilized soil samples in core tubes and stored sealed for at least 7 days. Each stabilized composite was subjected to heavy metal leaching tests.

This study confirmed the outcomes of other similar studies that fly ash if used properly is not a hazard to the environment when used for soil stabilization at the addition concentrations used in the sites[58].

Sushil et al. investigated the heavy metal content of fly ash and bottom ash from three major power plants in North India, using atomic absorption spectrometry. The ashes were analysed for the presence of Cr, Mn, Pb, Zn, Cu, Ni and Co and detectable levels of all were found in both fly ash and bottom ash. The concentrations of Cr and Zn were highest while Co concentration was less. The sites did not use ash pond lining in the construction of the ash ponds, hence leaching of the heavy metals was possible. The test results showed that all elements were present within detectable limits[59].

Erbe et al. conducted field studies at two sites in which coal combustion by-products were used to construct highway embankments to assess ground water quality impacts. The purpose of the study was to determine the potential for leachate to form within the pore water in the constructed embankments, and to evaluate whether the leachate is degrading the ground water quality. Pore and groundwater samples collected at the site had been analyzed for dissolved trace elements. Water quality results indicated that elevated concentrations of several trace elements (arsenic and manganese) and major ions (calcium, magnesium, chloride and sulfate) were found in fly ash pore water, indicating that leachate is forming within the fly ash fill. The data also indicated that the constituents are being attenuated in underlying soils and ground water beneath the embankments. The water quality test results indicated that the use of fly ash for highway embankments can adequately protect ground water quality[60].

Kaniraj et al. conducted detailed testing of fly ash samples regarding geotechnical utilization from a thermal power station in India. The morphology of the fly ash particles was studied by scanning electron microscopy and X-ray diffraction. The testing program also included the classification, compaction, consolidation and the falling head permeability test. The paper explained the details and the results of the tests, especially those of the consolidation and permeability behaviors. The results showed that the coeffcients of permeability and consolidation of the compacted fly ash were comparable to those of nonplastic silts. The values of coefficient of permeability were in the same range

as those of non-plastic silts. The compacted fly ash deposits, therefore, would be moderately permeable. The coefficient of permeability of fly ashes should be determined directly from permeability tests and not back-calculated from consolidation tests. Comparison of silty soils with the silt-like fly ash has been made through illustrative examples. The results showed that, as a foundation material, fly ash has a lesser bearing capacity than silt; fly ash exerts lower lateral thrust on retaining walls than silts; and embankments on soft soils have a higher factor of safety and settle less when they are made of fly ash than of silt[61].

Kalinski et al. performed a study to assess the effect of water content, cement content, curing time and compaction effort on the hydraulic conductivity of compacted cement stabilized fly ash samples. Test results showed that when compacting relatively dry mixtures (w <20%), k is independent of compaction effort, and is on the order of 10^{-5} cm/s. When compacting between water content of 20% and optimum water content, compaction effort affected k and at a given water content, k decreased by about an order of magnitude when increasing from standard to modified proctor effort. When wet of optimum, k is on the order of 10^{-6} cm/s regardless of compaction effort or water content. With respect to curing time, extended curing time had relatively little effect on k within a 60 day time frame. The hydraulic conductivities for the specimens measured during the study are suitable for geotechnical applications such as earth dams and highway base courses[62].

Kim et al. prepared three mixtures of fly and bottom ash with different mixture ratios (50, 75, and 100 fly ash content by weight) for testing. The hydraulic conductivity of the ash mixtures was measured by falling head tests using a rigid-wall compaction mold permeameter. The hydraulic conductivity of the compacted ash mixtures were found to decrease slightly with increasing fly ash content. This is due to the increasing specific surface with increasing fines content, which generates more resistance to water flow through voids between particles. The overall range of the values was similar to that of a fine sand/silt mixture or silt. Test results indicated that ash mixtures compare favorably with conventional granular materials[63].

Table 2.7. Hydraulic conductivity values of compacted fly ashes

Reference	Material	Hydraulic conductivity (cm/s)
Kaniraj et al. (2004)	Fly Ash	$5.96.10^{-6}$
Kalinski et al. (2006)	Fly Ash Cement content = 0% Cement content = 10% Cement content = 15%	 $3.59.10^{-5}$ $2.76.10^{-5}$ $1.39.10^{-5}$
Kim et al. (2005)	Fly Ash	$6.00.10^{-6}$

Wang et al. investigated microscopic study of concrete prepared from cement and fly ash which covers coal fly ash and biomass fly ash. Scanning electron microscopy, energy dipersive X-ray and environmental scanning electron microscopy analysis showed that both coal and biomass fly ash particles undergo significant changes of morphology and chemical compositions in concrete due to pozzolanic reaction, although biomass fly ash differs substantially from coal fly ash in its fuel resources[64].

Antiohos et al. examined whether and to what extent reactive silica of fly ashes affects the mechanisms occuring during their hydration. The work described a laboratory scale study on the influence of active silica of two high-lime fly ashes on their behavior during hydration. Volumes up to 30% of Greek high-calcium fly ashes, diversified both on their reactive silica content and silicon/calcium oxides ratio, were used to prepare mixtures with Portland cement. The new blends were examined in terms of compressive strength, remaining calcium hydroxide, generation of hydration products and microstructural development. It was found that soluble silica of fly ashes holds a predominant role especially after the first month of the hardening process and silica is increasingly dissolved in the matrix forming additional cementitious compounds with binding properties, principally a second generation CSH. The rate however, that fly ashes react in Fly ash-Cement systems seems to be independent of their active silica content, indicating that additional factors such as glass content and fineness should be taken into account for predicting the contribution of fly ashes in the final performance of pozzolanic cementitious systems[65].

3. EXPERIMENTAL STUDY

3.1. Soma Thermal Power Plant

Soma thermal power plant is located 2 kilometers out of Soma. Soma is a town in the province of Manisa that is a city located in the Aegean region of Turkey. The plant is formed of eight units, six of them with a capacity of 165 MW and the two with 22 MW. The overall annual electricity production is 7.5 x 10^6 MWh. The annual coal consumption of units one-four is 1.1 x 10^6 tons, that of units 5-6 is 1.6 x 10^6 tons, and that of units seven-eight is 150 thousand tons. The seventh and eighth are the oldest units, which were commissioned in 1957. The other units were commissioned in between 1983-1992.

Lignite coal is used to generate electricity in Soma thermal power plant. After coal is mined, it is transported to power plants by trucks. A conveyor belt carries the coal to a pulverizer, where it is ground to the fineness of talcum powder. The powdered coal is then blown into a combustion chamber of a boiler, where it is burned at around 1000±50ºC. Surrounding the walls of the boiler room are pipes filled with water. Because of the intense heat, the water vaporizes into superheated high-pressure steam. The steam passes through a turbine connected to a generator. The incoming steam causes the turbine to rotate at high speeds, creating a magnetic field inside wound wire coils in the generator and pushes an electric current through the wire coils out of the power plant through transmission lines. After the steam passes through the turbine chamber, it is cooled down in cooling towers and it again becomes part of the water/steam cycle. Several by-products, including solids and gases, are created in the electricity generation process. A substance called "clinker" or bottom ash (glassy particles of melted coal ash) settles at the base of the furnace. This material is periodically removed and disposed of. Fly ash, the noncombustible minerals found in coal (including ash, dust, soot, and cinders) travels upward with gaseous by-products. Fly ash can be captured in an electrostatic precipitator and then transported by pipes to a holding pond, where it settles. Gaseous by-products include carbon dioxide (CO_2), sulfur oxides (SO_x), and nitrogen oxides (NO_x). Sulfur oxides can be controlled by the installation of scrubbers at coal-fired power plants.

The lignite coal burned in all units have a minimum calorific value of 200 kcal/N. The fly ash is collected by electrostatic precipitators and handled both by dry and wet methods. The residues collected from units one-six are hauled to the lagoons commissioned in Yırca and Ayıtlı villages with 9 x 10 m^3 and 70 x 10^6 m^3 volumetric capacities respectively. The residues obtained from units seven and eight are deposited to the site next to the power plant. The related statistical figures are given in Table 3.1.[66].

Table 3.1. The statistical figures related with the coal combustion, calorific value and fly ash production of the Soma thermal power plant.

Units	Coal Consumption (tons/day)	Calorific Value (kcal/N)	Fly Ash Production (%)	Precipitator Efficiency (%)
1-2-3-4	4000	2200	37-43	98-99
5-6	6000	1550	52-64	99
7-8	500	3325	25	97

In Table 3.1, the fly ash production is defined in terms of percentage of coal consumption. The precipitator efficiency defines the amount of fly ash collected by the precipitator in per cent of fly ash production.

In eight out of 15 thermal power plants in Turkey, coal is used for energy production. In only one of these plants anthracite is used. In the rest of the plants lignite is used. Therefore, although the mineralogical properties of the fly ash obtained from different power plants may be somehow similar, the physical and chemical properties may vary depending on the operational conditions like the degree of coal pulverization, the firing temperature and handling and storage methods in these plants. The chemical analysis performed on spontaneously obtained samples from some of these plants are given in Table 3.2.[66].

Table 3.2. The chemical analysis results on samples obtained from some of the thermal power plants commissioned in Turkey.

	Afşin	Yenikoy	Kangal	Soma	Tunçbilek
SiO_2 (%)	30.78	17.54	38.67	49.00	53.00
Al_2O_3 (%)	10.41	9.94	16.63	24.22	19.63
Fe_2O_3 (%)	10.81	0.37	6.41	7.78	10.74
CaO (%)	32.59	33.10	23.63	11.60	12.02
MgO (%)	4.06	2.46	3.90	0.49	2.04
SO_3 (%)	12.23	33.75	6.00	4.35	0.57
Loss on Ignition (%)	0.27	0.45	2.54	2.08	1.15
ASTM Classification	TypeC	-	TypeC	TypeC	Type C

Afsin, Kangal, Soma and Tunçbilek fly ash may all be classified as Type C fly ash with respect to ASTM C 618, however, Yenikoy fly ash may not be classified by ASTM standards due to low SiO_2+Fe_2O_3+Al_2O_3 content. On the other hand, the $S0_3$ contents of Afsin, Yenikoy and Kangal fly ash are higher than the limits specified. According to the figures given in Table 3.2, the most suitable fly ash for use in construction industry is Soma and Tuncbilek fly ash that possesses cementitious property without necessity of desulphurization treatment. All statistical figures are obtained from EÜAŞ, Ankara.

3.2. Materials Used

3.2.1. Fly Ash

The fly ash is supplied from Soma Thermal Power Plant, located in the Aegean region of Turkey. Locally produced low calory lignite coal is used in this power plant. Approximately 30 per cent by weight of this coal turns into ash upon burning. Soma fly ash is self-cementitious, and four million tons are produced annually. The fly ash is mixed with water and disposed into an ash dam. Upon collection directly from the hopper at the power plant, the fly ash was sealed in bags and transported to the Karl Terzaghi Soil Mechanics and Geotechnical Engineering laboratory. Its exposure to air, moisture and light is prevented. The physical and chemical properties of fly ash was determined in AkçanSa cement factory laboratories in Büyükçekmece, İstanbul and is presented in Table 3.3.

Table 3.3. Physical and chemical characteristics of fly ash

Analysis Report

Chemical analysis	SiO_2 (%)	Al_2O_3 (%)	Fe_2O_3 (%)	CaO (%)	MgO (%)	SO_3 (%)	Na_2O (%)	K_2O (%)	Cl^- (%)	Loss on Ignition (%)	Specific Weight	Specific Surface Area(cm^2/g)
Fly Ash (FA)	36.94	17.2	4.76	33.22	1.36	3.82	0.34	1.82	0.0045	0.19	2.56	3206

Physical analysis	Fineness (%)	45 mm	90 mm	200 mm
Fly Ash (FA)		23.3	9.93	2.74

3.2.2. Snow

Natural snow is collected in the winter season from the university's garden and stored in special bags in a deepfreezer at -25 ^{0}C through the test period.

3.3. Samples

3.3.1. Sample Preparation

The moisture content-dry density relationship of fly ash was determined as described in ASTM D698[67]. The optimum water content and maximum dry density of Soma fly ash are 19,05%, and 14,92 kN/m^3, respectively.

During winter, natural snow was collected and stored in a deep freezer. Samples were prepared at optimum moisture content for the control group, and by adding 10 per cent natural snow by weight over optimum moisture content for the investigated group. For optimization, snow percentages of five to 30 per cent were studied. Adding 10 per cent natural snow over the optimum moisture content by weight gave the highest unconfined compressive strength values. Also at higher percentages of snow addition, compaction became difficult and lower compressive strength values were obtained.

The scope of adding natural snow was to provide extra water for hydration after the samples were molded into shape. This water was introduced by the thawing of snow. Also it was proposed that after the thawing period snow addition would increase the compressive

strength and improve the environmental properties by introducing small voids into the samples.

Miniature Harvard Compaction apparatus was used for the compaction of the samples. The compaction mold diameter was 3.6 cm and height was 7.6 cm. A miniature hammer was designed to apply standard compaction energy (600 kN-m/m^3). The fly ash was placed into the molds in three layers. The sample preparation equipments were cooled to -15^{0}C to prevent melting of snow during the sample preparation stage.

For hydraulic conductivity tests the specimens were compacted using standard proctor compaction effort and standart compaction molds[67]. After compaction, the specimens were sealed with plastic film and aluminum sheets and allowed to cure for 28 and 90 days. Three repetitions were made for each result.

3.3.2. Sample Curing

The compacted samples were extruded from the molds and were wrapped in plastic film, and then in aluminum sheets, and were stored in the curing room for one, seven, 14, 28, and 90 days at 21°C and 75 per cent humidity. At the end of the curing period, it was seen that the samples had lost only a small amount of moisture varying from 0.5 to 0.8 per cent.

3.4. Sample Testing

Unconfined compression, splitting tensile strength, hydraulic conductivity, pH, radioisotope activity comparison, temperature measurements during the curing period, thermographic measurements, microstructural analysis (XRD and ESEM studies), freeze-thaw analysis, thermal conductivity analysis, erosion pinhole test, heavy metal lechate analysis and length change determination tests were performed on the samples.

3.4.1. Unconfined Compression Testing

This test method consists of applying a compressive axial load to molded cylinders or cores at a rate which is within a prescribed range until failure occurs. The compressive strength of the specimen is calculated by dividing the maximum load attained during the test by the cross-sectional area of the specimen.

The values obtained will depend on the size and shape of the specimen, batching, mixing procedures, the methods of sampling, molding, and fabrication and the age, temperature, and moisture conditions during curing[68].

The unconfined compression test may be either strain-controlled or stress-controlled. The strain-controlled test is almost universally used, as it is simply a matter of attaching the proper gear ratio to a motor to control the rate of advance of a loading head. The test has been found to be somewhat sensitive to the rate of strain, but a strain rate between $^{1}/_{2}$ and two per cent/min (e.g., a 70-mm specimen at a one per cent strain rate would be compressed at the rate of 0.70 mm/min; 10 min = seven mm) appears to yield satisfactory results[69].

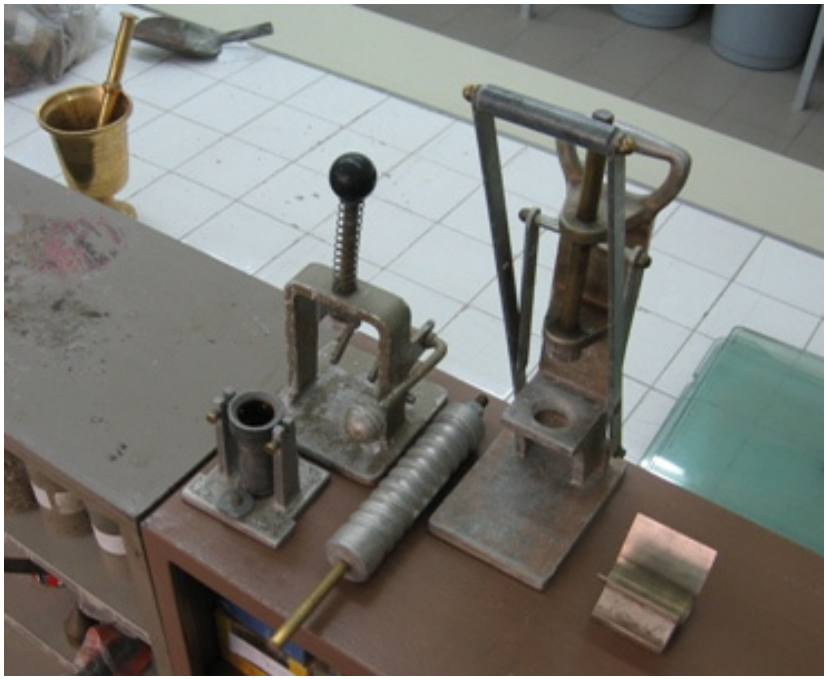

Figure 3.1. Miniature harvard compaction apparatus

Miniature Harvard Compaction apparatus shown in Figure 3.1 was used for the compaction of the samples. The compaction mold diameter was 3.6 cm and height was 7.6 cm. A miniature hammer was designed to apply standard compaction energy (600 kN-m/m^3). The fly ash was placed into the molds in three layers. The compacted samples were extruded from the molds and were wrapped in plastic film, and then in aluminum sheets, and were stored in the curing room for one, seven, 14, 28, and 90 days at 21°C and 75 per cent humidity. A total number of 80 samples were prepared. Eight repetitions were made for each data point.

3.4.2. Splitting Tensile Strength Testing

By definition the tensile strength is obtained by the direct uniaxial tensile test. But the tensile test is difficult and expensive for routine applications. The splitting tensile test appears to offer a desirable alternative, because it is much simpler and inexpensive. Furthermore, engineers involved in rock mechanics design usually deal with complicated stress fields, including various combinations of compressive and tensile stress fields. Under such conditions, the tensile strength should be obtained with the presence of compressive stresses to be representative of the field conditions. The splitting tensile strength test is one of the simplest tests in which such stress fields occur. Since it is widely used in practice, a uniform test method is needed for data to be comparable. A uniform test is also needed to insure positively that the disk specimens break diametrally due to tensile pulling along the loading diameter[16].

The test specimen shall be a circular disk with a thickness-to-diameter ratio (t/D) between 0.2 and 0.75. The diameter of the specimen shall be at least 10 times greater than the largest mineral grain constituent.

Miniature Harvard Compaction apparatus was used for the compaction of the samples. The compaction mold diameter was 3.6 cm and height was 7.6 cm. A miniature hammer was designed to apply standard compaction energy (600 kN-m/m^3). The fly ash was placed into the molds in three layers. The compacted samples were extruded from the molds and were wrapped in plastic film, and then in aluminum sheets, and were stored in

the curing room for one, seven, 14, 28, and 90 days at 21°C and 75 per cent humidity. After the curing period finishes, the samples were cut to a thickness-to-diameter ratio of 0.5. A total number of 80 samples were prepared. Eight repetitions were made for each data point.

3.4.3. Hydraulic Conductivity Testing

The coefficient of permeability is a constant of proportionality relating to the ease with which a fluid passes through a porous medium. Two general laboratory methods are available for determining the coefficient of permeability of a soil directly. These are the constant-head method and the falling-head method. Both methods use Darcy's law[69].

The falling-head method is usually used for cohesive materials (where the computed k is on the order of 10^{-4} cm/s and smaller). With a small k it may take several days to perform the constant-head test and a large amount of water would flow across the head control weir into the sewer[71].

Neither the constant-head nor the falling-head laboratory method provides a reliable value for the coefficient of permeability of a soil. One is fortunate if the value obtained is correct within one order of magnitude[73].

For hydraulic conductivity tests the specimens were compacted using standard proctor compaction effort[67]. After compaction, the specimens were sealed with plastic and aluminum foils and allowed to cure for 28 and 90 days. After curing, the specimens were placed in a compaction permeameter. Deaired, distilled water was used as the permeant. The hydraulic conductivity coefficient was obtained using the falling head method. Three repetitions were made for each result.

In the falling head permeability test, the coefficient of hydraulic conductivity, k, is calculated as

$$k = \frac{aL}{At} \ln \frac{h_i}{h_t} \tag{3.1}$$

where *a*=inside area of the burette; A=area of the specimen; L=thickness of the specimen; t=elapsed time between the two head loss observations; h_i = initial head loss across the specimen at the beginning of the observation; and h_t = head loss at t. Because the burette readings were noted at every five minute interval over a period of 35 min, there were a large number of combinations of t, h_i , and h_t , in which the data could be used to calculate the value of k by Eq. 4.1. The procedure suggested by Bardet was used[72]. The value of k was calculated for each of the seven elapsed times from the beginning of the hydraulic conductivity test, and the average of these values, k_{av} , were determined.

3.4.4. pH Measurements

The pH of water is a critical parameter affecting the solubility of trace minerals, the ability of the water to form scale or to cause metallic corrosion, and the suitability of the water to sustain living organisms. It is a defined scale, based on a system of buffer solutions with assigned values. In pure water at 25°C, pH 7.0 is the neutral point, but this varies with temperature and the ionic strength of the sample. Pure water in equilibrium with air has a pH of about 5.5, and most natural uncontaminated waters range between pH 6.0 and pH 9.0.

The true pH of an aqueous solution or extract is affected by the temperature. The electromotive force between the glass and the reference electrode is a function of temperature as well as pH. The temperature effect can be compensated automatically in many instruments or can be manually compensated in most other instruments. The temperature compensation corrects for the effect of changes in electrode slope with temperature but does not correct for temperature effects on the chemical system being monitored. It does not adjust the measured pH to a common temperature; therefore, the temperature should be reported for each pH measurement[74].

The pH meter shown in Figure 3.2 and associated electrodes are standardized against two reference buffer solutions that closely bracket the anticipated sample pH. The sample measurement is made under strictly controlled conditions and prescribed techniques.

The pH measurements of the leaching fluid of cured fly ash samples were measured with an Orion 710A pHmeter within ASTM D1293[74]. Three repetitions were made for each result.

Figure 3.2. pH meter

3.4.5. Temparature Measurement of Fresh Specimens

The temperature changes of the specimens with respect to time were measured within ASTM C1064[75]. This test method provides a means for measuring the temperature of freshly mixed specimens. The specimen is prepared at standard compaction energy, CBR molds are used when compacting the specimen to minimize the effect of outside air temperature. The thermocouple is positioned so that the end of the temperature sensing portion is submerged 75 mm into the freshly mixed sample. The void left by the placement is closed gently by pressing the ash around the thermocouple at the surface of the concrete to prevent ambient air temperature from affecting the reading.

The thermocouple is left in the freshly mixed sample for a period of 800 minutes, the temperature is recorded within every five minutes. The temperature of the freshly mixed specimen is measured to the nearest 0.1°C. The test is conducted and the measurements are recorded at the curing room.

3.4.6. Radioisotope Activity Comparison

Alpha, beta and gamma radiation are the three primary types of radiation. Alpha particles are fast moving helium atoms. They have high energy, typically in the MeV range, but due to their large mass, they are stopped by just a few inches of air, or a piece of paper. Beta particles are fast moving electrons. They typically have energies in the range of a few hundred keV to several MeV. Since electrons are lighter than helium atoms, they are able to penetrate further, through several feet of air, or several millimeters of plastic or less of very light metals. Gamma particles are photons, just like light, except of much higher energy, typically from several keV to several MeV. Depending on their energy, they can be stopped by a thin piece of aluminum foil, or they can penetrate several inches of lead.

Determination of the radioactivity content of fly ash can be accomplished using gamma spectrometry, with a minimum of sample preparation and good sample throughput. Other techniques, such as alpha spectrometry can also be applied. However, their use for the analysis of fly ash is in most cases not justified, as they are labor intensive and costly, while the activity levels found in fly ash are usually easily and accurately determined by gamma spectroscopy.

The radioisotope activity analysis was conducted at the Çekmece Nuclear Research and Training Center (ÇNAEM) with a gamma analyst integrated gamma spectrometer shown in Figure 3.3; the detector assembly includes a standard coaxial HPGe detector. The materials under study were hermetically sealed in 282 ml plastic cylindrical boxes. To allow for equilibrium of 226Ra and 232Th with their decay products, all specimens were analyzed four weeks after the boxes were sealed.

Figure 3.3. Gamma spectrometer

3.4.7. Thermographic Measurements

The thermal images were captured by a thermal imager shown in Figure 3.4. Thermal imaging, also called thermography, is the production of non-contact infrared or heat pictures from which temperature measurements can be made. Portable infrared cameras scan samples, then instantly convert the thermal images to pictures for monitoring or quantitative temperature analysis. This setup contained a thermal camera provided with an FPA type detector with a resolution of 120 x 120 pixels. The object to be measured was placed in front of a rusty iron background. This allowed a homogeneous distribution of the radiation over the surface with a clear difference in radiation between object and background. Rusty iron is characterized by a low emissivity and reflection. An automatic calibration for the ambient and camera temperature and for the air humidity was provided. Thermographic images were recorded with the camera and analyzed with software to obtain the temperature variations.

Figure 3.4. Thermal imager

3.4.8. X-Ray Diffraction Analysis

The investigations of the microstructural changes of the specimens by the X-ray Diffractometer were carried on at Boğaziçi University Advanced Technologies Research and Development Center shown in Figure 3.5. XRD patterns were obtained using a Rigaku powder diffractometer (Model D-max II) with monochromated Cu-Kα radiation. During XRD analysis powder diffraction method was used, samples were finely powdered and surface-dried in air. The samples were run from 5.0^0 to 70.0^0 2θ on a XRD using 40 KV and 40 mA monochromatic copper radiation at 1.0^0 2θ/min with a step size of 0.02^0 2θ. Peaks were assigned by reference to the JCPDS database.

Figure 3.5. X-ray diffractometer

3.4.9. Environmental Scanning Electron Microscope Analysis

In this part of the study, environmental scanning electron microscope (ESEM) analysis were conducted on both control and natural snow added compacted fly ash specimens. Magnifications of 350, 2000 and 4000 were selected to examine the matrix in ESEM analysis. The investigations of the microstructural changes of the specimens by the ESEM in the gaseous secondary electron mode (GSE) were carried on at Boğaziçi University Advanced Technologies Research and Development Center shown in Figure 3.6. The analysis were performed by means of a Philips XL30 ESEM-FEG/EDAX machine without any surface preparation on the specimens.

The environmental scanning electron microscope is a new type of high-resolution microscope, which allows the examination of specimens in the presence of gases. As a result, wet or dry, insulating or conducting, and generally all specimens can now be viewed with no or minimal preparation.

Figure 3.6. Environmental scanning electron microscope

3.4.10. Resistance of Samples to Rapid Freezing and Thawing

This test covers the determination of the resistance of specimens to rapidly repeated cycles of freezing and thawing in the laboratory by rapid freezing and thawing in water ASTM C666 Procedure A. This procedure is intended for use in determining the effects of variations in the properties of the specimens, on the resistance of the specimens to the freezing and thawing cycles specified in the ASTM procedure.

The freezing and thawing apparatus consists of suitable chambers in which the specimens may be subjected to the specified freezing and thawing cycle (Figure 3.7), together with the necessary refrigerating and heating equipment and controls to produce continuously (Figure 3.8), and automatically, reproducible cycles within the specified temperature requirements. Each specimen is supported at the bottom of its container in such a way that the temperature of the heat exchanging medium has not been transmitted directly through the bottom of the container to the full area of the bottom of the specimen,

thereby subjecting it to conditions substantially different from the remainder of the specimen.

Figure 3.7. Freeze-thaw cabinet

The nominal freezing-and-thawing cycle for this test consisted of alternately lowering the temperature of the specimens from +4 to −18°C and raising it from −18 to +4°C in 5 hours[76].

The specimens used in this test were prisms made and cured in accordance with the ASTM C666 requirements. Specimens used were 76mm. in width, 102mm. in depth and 405mm. in length. A total number of 16 samples were prepared.

Figure 3.8. Freeze-thaw apparatus refrigerating and heating equipment and controls

3.4.11. Thermal Conductivity Analysis

This test establishes the principles for the design of a hot box apparatus and the minimum requirements for the determination of the steady state thermal performance of building assemblies when exposed to controlled laboratory conditions. The hot box apparatus is required to establish and maintain a desired steady temperature difference across the test specimen for the period of time. The elapsed time required is that necessary to ensure constant heat flow and steady temperatures, and, for an additional period adequate to measure these quantities to the desired accuracy.

To determine the resistance, R, of any specimen, it is necessary to know the area, A, the net heat flow, Q and the temperature differences, Δt, all of which shall be determined under such conditions that the flow of heat is steady. The area and temperatures are measured directly. The inside chamber temperature is measured with the thermocouples and the surface temperatures of the specimens are measured using an infrared thermal

camera. The heat flow rate through the metering chamber walls is limited by the use of highly insulated walls.

The major components of a hot box apparatus are the metering chamber on one side of the specimen; the climatic chamber on the other; the specimen frame providing specimen support and perimeter insulation; and the surrounding ambient space. These elements shall be designed as a system to provide the desired air temperature, air velocity, and radiation conditions for the test and to accurately measure the resulting net heat transfer[77].

The samples for this test were prepared in special prism molds which were 40mm.x40mm.x160mm. in dimensions.

3.4.12. Erosion Analysis (Pinhole Test)

This test presents a direct, qualitative measurement of the dispersibility and consequent colloidal erodibility of specimens by causing water to flow through a small hole punched in the specimen shown in Figure 3.9.[78].

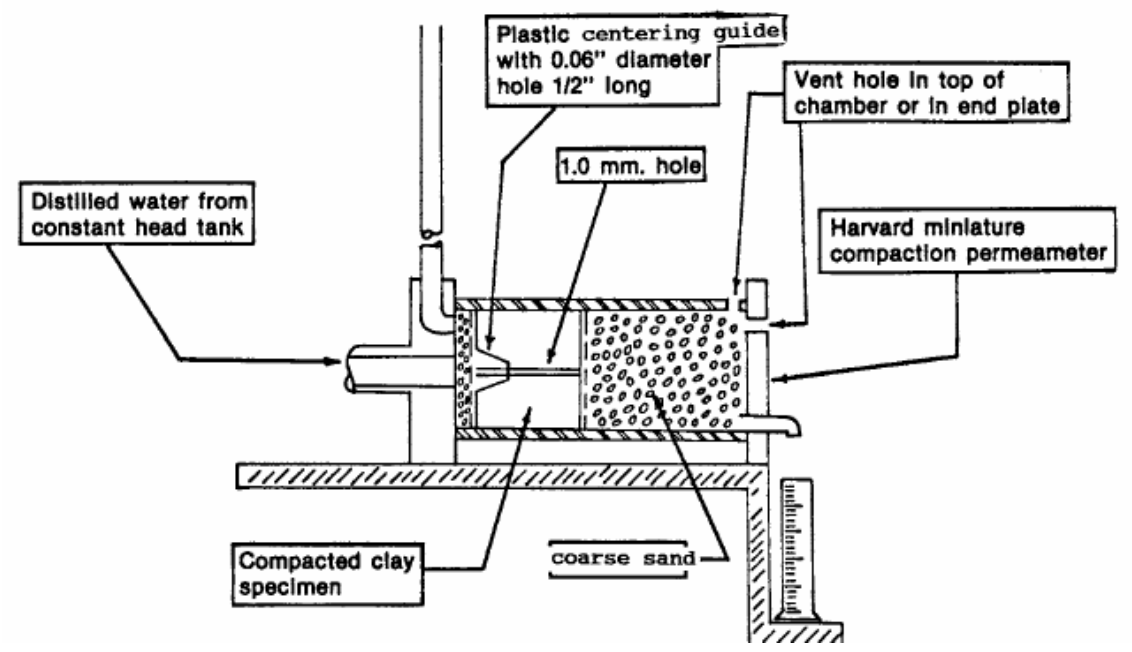

Figure 3.9. Schematic drawing of the pinhole test equipment

Test results are evaluated from the appearance of the flowing solution emerging from the specimen, the rate of flow, and the final size of the hole through the specimen. These observations provide the basis for classifying the specimen.

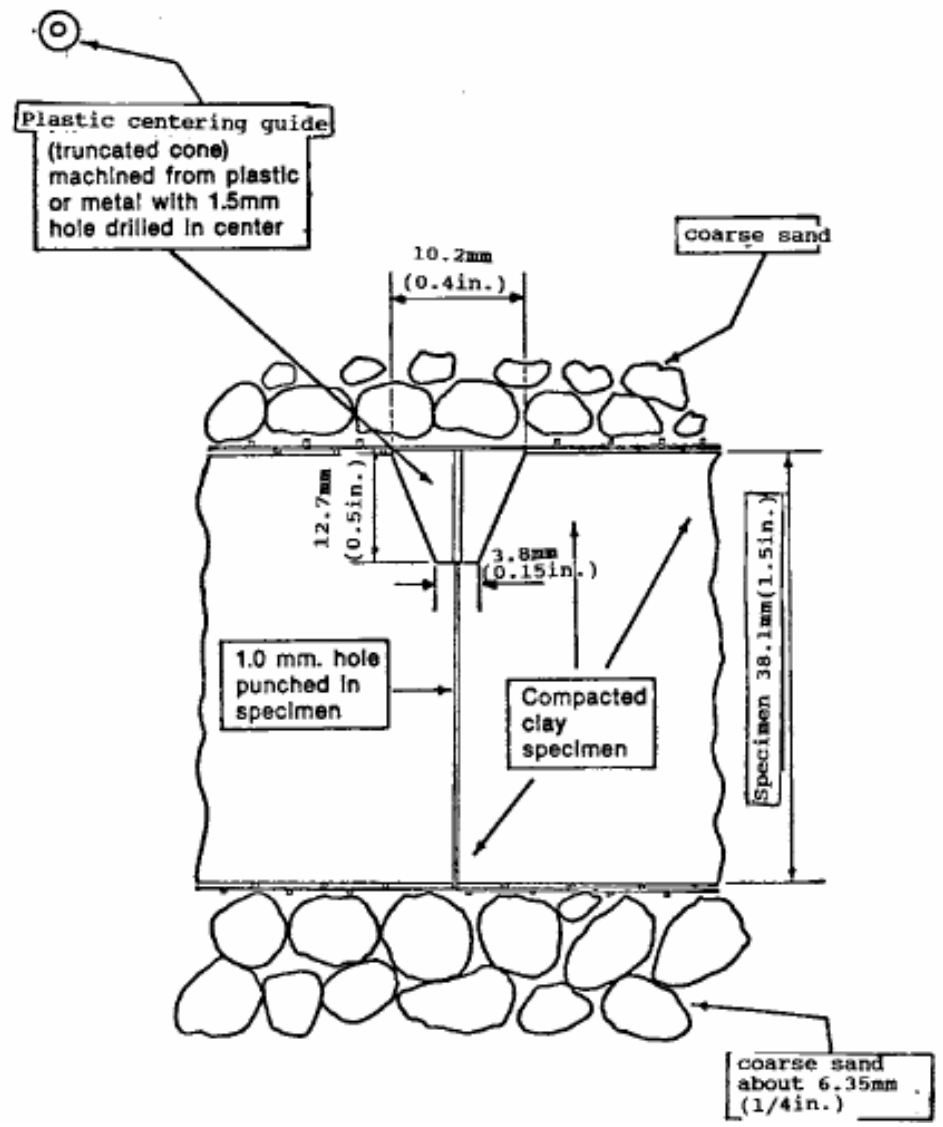

Figure 3.10. Schematic drawing of pinhole test specimen

The 38 mm long specimen is compacted into the pinhole test cylinder on top of the coarse sand and wire screen, which have been previously placed in the cylinder. When using the Harvard compaction and permeability equipment approximately 95 per cent of maximum standard dry unit weight is achieved by compacting the specimen in five lifts with 16 tamps on each lift using a 6.8 kg spring on the Harvard compaction test tamper.

The truncated cone centering guide with the 1.5mm diameter hole is inserted into the center of the top of the specimen using finger pressure shown in Figure 3.10[78]. Care had been taken to ensure that the nipple is inserted vertically with the top of the nipple flush with the top of the soil specimen so that the pinhole is normal to the specimen surface. The punch is removed from the specimen and the wire screen is carefully placed on top of the specimen with centering guide in place and the remaining void in the top of the test cylinder is filled with coarse sand. Then the top plate is assambled; the head (distilled water) source, and the head measuring device is connected. The assembled apparatus is placed in horizontal position shown in Figure 3.11 and Figure 3.12.

Figure 3.11. Pinhole test setup

The test is started by introducing distilled water into the apparatus so that a hydraulic head at the level of the pinhole is 50 mm. The time is recorded at start of the test. With an appropriate graduated cylinder, the quantity of effluent flow is measured as it emerges from the specimen. The test is continued at different head levels. After the test has been finished, the size and shape of the hole through the specimen at the end of the test is observed and recorded[78].

In evaluating test results from the samples, the cloudiness of the effluent emerging from the specimen is more important than the rate of flow. It is also important that characteristics of the hole at the end of the test be carefully observed and recorded.

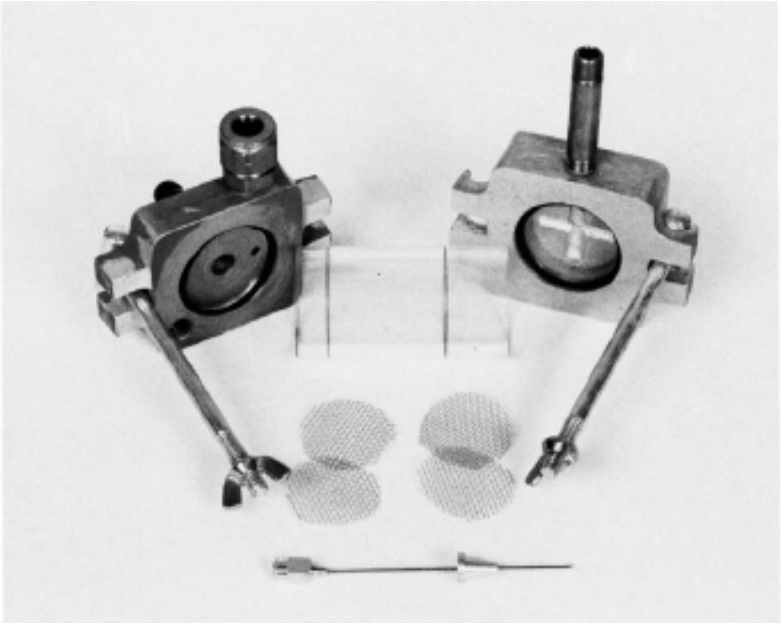

Figure 3.12. Pinhole test mold, screens, nipple and needle

3.4.13. Leachate Analysis

Column leaching tests were conducted to provide a more realistic assessment of leaching from the samples and to determine the leaching and transport parameters[79]. The specimens for the leaching tests were prepared in standard Proctor mold using standard Proctor compaction effort. The specimens were compacted in rigid-wall compaction permeameters operated in an up-flow mode[80].

Hydraulic gradients between seven and 10 were applied to make sample collection convenient. These gradients are larger than exist in the field (typically about one). However, it is reported that metal leaching from fly ashes is independent of flow rate[81]. Thus, the larger gradients are believed to have little impact on the test results.

Effluent from the column test (leachate) was collected in airtight sampling bags. A portion of leachate (350 ml) was collected for heavy metal determination test. The pH, volume, and time of collection of the leachate were recorded. Leachate samples were preserved and subjected to several tests and the results are analyzed by atomic absorption spectrophotometer at Bogazici University Environmental Sciences Laboratory shown in Figure 3.13.

Figure 3.13. Atomic absorption spectrophotometer

3.4.14. Length Change Determination

In the length change determination test, an increase or decrease in the linear dimension of the cured test specimens are measured along the longitudinal axis, due to causes other than applied load.

The interior surfaces of the molds are thinly covered with mineral oil. The specimens were compacted in the special shrinkage molds (40mm.x40mm.x160mm.) using standard Proctor compaction effort shown in Figure 3.14. After compaction, the gage studs are set and kept clean, free of oil, grease, and foreign matter.

The reference bar in the instrument is placed in the same position each time a comparator reading is taken. The hole in the base of the comparator into which the gage stud on the lower end of the bar fits is cleaned before taking measurements. The comparator indication of the length of the reference bar is read and recorded[82].

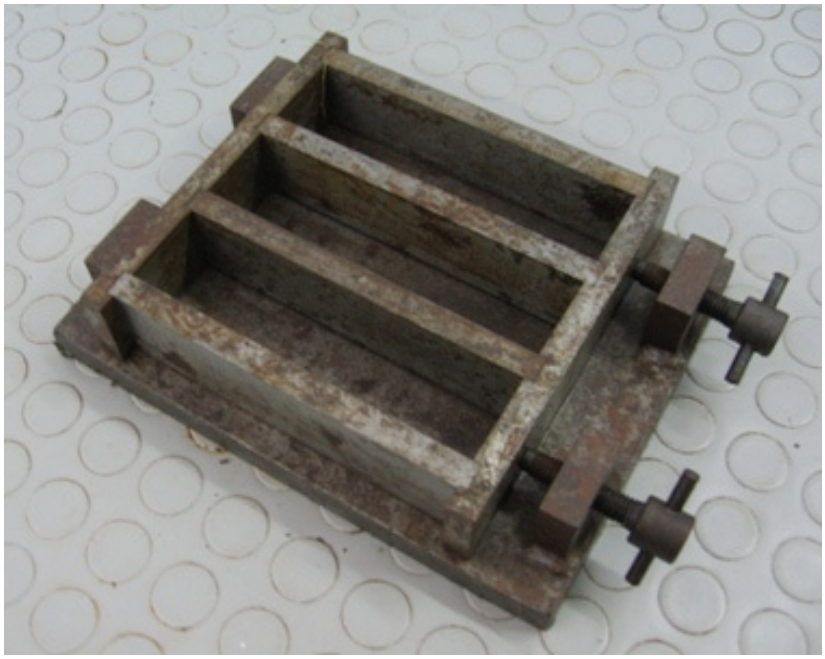

Figure 3.14. Shrinkage mold

4. MICROCHEMICAL AND MICROFABRIC INVESTIGATION

4.1. X-Ray Diffraction Analysis

X-Ray diffraction has long been used as definitive technique for identification of crystalline mineral components and other crystalline phases. XRD results give useful information in materials such as fly ash, where the individual crystals are too small to be reliably identified by other techniques.

The X-ray diffraction spectra of the fly ash, and samples compacted at optimum moisture content, and cured for one, 28, 90 days and five years are presented in Figure 4.1. In Figure 4.2., the X-ray diffraction spectra of the fly ash and snow-added samples compacted at optimum moisture content and cured for one, 28, 90 days and five years are shown. There are several crystalline phases as determined by the X-ray diffractometer such as; quartz (SiO_2), mullite ($Al_6Si_2O_{13}$), calcite ($CaCO_3$), ettringite ($Ca_6Al_2(SO_4)_3(OH)_{12}.26H_2O$) and thaumasite ($Ca_3Si(OH)_6(CO_3)(SO_4).12H_2O$). In the Figures 4.1 and 4.2, ettringite, thaumasite, mullite, quartz and calcite are represented by letters E, T, M, Q, and C, respectively (Figure 4.1 and Figure 4.2). With increasing curing time, the formations of thaumasite and ettringite minerals are observed. Ettringite peak intensity increases with increasing curing time. Due to smaller amount of water in its atomic structure, thaumasite is seen in samples compacted at optimum water content. Ettringite's atomic structure consists of more water and is dominant in the samples compacted with snow where fifty per cent more water is available for reactions. The peaks of the ettringite and thaumasite minerals are sharper and show a rapid increase in the one, 28, 90 days and five years-cured snow-added fly ash samples (FI1, FI28, FI90 and FI5Y) (Figure 4.1 and Figure 4.2). In Figures 4.1 and 4.2 raw fly ash (FA) diffraction pattern show a hump, however as curing period approaches five years this hump gets lost, this means that raw fly ash has an amorphous structure and as curing period approaches to five years the structure is converted into a crystalline structure. This means that the matrix is transformed into a more ordered structure.

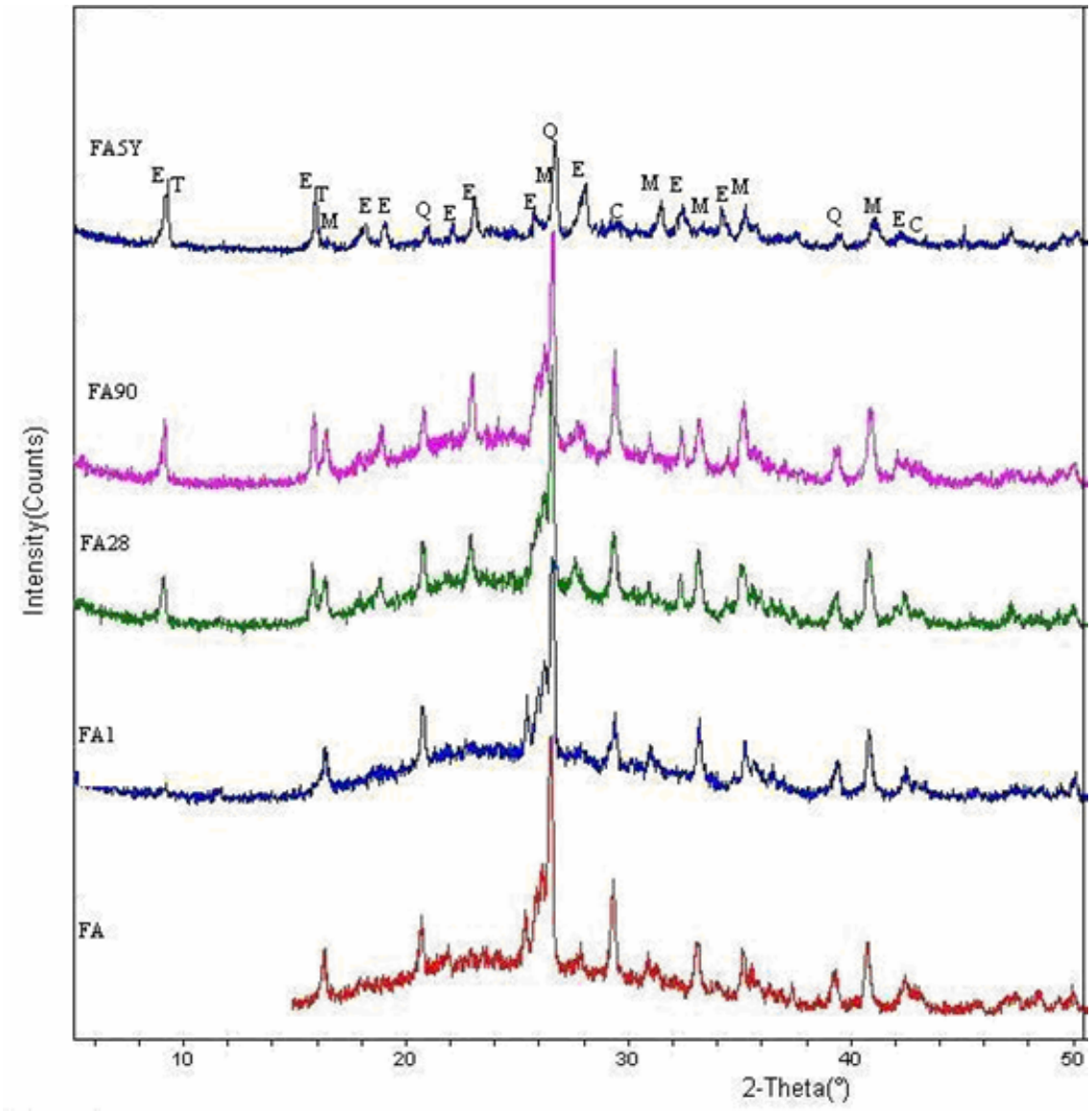

Figure 4.1. X-Ray diffraction patterns of raw fly ash (FA), fly ash cured for one day at optimum moisture content (FA1), fly ash cured for 28 days at optimum moisture content (FA28), fly ash cured for 90 days at optimum moisture content (FA90), fly ash cured for five years at optimum moisture content (FA5Y).

Results will be testified in the next sections with the observations in the improved engineering properties. Although the intensity of the calcium silicate peaks is getting relatively higher with hydration age, the presence of mullite after five years indicate that the hydration of the phases is not complete in both control and snow-added fly ash samples. This fact indicates that additional CAH will probably be produced even after five years of hydration.

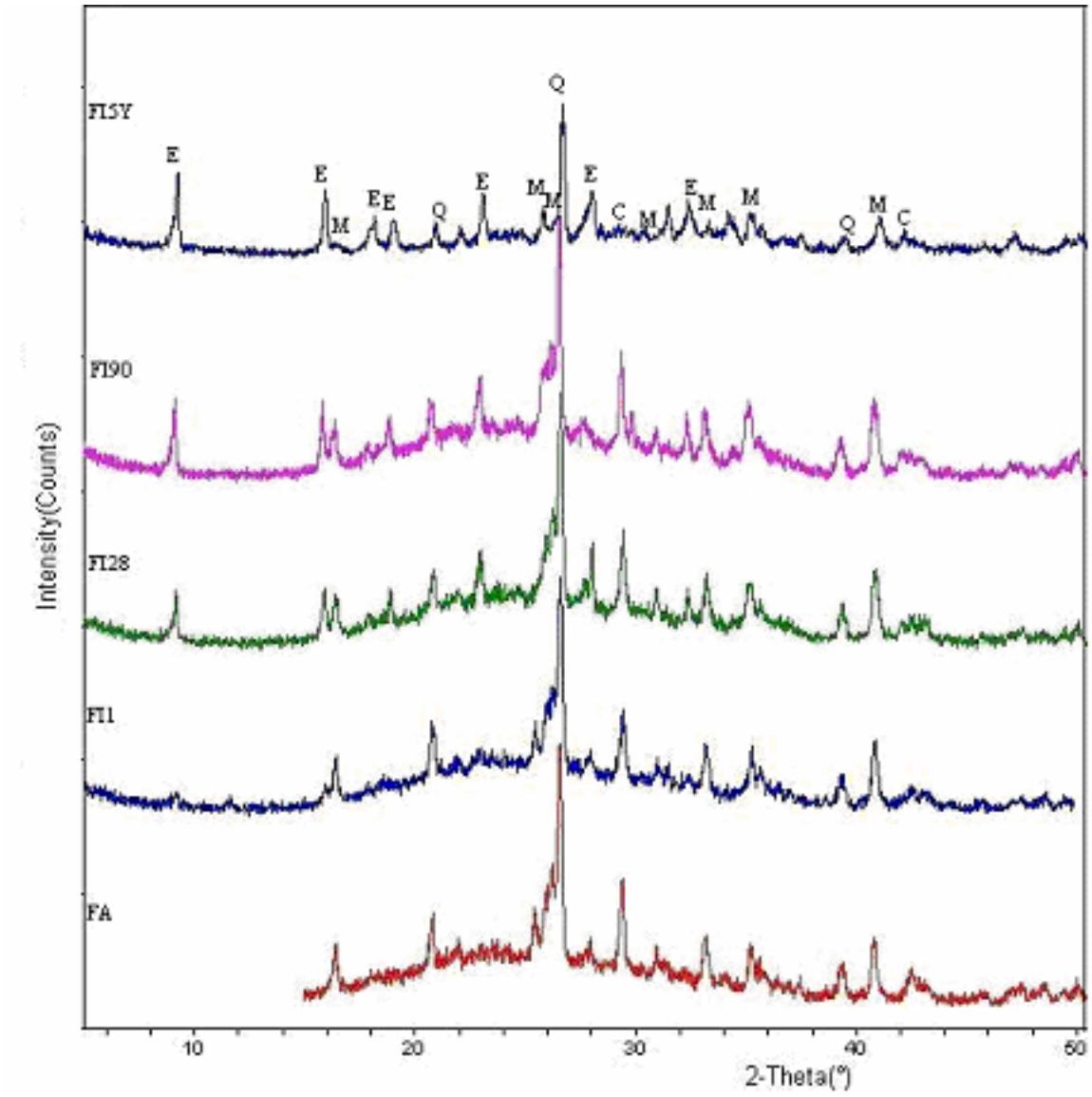

Figure 4.2. X-Ray diffraction patterns of fly ash (FA), snow-added fly ash cured for one day (FI1), snow-added fly ash cured for 28 days (FI28), snow-added fly ash cured for 90 days (FI90), snow-added fly ash cured for five years (FI5Y).

A noticable difference related to the formation of hydration products in tested specimens is the generation of ettringite phases with curing time. Ettringite is formed as early as in one day in both mixes as a result of the reaction of Ca^{+2} ions that are present in the pore solution, with the aluminate rich fly ash phases. Later on, a significant intensification of ettringite peaks are observed, accompanied by the production of calcium aluminate hydrates. In the literature there is agreement that the production of ettringite phases, is the outcome of the increasing dissolution of aluminate ions from the fly ash glass

[85,86]. However, this is not the case in this study, as the thaumasite seem to grow independently of the ettringite ones. This is remarkable in the control fly ash samples (FA), where especially after the first month of hydration a simultaneous intensification of the peaks representing the aforementioned phases is observed.

The consistent production of pore filling ettringite, even at late curing periods, obviously contributes to the final strength of control fly ash and snow-added fly ash specimens and provides an additional explanation for the superiority of the snow-added fly ash samples at later ages. The lower increase rate (with respect to snow added fly ash samples) in the peak intensities of the control fly ash samples' XRD patterns correspond to the main hydrates, CSH, implies the poor crystallinity of both the initial gel and the pozzolanic CSH formed afterwards.

4.2. Environmental Scanning Electron Microscope Analysis

An environmental scanning electron microscope (ESEM) study was carried out to observe the microfabric development of the control and snow-added fly ash specimens cured for different periods varying from one day to five years. ESEM examinations verified the results reported in the previous sections and provided an image of the microstructural development of the tested specimens. In this approach, special attention was given in the snow-added fly ash samples that presented higher performance at the end of the curing period, the mixture containing 10 per cent by weight natural snow. Figure 4.3 and 4.4 show the microfabric of the matrix at one day of hydration. For the control samples unreacted fly ash particles (FA) retaining their smooth and spherical shape are recognizable, while some others have already been covered by hydration products (mostly CSH). Rodlets are not present in the matrix which indicate the presence of ettringite (very tiny). At this age the snow crystals act mainly as a catalyzer, promoting the precipitation of hydration products formed and the hydration of calcium silicate phases of the fly ash.

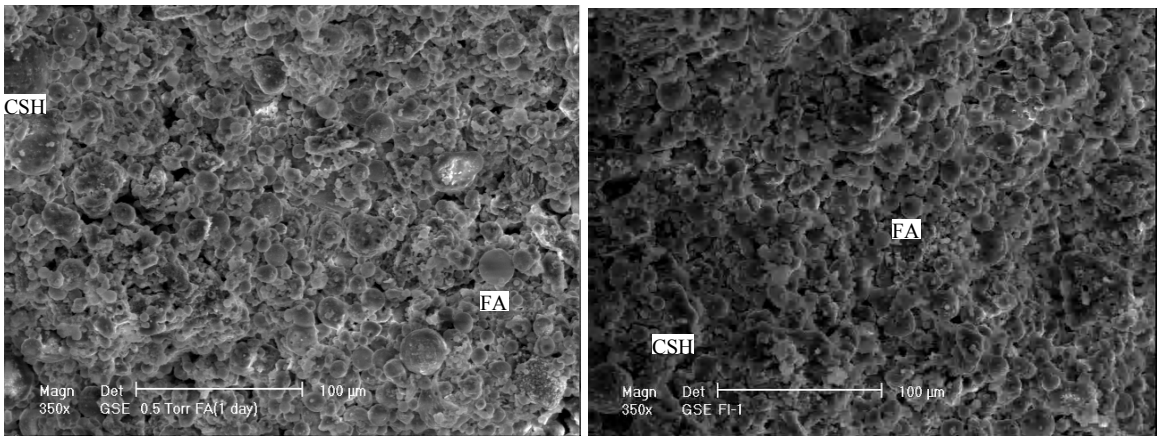

Fly Ash one day cured(FA1)(350x) Fly Ash + snow one day cured(FI1)(350x)

Figure 4.3. The Environmental scanning electron microscope (ESEM) micrographs after one day curing. (350x)

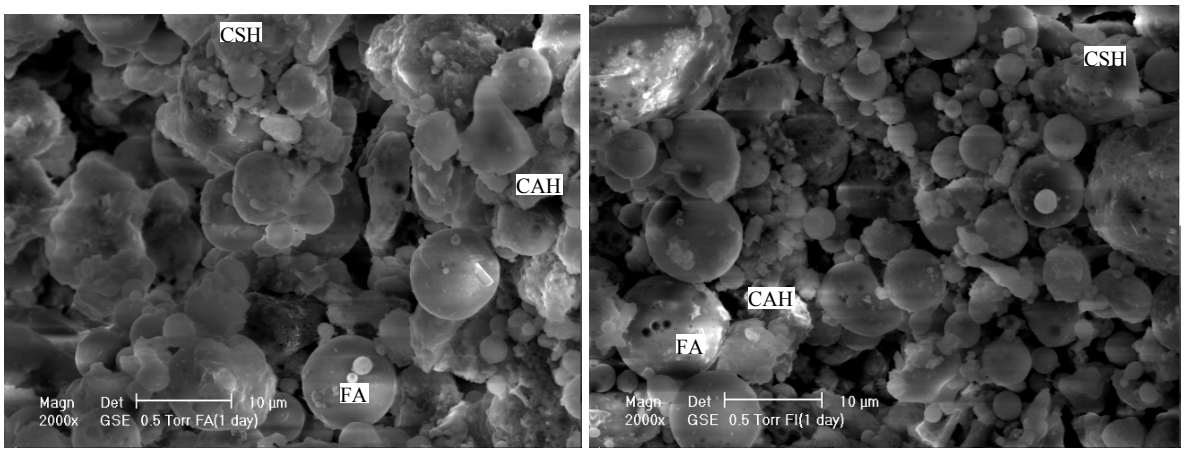

Fly Ash one day cured(FA1)(2000x) Fly Ash + snow one day cured(FI1)(2000x)

Figure 4.4. The Environmental scanning electron microscope (ESEM) micrographs after one day curing. (2000x)

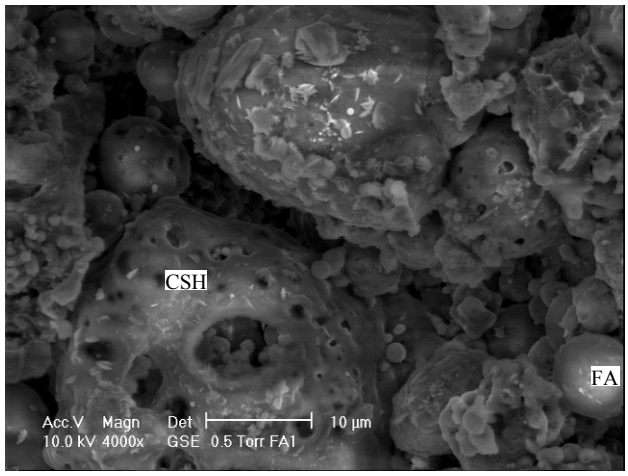

Fly Ash one day cured(FA1)(4000x)

Figure 4.5. The Environmental scanning electron microscope (ESEM) micrographs after one day curing. (4000x)

The numerous voids visible in the structure of the control and snow-added specimens at one day, decrease substantially after 28 days, leading to a more compact morphology shown in Figure 4.6 and 4.7. At this age, fly ash particles have been encapsulated into the matrix of calcium aluminates and ettringite phases are formed. The formation of this network is to a large extent ascribed to the extra water (10 per cent) supplied by snow addition over optimum moisture content of fly ash. The strong presence of Ca^{2+} and Al^{3+} ions in the hydration products implies that dissolution of alkalies by some fly ash particles has taken place. X-ray mapping and elemental distribution analyses on a reacted fly ash particle at this age shown in Figure 4.5, revealed the high presence of alkalies and Ca^{2+} ions in the exterior glass hull of the ash confirming that these species are available from the ash particles from the very early ages. During the same analysis, silica was detected in the interior glass matrix of the ash particle. This indicates that glassy silica is not readily dissolved into the matrix. There is a need for the exterior glass shell of fly ash to be broken down, so as silica will run freely in the pore solution, leading to the formation of products with binding properties. The dense structure formed by the addition of snow reinforces the already present ettringite, providing an explanation for the early age strengths. This is consistent with the improved engineering properties of the snow-added fly ash specimens as will be stated in the following sections.

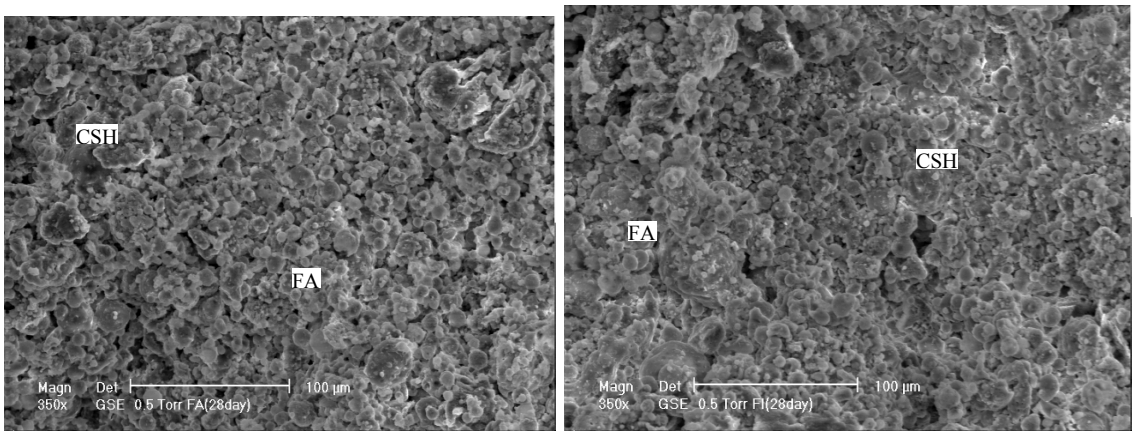

Fly Ash 28 days cured (FA28)(350x) Fly Ash + snow 28 days cured (FI28)(350x)

Figure 4.6. The Environmental scanning electron microscope (ESEM) micrographs after 28 days curing. (350x)

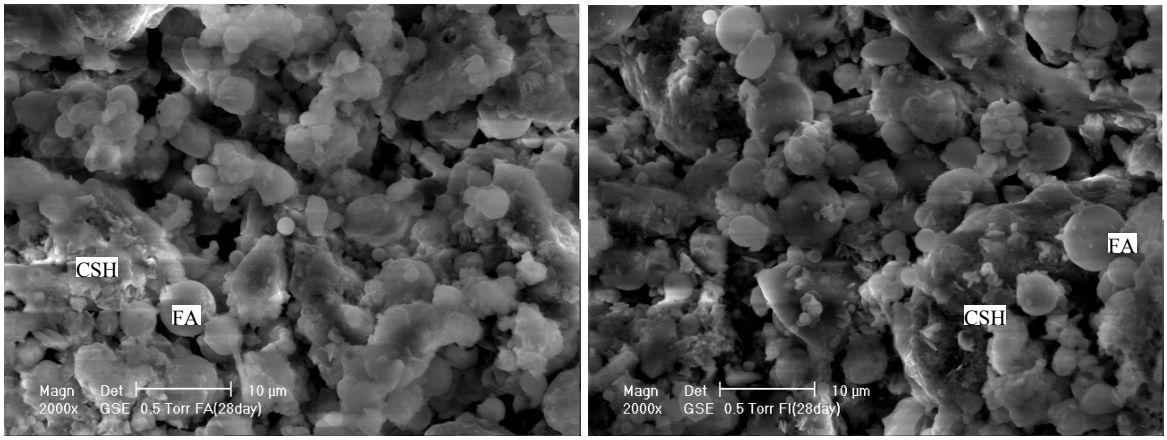

Fly Ash 28 days cured(FA28)(2000x) Fly Ash + snow 28 days cured(FI28)(2000x)

Figure 4.7. The Environmental scanning electron microscope (ESEM) micrographs after 28 days curing. (2000x)

One month after curing, breaking of the fly ash glass has progressed leading to the formation of a flocculent CSH gel that surrounds the majority of the particles. This is an indication that pozzolanic reaction is evolving and that part of the amorphous silica in the ash is released into the matrix, combining with available extra water and forming a second generation CSH, improving the strength of the system. Numerous fly ash particles have been completely covered by hydrated crystals shown in Figure 4.7.

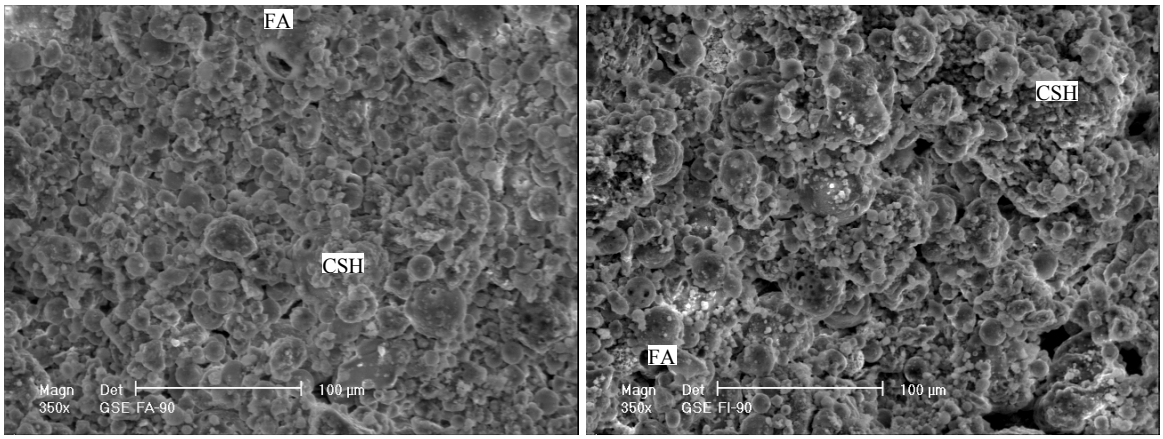

Fly Ash 90 days cured (FA90)(350x) Fly Ash + snow 90 days cured (FI90)(350x)

Figure 4.8. The Environmental scanning electron microscope (ESEM) micrographs after 90 days curing. (350x)

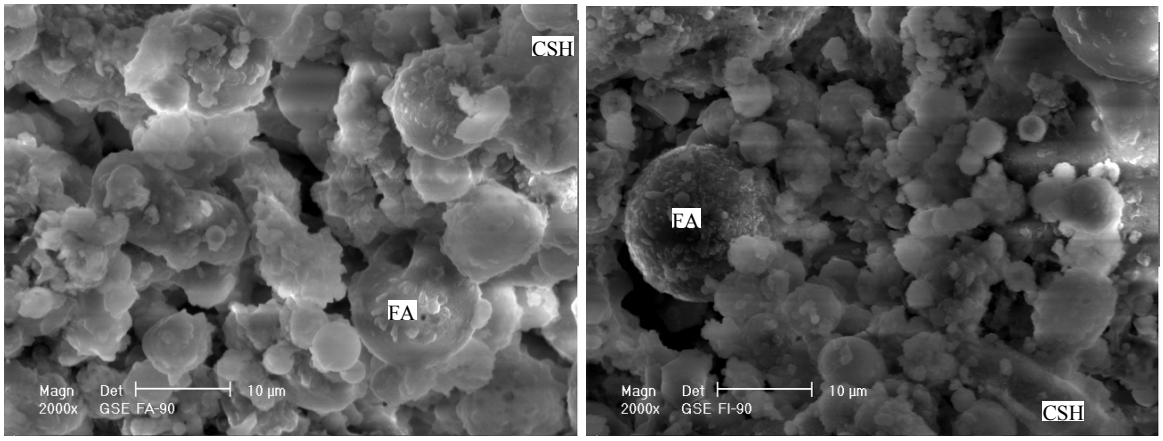

Fly Ash 90 days cured(FA90)(2000x) Fly Ash + snow 90 days cured(FI90)(2000x)

Figure 4.9. The Environmental scanning electron microscope (ESEM) micrographs after 90 days curing. (2000x)

After 90 days the matrix of the snow-added fly ash sample has further densified (Figure 4.8 and 4.9), a fact that corresponds to its higher strength. Silica from the ash particles is increasingly dissolved, joins the pore solution, reacts with still available calcium aluminate hydrate, and provides additional pozzolanic CSH. The binding properties of this gel supplement the filling effect of the ashes than remain intact, leading in a subsequent decrease of the pores in the matrix. Ettringite was also detected during the XRD test. Obviously these phases continued to develop and needle crystals crossed each other to form an improved and frame microstructure.

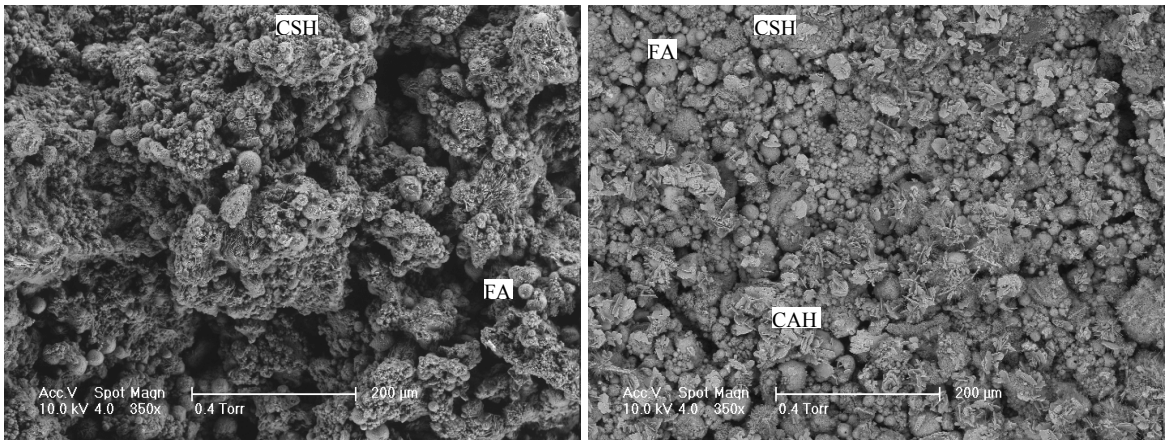

Fly Ash five years cured (FA5Y) Fly Ash + snow five years cured (FI5Y)

Figure 4.10. The Environmental scanning electron microscope (ESEM) micrographs after five years curing. (350x)

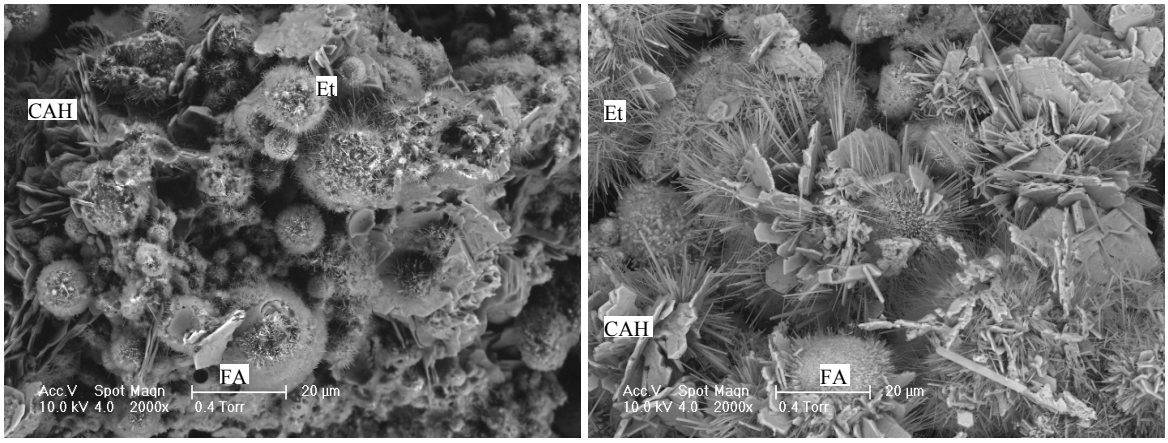

Fly Ash five years cured(FA5Y) Fly Ash + snow five years cured(FI5Y)

Figure 4.11. The environmental scanning electron microscope (ESEM) micrographs after five years curing. (2000x)

Figure 4.10 and Figure 4.11 show a typical microfabric of fly ash samples cured for time periods of five years. Typical examples of ettringite ($Ca_6Al_2(SO_4)_3(OH)_{12}.26H_2O$) growth on the surface of spherical fly ash particles are seen. Ettringite is also observed growing inside the void spaces of the fly ash. There are abundant sulfate and aluminum ions available in the system to form ettringite. The availability of calcium ions in solution is critical in determining the ettringite formation. For the formation of thaumasite, carbonate ions must also be available in the system. The snow-added fly ash samples have a void ratio 30 per cent larger than that of fly ash samples compacted at optimum water

content. This higher void ratio is compensated by formation of more cementitious minerals, which results in nearly 70 per cent higher strength. The open fabric is easily seen for the control samples.

When incorporating snow in high calcium fly ash systems, the melting snow present in the matrix significantly affects the hydration. This effect seems to be substantial especially after the first month of the hardening process, when silica is dissolved in the matrix to form additional cementitious compounds with binding properties. Snow addition is found to be critical both in the strength development and in the mineral formation of such samples especially after the first month of the hardening process. By 10 per cent replacement of fly ash with snow, a high reactive fly ash was found to accelerate the strength of the system and the formation of hydration phases. A synergetic effect that upgraded the final performance of the examined mixtures was related to the persistent appearance of the ettringite phases even at later ages, attributed largely to the introduction of extra water in the system by snow melting.

5. TEST RESULTS AND EVALUATION

5.1. Physical Properties of the Compacted Samples

The physical properties of the compacted samples and their comparison are summarized in Table 5.1. The compacted dry unit weight versus moisture content relationship of control fly ash and natural snow added fly ash samples are shown in Figure 5.1. Figure 5.1 displays the compaction curves of the mixtures containing zero and 10% natural snow. The results of the compacted specimens shown in Table 5.1 indicated that the dry unit weight of snow added fly ash samples decreased by 12 per cent. Also with addition of snow, the total water content of the sample increased by 48 per cent. The test results on the samples show that as the natural snow content increased from zero to 10 per cent, the optimum moisture content increased, while the maximum dry unit weight decreased as can be seen in Figure 5.1. When natural snow is added into the mixture by 10%, the natural snow particles distributed in the matrix created air voids and an air-entrained structure achieving a 12% lower dry unit weight.

Table 5.1. Comparison of the properties of compacted fly ash and compacted fly ash & snow

	Fly Ash (FA)	Fly Ash + Snow (FI)	% Change
Dry Unit Weight (kN/m^3)	13.41	11.78	12% decrease
Water Content w%	19.54	28.89	48% increase
Void Ratio e	0.90	1.17	30% increase

The void ratio of snow-added fly ash is 30 per cent higher than that of fly ash compacted at optimum water content. The higher void ratio of snow-added fly ash (FI) is particularly important for insulation capability and freeze-thaw resistance. The amount of fly ash (FA) to compact the same volume of embankment will decrease, causing significant cost savings. For embankments constructed on soft soils, the 12 per cent lower unit weight

of snow-added embankment will decrease the settlement of the embankment while increasing the factor of safety against the bearing capacity failure.

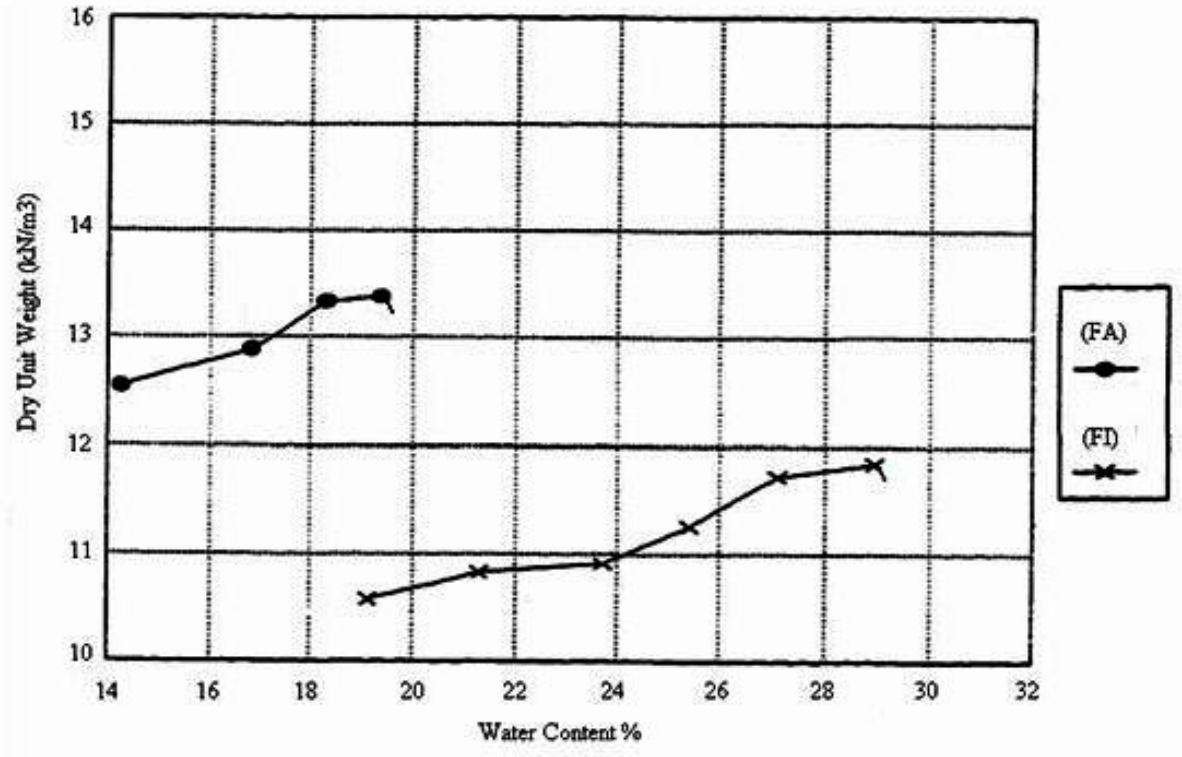

Figure 5.1. Compacted dry unit weight-moisture content relationship of control fly ash and natural snow added fly ash samples

5.2. Settlement and Stress Increase In Soil From Embankment Construction

The construction of highway embankments requires substantial amounts of fill materials. Soils, being the common source for such fill, are usually transported from nearby borrow areas. Fly ash can be viewed as one of the viable alternatives for soils. It can offer several advantages over many soils and rocks. Fly ash has a lower unit weight than most soils. This property can be useful, especially when the compressibility of the underlying soil is a source of concern. Relatively high shear strength can be obtained if the coal ash is compacted appropriately. High shear strength allows for steeper slopes and higher embankments. By adding natural snow into the fly ash samples, lower unit weight and higher shear strength are achieved, therefore the slopes can be constructed steeper and higher and the amount of fly ash to compact the same volume of embankment will decrease

which will cause significant cost savings. For embankments constructed on soft soils, the 12 per cent lower unit weight of snow-added embankment will decrease the settlement of the embankment and the underlying soil will be less exposed to stresses as can be seen in the following example.

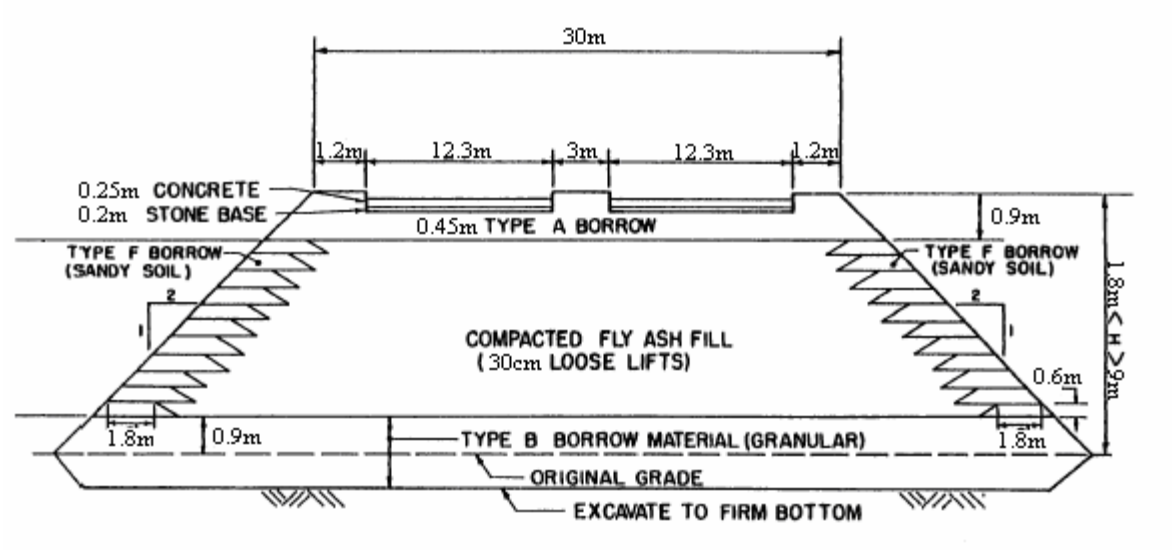

Figure 5.2. Typical fly Ash embankment section in the I-495 and Edgemoor road interchange, Delaware.

The distribution of stresses within the underlying soil is determined by assuming that the soil is a semi-infinite, homogenous, linear, isotropic, elastic material. A typical fly ash embankment shown in Figure 5.2[87] constructed with the control fly ash sample will exert 19 kPa vertical stress increase to the underlying soil at a depth of three meters below the embankment. Slope angle is 26.5^0(two : one). A typical embankment constructed with the natural snow added fly ash will exert 16,9 kPa vertical stress increase to the underlying soil at a depth of three meters below the embankment. The underlying soil will be less exposed to stresses with the natural snow added fly ash embankments as seen in this example. Also the slopes can be constructed steeper. For the natural snow added fly ash embankment to exert the same amount of vertical stress, the embankment can be constructed with a slope angle of $36,8^0$ (four : three) which will also allow to get less right of way. If the embankment was constructed with the traditional embankment construction materials(soil), the vertical stress increase three meters under the embankment would be 26,9kPa which means that underlying soil will be exposed to 37% less vertical stress if the

embankment is constructed with natural snow added fly ash. The influence factor chart shown in Figure 5.3 is used to calculate the vertical stress increase under the embankment section[88].

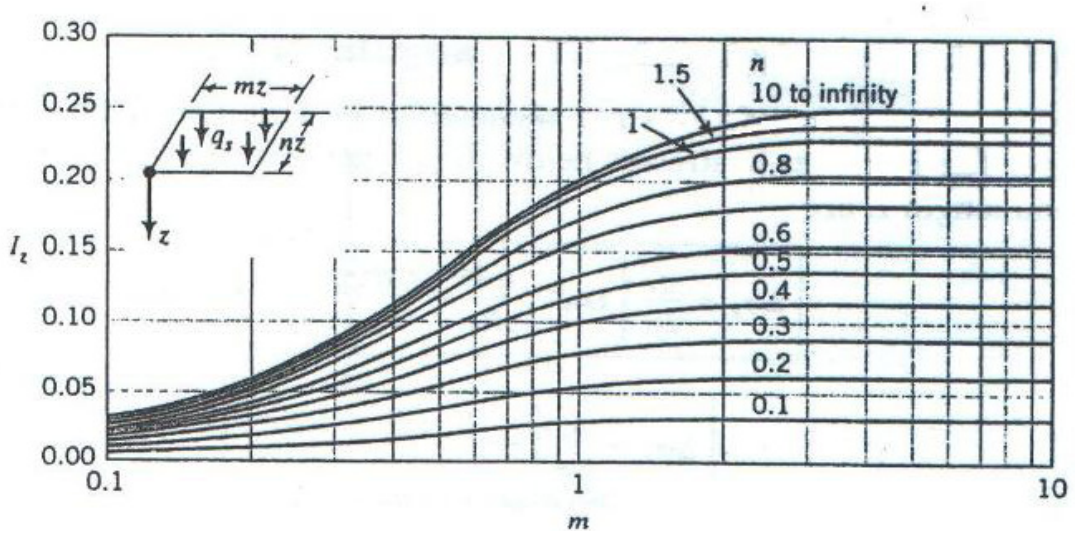

Figure 5.3. Influence factor for calculating the vertical stress increase under the corner of a rectangle.

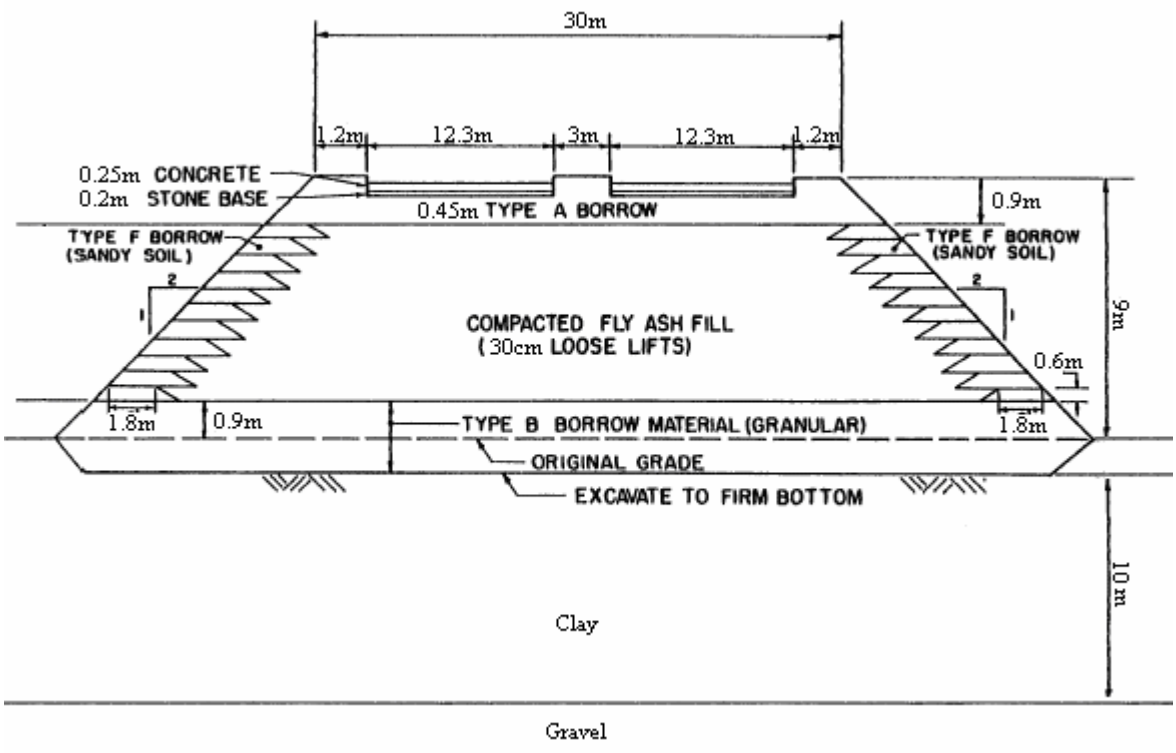

Figure 5.4. Typical fly ash embankment section resting on a clay layer

Let us assume that the embankment shown in Figure 5.4 is constructed on a 10 meter thick clay layer with an average modulus of volume compressibility $m_v = 5 \times 10^{-5}$ m^2/kN. The primary consolidation settlement values will be 43.5mm for the embankment constructed with the control fly ash, 38.5mm for the embankment constructed with the natural snow added fly ash and 62 mm for the embankment constructed with the traditional embankment construction materials. These results testify the advantages of embankment construction using natural snow added fly ash samples.

5.3. Unconfined Compression Tests

The unconfined compressive strength values of fly ash (FA) and snow-added fly ash (FI) samples cured at the curing room and at the outdoor conditions are presented in Figure 5.5 for curing periods from one day to 90 days. The stress strain curves obtained by averaging the data of eight samples are presented in Figure 5.6. The temperature variation of the outdoor curing conditions are presented in Figure 5.7. From one to seven days curing period, the increase amount in the strength values are lower with respect to seven-28 days curing results. This strength rate increase after seven days curing can also be seen in the ESEM and XRD observations in the previous sections. The strength development in snow-added fly ash (FI) is much faster, and after 14 days of curing, the strength difference becomes more pronounced. The higher strength gain after 28 and 90 days is due to the excess water provided by the added natural snow which causes more crystal formation, and the slower hydration rate which causes larger size crystal development. The cementation reactions continue in the presence of free water. The excess 10 per cent water, added in the form of natural snow, provided a satisfactory environment for development of cementitious minerals, leading to higher strength. The curing conditions (temperature and humidity controlled curing room and outdoor curing conditions shown in Figure 5.8) represented similar results for 28 days curing period. The strength gain for the samples cured at the outdoor conditions gave lower strength values because of the changes in the curing temperature ranging from zero to 15^0C. The cementitious mineral formation rate is decreased at temperatures approaching the freezing values.

The unconfined compressive strength of snow-added fly ash is 70 per cent higher than that of fly ash after 90 days of curing, which will lead to higher embankment stability and the possibility of steeper side slopes.

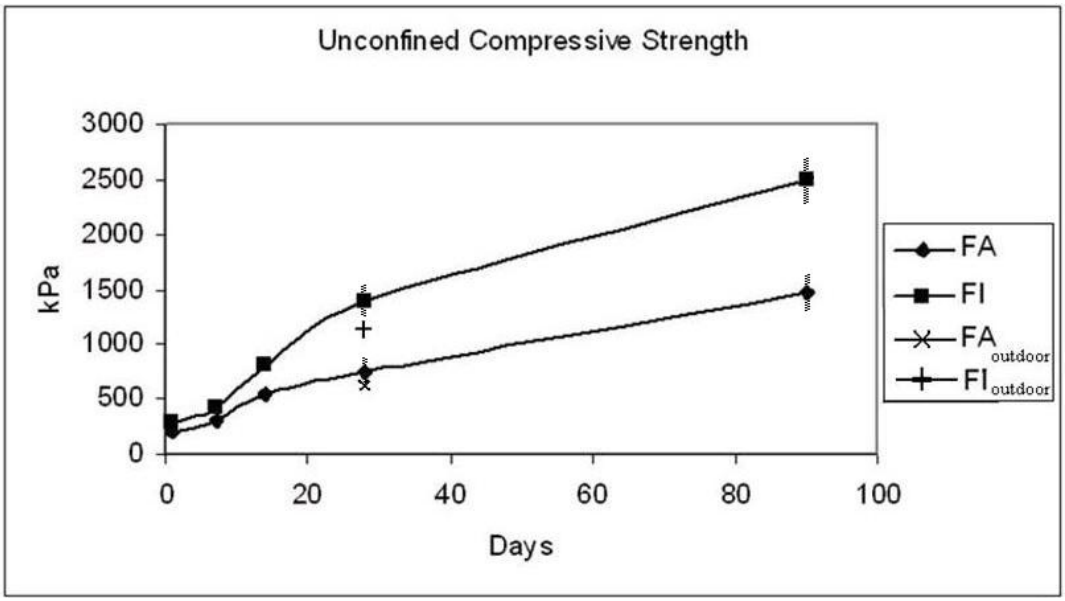

Figure 5.5. Variation of the unconfined compressive strength values of fly ash (FA) and snow-added fly ash (FI) with time.

The stress strain curves obtained by averaging the data of eight samples are presented in Figure 5.6. The shape of the stress-strain curves for snow-added fly ash samples cured for 28 and 90 days states that, the pores are first squeezed up to 0.004 strain, and afterwards the rate of strength gain increased. At 0.008 strain the sample failed. For fly ash only samples, the stress strain curves are flatter. The stress strain curve for 90 days-cured fly ash (FA90) samples is very similar to the stress strain curve of 28 days-cured snow-added fly ash (FI28) samples. Given that the void ratio of snow-added fly ash is approximately 30 per cent higher than that of fly ash samples, the strength improvement due to snow addition is very remarkable.

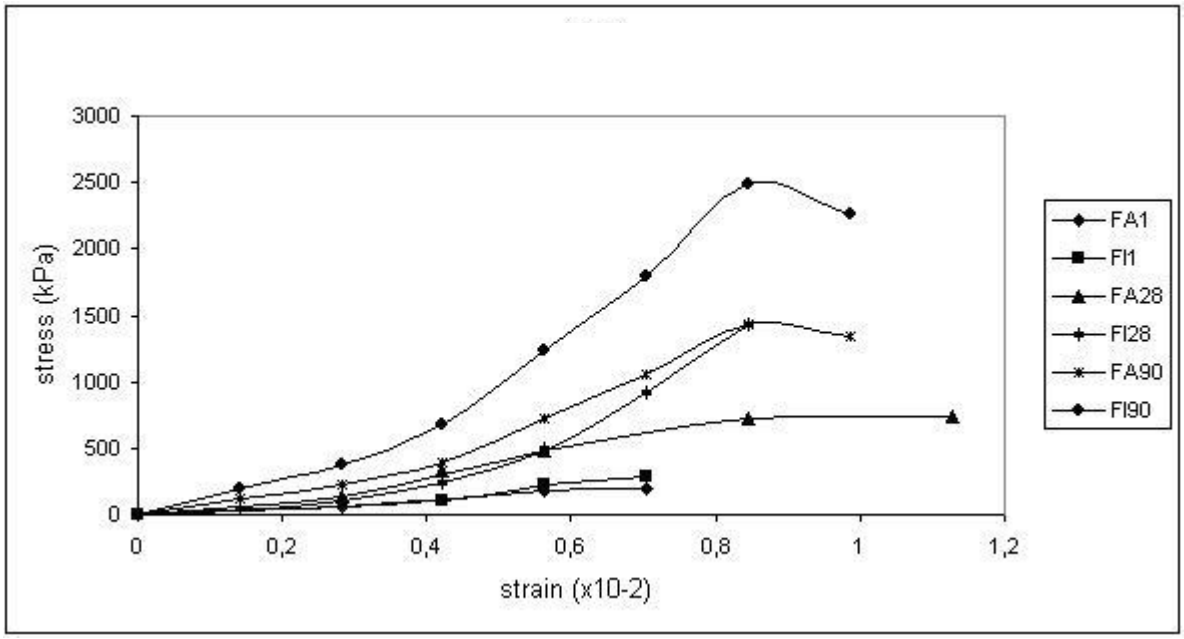

Figure 5.6. Stress-strain curves for samples cured at different time periods (FA1, FA28, FA90, fly ash cured for one, 28, and 90 days at optimum moisture content; FI1, FI28, FI90, snow-added fly ash cured for one, 28, and 90 days).

One of the main products of the reaction between fly ash and water is calcium silicate hydrate (CSH) which is the main source of strength development. CSH is the largest component of the matrix and is the most important component in the hydration process. As the CSH hydrates further, the coating thickness grows forcing the outward spines of adjacent particles to interlock to form solid bonds. The effect is to bond the fly ash grains together with the CSH coating[23].

Hydration of the CSH is not accompanied by an increase in volume. These CSH crystals will only occupy free space in the matrix. The snow-added fly ash samples have 30 per cent more voids than that of the control samples, this leads to more space for CSH crystals to develop which explain the higher unconfined compressive strength values.

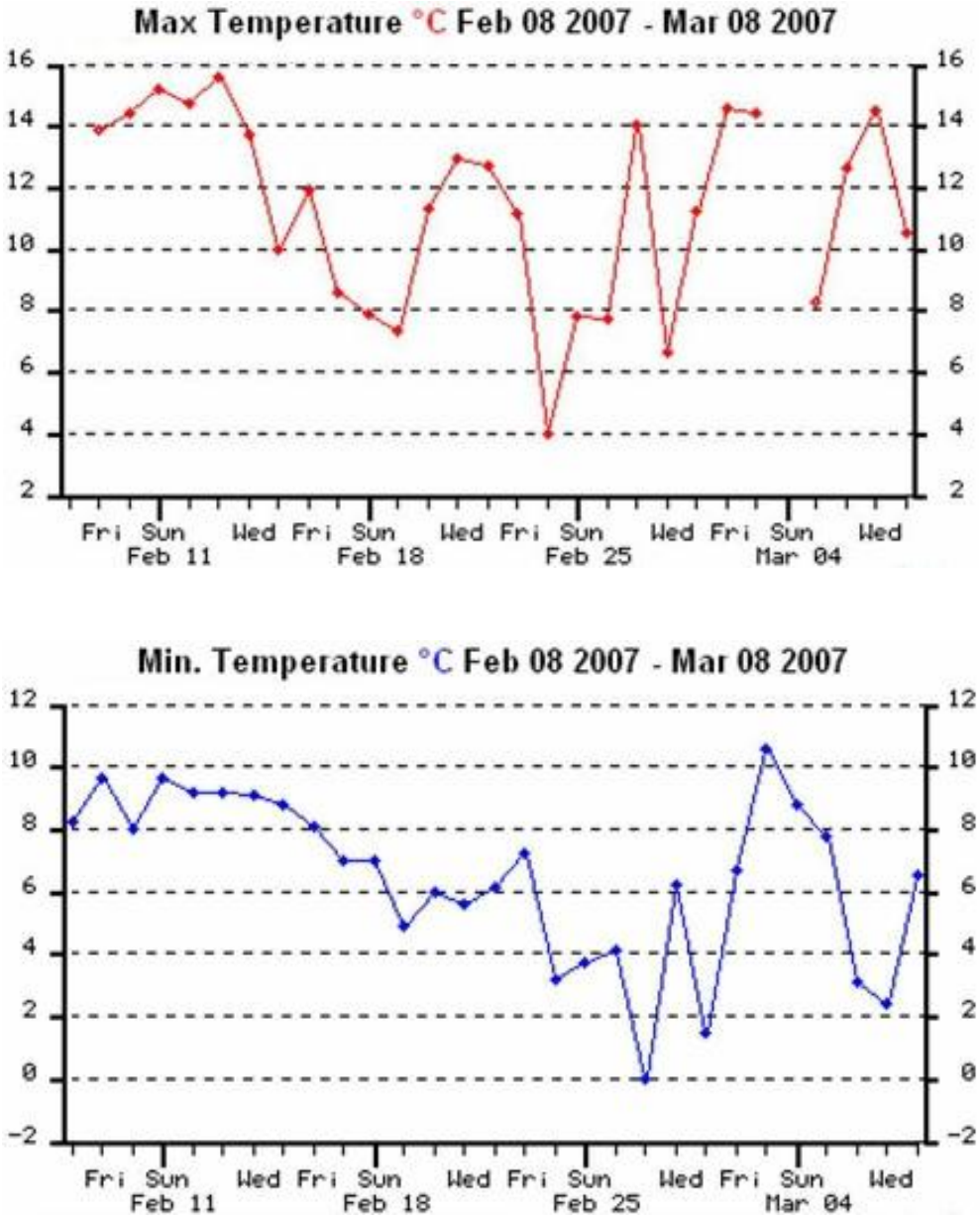

Figure 5.7. The temperature variation of the outdoor curing conditions

5.4. Splitting Tensile Strength Tests

When fly ash is used as a base or sub base layer in a highway pavement, the tensile stresses become important due to the traffic load acting on the pavement. Splitting tensile tests were conducted to observe the behavior of fly ash and snow-added fly ash samples. Splitting tensile strength values of fly ash and snow-added fly ash are given in Figure 5.8 for curing periods between one to 90 days. A similar trend to the one observed for unconfined compressive strength values is observed for curing periods from seven to 90

days. From one to seven days curing period the increase amount in the strength values are lower with respect to seven to 28 days curing results. This strength rate increase after seven days curing can also be seen in the ESEM and XRD observations in the previous sections. The tensile strength values are approximately 10 per cent of unconfined compressive strength values. The tensile strength of snow-added fly ash is 85 per cent higher than the tensile strength of fly ash after 90 days of curing. This observation again confirms the superior performance of snow addition to fly ash. While comparing these two values, the higher void ratio of snow-added fly ash must be kept in mind, stating the effectiveness of the developed technology.

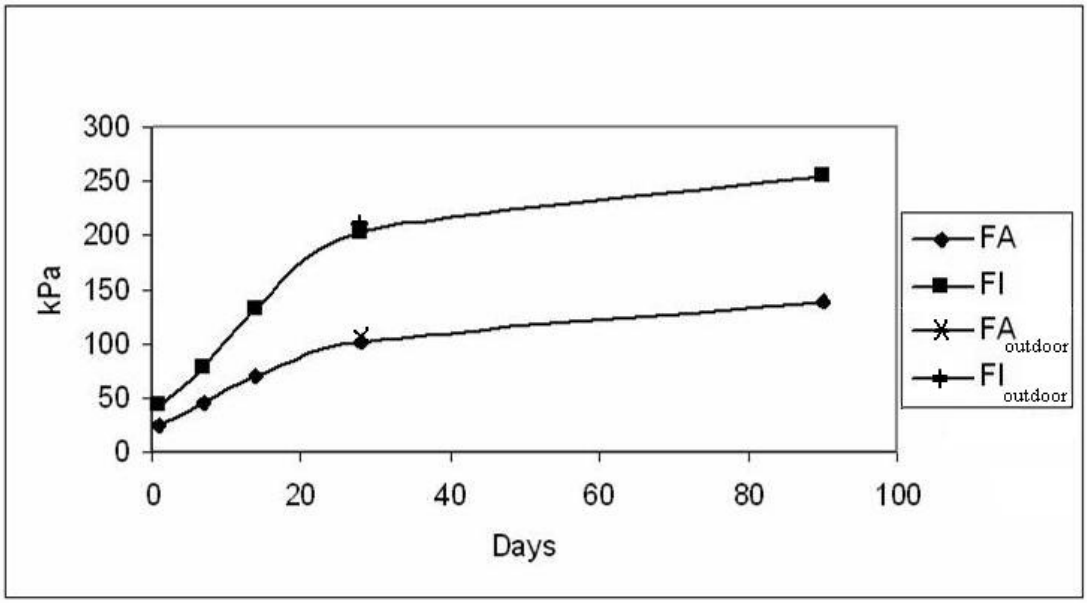

Figure 5.8. Variation of the splitting tensile strength values of fly ash (FA) and snow-added fly ash (FI) with time.

5.5. Hydraulic Conductivity Tests

The hydraulic conductivity coefficient values (k_{av}) for 28 and 90 days cured fly ash and snow-added fly ash are presented in Table 5.2 and Figure 5.9.

The values of k_{av} vary from 3.49×10^{-7} to 8.65×10^{-7} cm/s for fly ash control samples, which are typically in the range of the hydraulic conductivity coefficient of clay. The compacted fly ash, therefore, would be practically impermeable. The values of k_{av} vary

from $1.01x10^{-4}$ to $1.83x10^{-4}$ cm/s for snow-added fly ash samples, which are typically in the range of the hydraulic conductivity coefficient of silty sand. The compacted snow-added fly ash samples, therefore, would be summarized as low permeable.

The snow-added fly ash samples, therefore, cannot be used in seepage barriers such as liners. Clay-like admixtures should be added to the fly ash to reduce its hydraulic conductivity. However, in embankments and retaining walls the snow-added fly ash would demonstrate higher performance than that of the compacted fly ash control samples, because it possesses better drainage characteristics and no tension cracks would develop.

The higher void ratio of snow-added fly ash caused two to three orders of magnitude increase in hydraulic conductivity values. Although this increase in hydraulic conductivity value seems to create problems for leaching potential for heavy metals due to higher percolation of water in fly ash, the increased strength of snow-added fly ash will make it less prone to leaching as will be presented in section 5.12. The snow-added fly ash samples have a stiffer matrix and stronger bonds than that of the fly ash samples compacted at the optimum moisture content, this stronger bonds and stiffer matrix despite the 30 per cent increase in the void ratio lead to less leaching of the heavy metals.

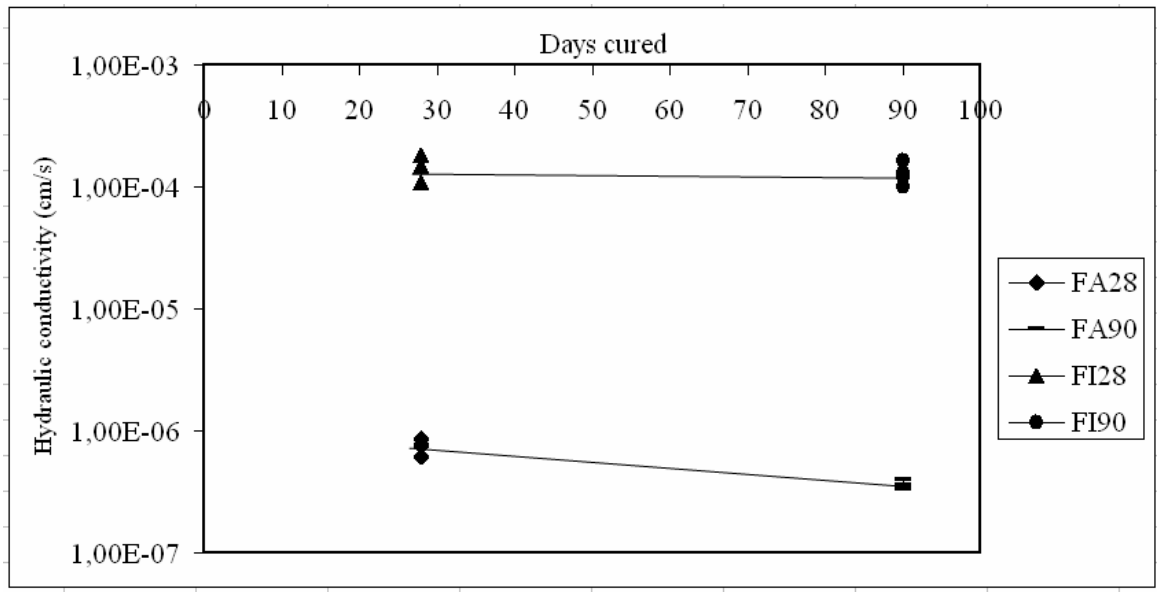

Figure 5.9. Comparison of the hydraulic conductivity values of 28 and 90 days cured compacted fly ash and compacted fly ash & snow

With respect to curing time, extended curing time has a considerable effect on k. Since most strength gain and pozzolanic reaction occurs within the first 28 days of hydration, it is unlikely that k would change significantly beyond 90 days.

Although the self-hardening nature of the class C fly ash is appreciable, its hydraulic conductivity does not vary significantly with time. Therefore, embankments and backfills constructed of snow-added fly ash may continue to remain moderately permeable after construction as well.

Table 5.2. Comparison of the hydraulic conductivity values of 28 and 90 days cured compacted fly ash and compacted fly ash & snow

28 days cured	FA28 (cm/s)	FI28 (cm/s)	FA90 (cm/s)	FI90 (cm/s)
Sample 1	$7{,}72.10^{-7}$	$1{,}47.10^{-4}$	$3{,}27.10^{-7}$	$1{,}01.10^{-4}$
Sample 2	$8{,}65.10^{-7}$	$1{,}83.10^{-4}$	$3{,}49.10^{-7}$	$1{,}21.10^{-4}$
Sample 3	$6{,}11.10^{-7}$	$1{,}09.10^{-4}$	$3{,}98.10^{-7}$	$1{,}65.10^{-4}$
Average of the three test samples	$7{,}50.10^{-7}$	$1{,}46.10^{-4}$	$3{,}58.10^{-7}$	$1{,}29.10^{-4}$

5.6. pH Measurements

pH of the effluent from the leaching tests was measured and recorded immediately after collecting the leachate samples. The pH of the influent (deaired-distilled water) was 7.0.

The pH measurements represented a small difference between control fly ash samples and snow-added fly ash samples compacted at optimum moisture content as represented in Table 5.3. pH of the leachate from the leaching tests is also shown in Figure 5.10 as a function of natural snow content and curing period. pH values of the leachate decreases with increasing curing period for control fly ash samples, however the pH value increases with increasing curing period for snow-added fly ash samples. Within the 28 days curing

period the total amount of voids in the fly ash mixtures increase with 10 per cent natural snow addition, which is primarily responsible for higher pH at higher fly ash content. As the curing period reaches 90 days, the voids are more occupied with the hydration products and the pH values of natural snow-fly ash mixtures show an increasing trend as shown in Figure 5.10. The average pH of the leachate was highest for control fly ash cured for 28 days and lowest for control fly ash samples cured for 90 days. For most cases, pH of the leachate increases appreciably when the fly ash content increases. In this study as the curing period reaches 90 days the pH values of the control fly ash specimens decreased and the pH values of snow-added fly ash samples increased. The increasing trend in the snow-added fly ash samples gave rise to less leaching of metals and the decreasing trend in the control fly ash samples caused an increase in heavy metal leaching as will be presented in section 5.12.

Table 5.3. Comparison of the leaching fluid pH values of 28 days cured compacted fly ash and compacted fly ash & snow

	Fly Ash (FA)	Fly Ash + Snow (FI)
28 days cured	12,44	12,14
90 days cured	12,10	12,32

pH is one of the most important factors affecting heavy metal leaching from fly ash. The leachability of cationic metals such as cadmium, chromium, zinc, lead, mercury, and silver increases with decreasing pH.

Mineralization of Coal Combustion ByProducts (CCBs) have shown to play an important role in the mobility of constituents from CCBs. These reactions take extended periods of time and occur over days or even months. Ettringite is a mineral having the nominal composition $Ca_6Al_2(SO_4)_3(OH)_{12}•26H_2O$, is an example of a hydrated mineral. Direct evidence of ettringite formation is seen both in control fly ash and snow-added fly ash samples by using the XRD methods. If the proper ingredients: aluminum, calcium, sulfate and alkalinity are present, ettringite forms[83]. Ettringite is the primary hydration

product that forms when coal ash and water combine under alkaline conditions with a nominal pH between 11.5 and 12.5. Although this optimal pH range is required for ettringite formation, the bulk pH of samples may be below this limit and ettringite can still form. This is because of localized high pH at the ash granule-water interface. Because ettringite formation can result in very efficient removal of select oxyanionic species, its formation in ash projects is highly desirable.

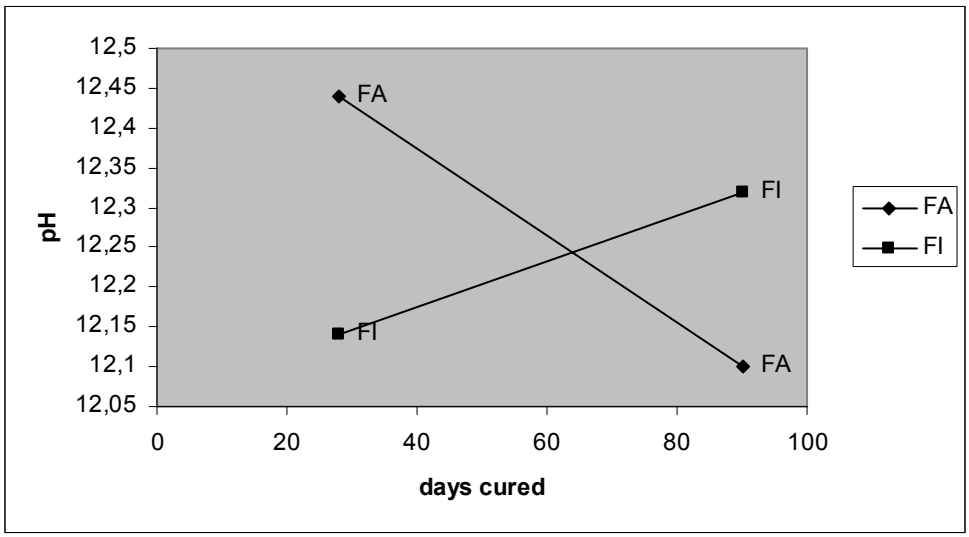

Figure 5.10. pH values of fly ash (FA) and snow-added fly ash (FI) with time.

The final pH levels of all the control fly ash and snow-added fly ash sample leachates are alkaline. The general observation for these pH determinations is that all of the mixtures were potentially capable of ettringite formation.

5.7. Temperature Measurement of Fresh Specimens

The temperature of control fly ash was measured to be 24^0C when the hydration process began, and the temperature decreased to 21^0C after five hours shown in Figure 5.11. In the case of water and 10 per cent by weight snow-added fly ash, the temperature dropped down to 3^0C after 70 minutes, and began to rise reaching 21^0C after 10 hours. The drop in temperature slows down the hydration process in the first hours of hydration, providing longer time for cementitious minerals to develop. Definitely the effect of higher

water content provided with the addition of snow is the main contributor in more cementitious mineral formation leading to higher strength.

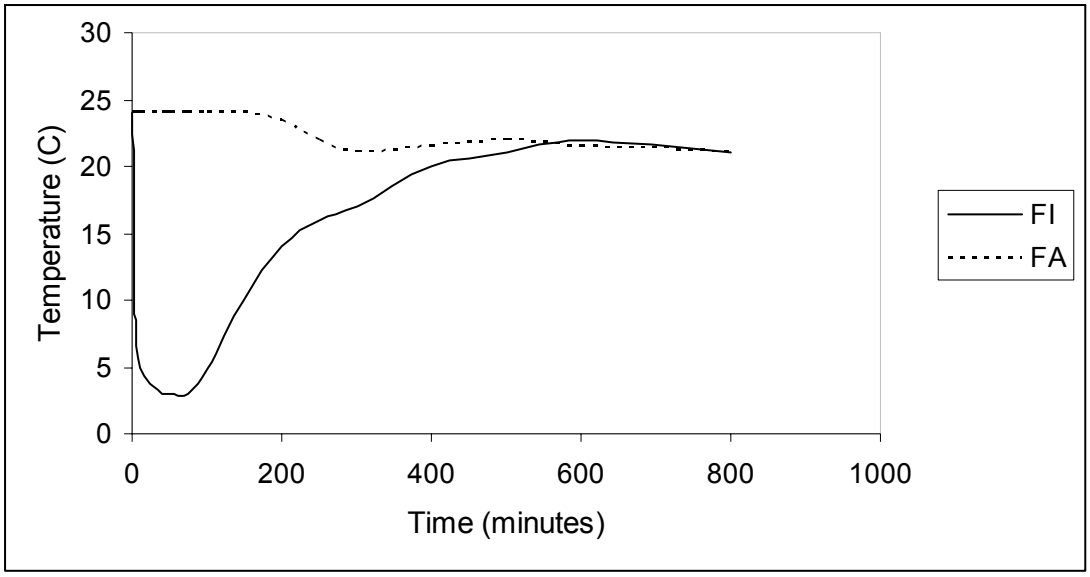

Figure 5.11. Temperature variation of fly ash (FA) and snow-added fly ash (FI) with time.

The temperature change of the compacted samples during the initial phase of hydration is observed with an infrared camera. An advantage of visualization with an infrared camera is the possibility of registering almost continuously time sequences, which allows analyses of phases with a strong transient character. A sequence of temperature profiles derived from infrared images obtained during the first minutes of curing of the samples are presented in Figure 5.12. The images represent the surface of the compacted samples.

In each image, the temperature is scaled to the respective minimum and maximum to obtain the best possible contrast. The minimum and maximum temperatures are presented in degrees centigrade on the scale below each figure. In Figure 5.12.b., the minimum temperature recorded in snow-added fly ash is 8^0C after five minutes of curing. After 240 minutes the recorded temperatures at the surface of the samples are similar for fly ash and snow-added fly ash.

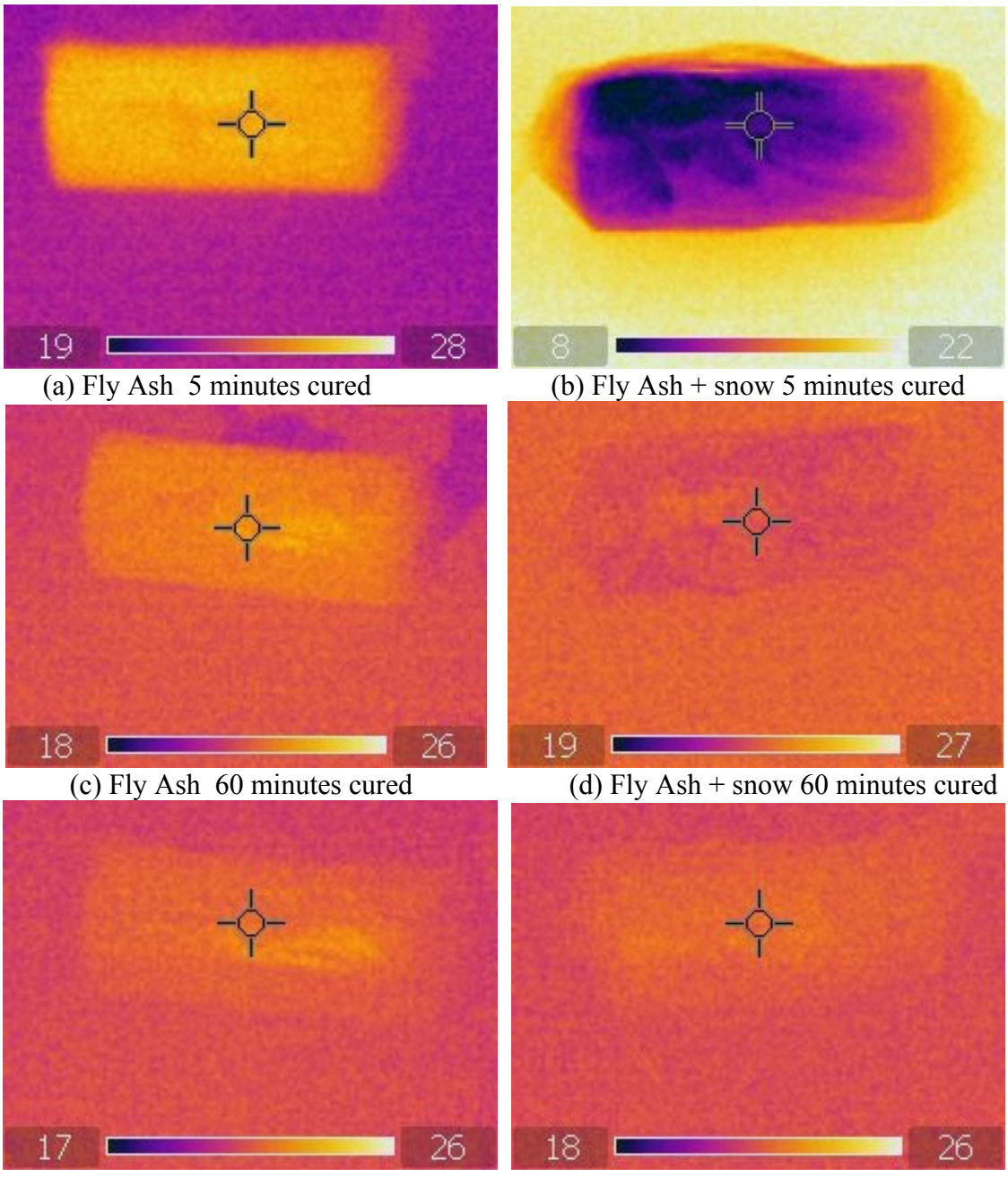

(a) Fly Ash 5 minutes cured (b) Fly Ash + snow 5 minutes cured

(c) Fly Ash 60 minutes cured (d) Fly Ash + snow 60 minutes cured

(e) Fly Ash 240 minutes cured (f) Fly Ash + snow 240 minutes cured

Figure 5.12. The Thermal imager images after 5, 60 and 240 minutes curing at 21^0C.

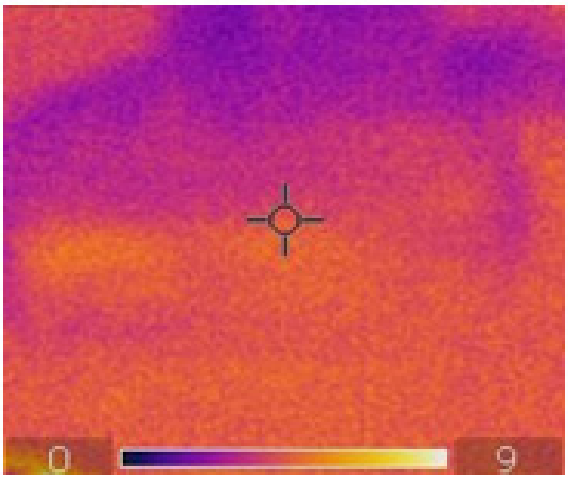

(a)Fly Ash 5 minutes cured

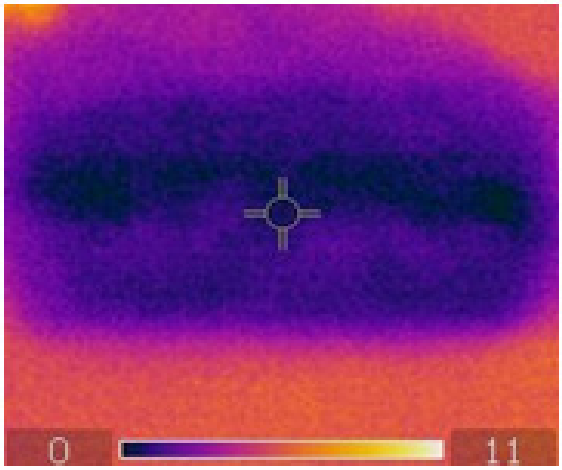

(b) Fly Ash + snow 5 minutes cured

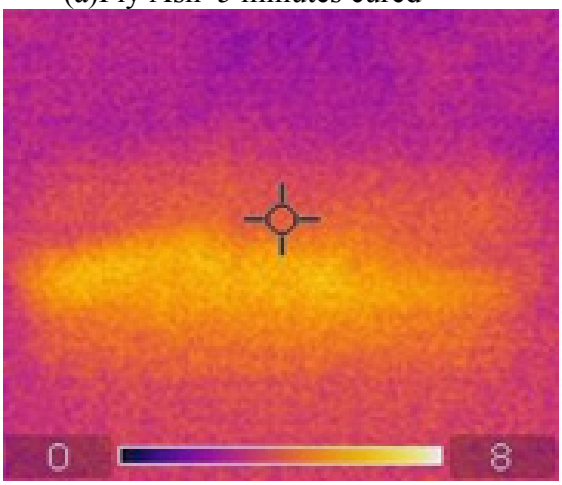

(c) Fly Ash 60 minutes cured

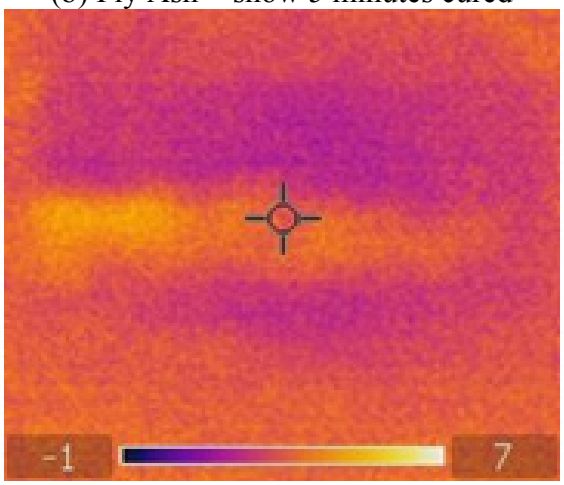

(d) Fly Ash + snow 60 minutes cured

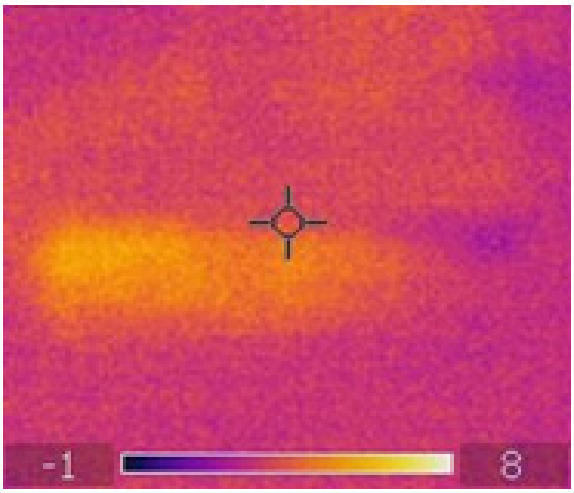

(e) Fly Ash 240 minutes cured

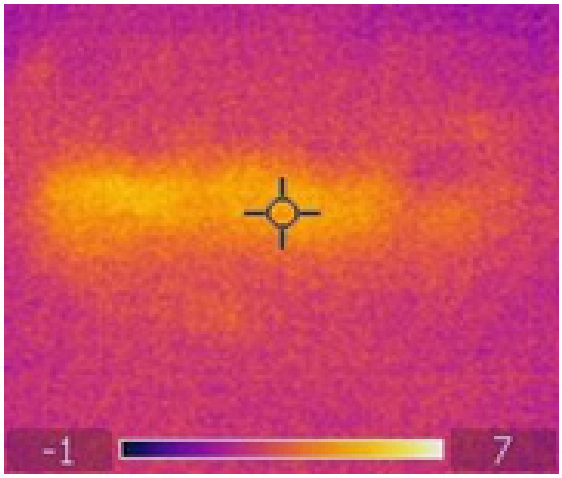

(f) Fly Ash + snow 240 minutes cured

Figure 5.13. The Thermal imager images after 5, 60 and 240 minutes curing at 2^0C.

Natural snow addition to fly ash samples lead to lower hydration degrees for the first four hours curing. The emphasis here is on the influence of natural snow on the setting and hardening process of fly ash specimens. Natural snow addition causes a retardation of 4 hours. The thermal images of samples FA and FI describe the effect of natural snow addition in delaying the hydration stage. The delayed setting and hardening stages of fly ash samples can be attributed to natural snow addition to fly ash samples.

In Figure 5.13 the thermal imager images after five ,60 and 240 minutes curing at $+2^0$C is presented. The minimum temperature recorded in snow-added fly ash sample is -1^0C after five minutes of curing. After 240 minutes, the recorded temperatures at the surface of the samples are similar for control fly ash and snow-added fly ash samples. This similarity demonstrates that the hydration rate is slowed by snow addition both in laboratory and field conditions. Figure 5.12 represents the laboratory test conditions. Figure 5.13 represents the field conditions. X-ray diffraction method is used to analyze the degree of hydration of control fly ash and snow-added fly ash samples. The results are presented in section 4.1.

5.8. Radioisotope Activity Comparison

Lignite, like all minerals, contains natural radionuclides from the uranium, thorium and radon series. These nuclides will therefore be present in fly ash, and their activity concentration should be determined prior to using these ashes in several applications. The radioactivity of fly ash may also become an important concern depending on the source of coal used in the thermal power plants.

Gamma radiation is more harmful to living organisms when compared to other sources of radiation. High levels of gamma rays can produce dangerous ionization of the tissue and cause skin cancer.

Alpha particles are made of two protons and two neutrons. This means that they have a charge of +2, and a mass of four (the mass is measured in "atomic mass units", where each proton & neutron is equal to one). Alpha particles are relatively slow and heavy. They have a low penetrating power, anybody can stop them with just a sheet of paper.

Beta particles have a charge of minus one, and a mass of about $1/2000^{th}$ of a proton. This means that beta particles are the same as an electron. They are fast, and light. Beta particles have a medium penetrating power, beta particles can be stopped by a sheet of aluminium or plastics such as perspex.

Gamma rays are waves, not particles. This means that they have no mass and no charge. Gamma rays have a high penetrating power, it takes a thick sheet of metal such as lead, or concrete to reduce the gamma rays significantly.

Determination of the radioactivity content of fly ash can be accomplished using gamma spectrometry, with a minimum of sample preparation and good sample throughput. The activities of ^{235}U, ^{226}Ra, ^{238}U, and ^{232}Th of the fly ash and snow-added fly ash samples compacted at optimum moisture content are determined and presented in Table 5.4. The snow-added fly ash samples compacted at optimum moisture content represented a 31-42 per cent decrease in radiation amounts in Bq/kg. This decrease in the radiation values is because of the 30 per cent increase in the void ratio and the firm cementitious matrix produced as a result of the hydration process of the snow-added fly ash samples.

Table 5.4. Comparison of the radioisotope activities of 28 days cured compacted fly ash and compacted fly ash & snow

	Fly Ash (FA) (Bq/kg)	Fly Ash + Snow (FI) (Bq/kg)	% Change
^{235}U	12±2	7±2	42% decrease
^{226}Ra	248±6	154±3	38% decrease
^{238}U	207±6	142±4	31% decrease
^{232}Th	51±4	35±2	31% decrease

More recently, The International Union of Producers and Distributors of Electrical Energy (UNIPEDE) produced a report[84] that reviewed various features of fly ash including the radiological properties. UNIPEDE summarized the radioactivity from fly ash around Europe as in Table 5.5

Table 5.5. Radioactivity in fly ash in Bq/kg (UNIPEDE)

Reports from	Fly Ash from	U-Series			Th-Series		
		Min	Max	Average	Min	Max	Average
Germany	Germany	93	137	119	96	155	121
	UK	72	105	89	3	94	68
	Australia	7	160	90	7	290	150
	Poland			350			150
Italy	Italy	130	210	170	100	190	140
Denmark	Denmark	120	210	160	66	190	120
Sweden	Sweden	150	200		150	200	
Belgium	Belgium	112	316	181	88	277	150
Spain	Spain	80	106	91	77	104	89
Germany				189			118
Czech Rep.	Czech Rep.	35	190	129	62	142	90

UNIPEDE refer to the World Energy Conference Report that suggests an average specific activity concentration of 200 Bq/kg. It is clear from the table that some countries may have some difficulties with such limits.

From the experimental results it can be seen that the control fly ash specimens' 238U and 226Ra activity values are over the critical limits (200Bq/kg). However, snow-added fly ash specimens' 238U, 226Ra, 235U and 232Th activity values are under the limiting value 200Bq/kg.

For control fly ash samples the values for 226Ra and 238U are higher than that of the reference level, while 235U and 232Th activites are within the critical limits. For snow-added fly ash samples the values for 226Ra, 238U, 235U and 232Th activities are within the critical limits.

The relatively higher radon, uranium and thorium content of control fly ash samples may be attributed to the higher unit weight and weak CSH gel structure.

During the 28 days curing period, it is evident that the radioisotope activity is mainly controlled by the emanation from the superficial pores. The decrease in radioisotope activities for snow-added fly ash samples can be directly linked with the extra moisture obtained by snow melting in the superficial pores, the radon atoms are trapped inside superficial pores by moisture. The lower radioisotope activity rates for 28 days curing period is suggested to be due to high moisture content of the superficial pores and the consequent inhibition of diffusion of radon atoms from the pores.

The results show that the snow-added fly ash samples pose less radiation than that of the control fly ash samples and indicate that the snow-added fly ash samples examined in this work could be used in embankment construction without exceeding the proposed radioactivity criterion level. It is desirable to select the construction materials of low specific radioactivity for use in road construction.

It should be noted that fly ash, even when coming from a single power plant, is not homogenous with respect to radioactivity content. Therefore, the radioactivity levels in fly ash may vary considerably. Detailed investigation of the issue should be performed even depending on the sampling location within the power plant.

In cases where ash is used on a large scale, such as road construction, where guidelines for acceptable radioactivity levels do not exist, laboratory analyses should be supplemented with in situ gamma spectrometry and dosimetry. In situ spectrometry can be performed using Ge detectors, similar to those used in a laboratory setting, while basic dosimetry can be performed with a simpler, appropriately calibrated instruments.

5.9. Resistance of Samples to Rapid Freezing and Thawing

An automatic environmental freeze-thaw cabinet was used to carry out the accelerated freeze-thaw test. The freezing and thawing apparatus consisted of suitable chambers in which the specimens are subjected to the specified freezing and thawing cycles, together with the necessary refrigerating and heating equipment and controls to produce continuously, and automatically, reproducible cycles within the specified temperature requirements as seen in Figure 5.14.

(a)

(b)

Figure 5.14. Automatic environmental cabinet used to carry out the accelerated freeze-thaw test

The apparatus is so arranged that, except for necessary supports, each specimen is completely surrounded by not less than one mm, nor more than three mm of water at all

times while it is being subjected to freezing and thawing cycles. Each specimen is supported at the bottom of its container in such a way that the temperature of the heat-exchanging medium will not be transmitted directly through the bottom of the container to the full area of the bottom of the specimen, thereby subjecting it to conditions substantially different from the remainder of the specimen. A flat spiral wire (D=3mm) is placed at the bottom of the containers.

Figure 5.15. Resonant frequency test setup

The fundamental resonant frequencies were determined using the forced resonance method. The supported specimens were forced to vibrate by an electromechanical driving unit. The specimen response was monitored by a lightweight pickup unit on the specimen. The driving frequency is varied until the measured specimen response reached a maximum amplitude. The value of the frequency causing maximum response is the resonant frequency of the specimen. Figure 5.15 represents the resonant frequency measurement test setup.

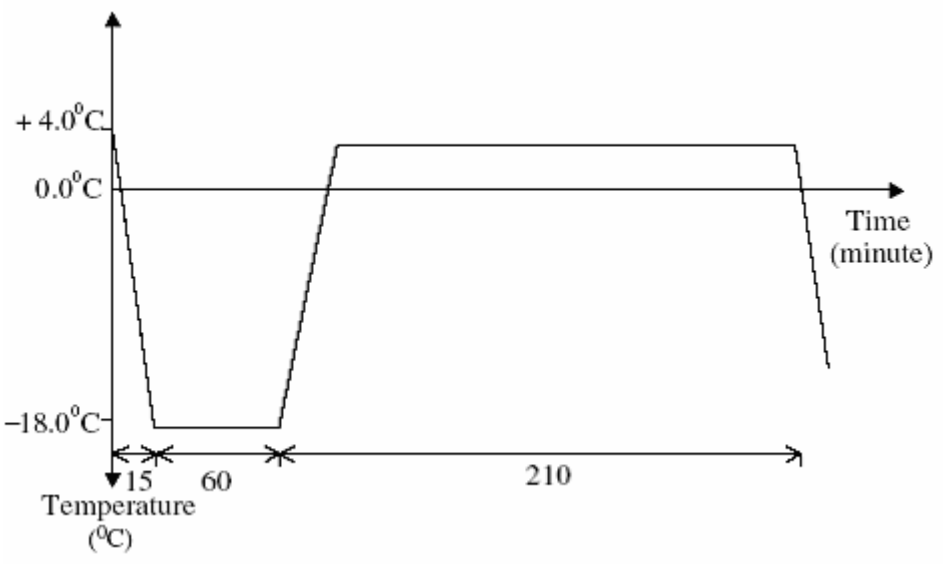

Figure 5.16. Freeze-thaw cycle of the specimens (ASTM C666 procedure A)

During the test it was also noted that at the end of the thawing phase ice was not melting completely. This would have resulted in prolonged freezing time as opposed to freezing and thawing cycle. Hence a trial test was carried out to change the cycle to ensure thawing and this cycle was adopted for the study (Figure 5.16).

Weight change was also monitored during the test. As the test proceeded, samples developed cracks along the sides about mid depth and the lower and upper part of the samples started to break off. Hence deterioration was noted by a decrease in weight and damage was assessed by rating based on visual observation and weight change, as given in Table 5.6. These cracks became more prominent and widespread as the test progressed, resulting in spalling and eventual breaking down of the samples. The progress of deterioration was monitored by visual inspection and rating on a scale of zero–five, zero being no damage and five being total break down. Table 5.7 gives the visual observation data during the test.

Table 5.6. Visual rating

Rating	Description
1	Less than 25% of surface has exposed aggregate
2	Wide spread surface scaling.
3	Scaling along with cracks on the sides and bottom of the slabs.
4	Well developed cracks reaching the top surface
5	Fully broken

Table 5.7. Development of deterioration of the test specimens

Specimens														
Days cured	90							180						
No. of FT cycles	0	5	18	33	65	91	121	0	5	18	33	65	91	121
	Visual ratings													
Fly Ash(FA)	-	-	2	3	4	5	-	-	-	2	3	4	5	-
Fly Ash + snow (FI)	-	-	1	1	2	3	5	-	-	1	1	2	3	5

Damage to the fly ash structure due to freeze-thaw occurred because of the hydraulic pressure developed when water in the saturated pores freezed and increased its volume and certain amount of water forced out of the pores; the osmotic pressure caused due to the movement of water from the smaller pores to the larger pores, where ice is formed, in order to re-establish equilibrium between the concentrations of solutions in the pores.

In the case of control fly ash samples the specimens started to indicate deterioration within 18 cycles of freezing and thawing. By 91 cycles, fly ash samples had broken down (Table 5.7). There appears to be not much difference in the freeze-thaw durability of 90 and 180 days cured fly ash specimens. The snow-added fly ash samples showed a more durable behavior. This is because of the variation of the pore structure in the matrix. It could be seen from Table 5.7 that the control fly ash specimens deteriorated much faster than snow-added fly ash samples. Test was continued for up to 121 cycles for snow-added samples and at 91 cycles still the visual rating was only 3 for the snow-added fly ash samples. This indicates that 10 per cent snow addition to the matrix can improve the freeze-thaw durability of compacted fly ash samples to a certain extent.

It can be seen that at around 18 cycles, fly ash samples had lost about 75 g. (cumulative) through scaling. In the case of snow-added fly ash samples a similar cumulative scaling weight was found only after around 65 cycles and still the samples were not broken (Figure 5.18 and Figure 5.21). These snow-added fly ash samples lasted through out the 121 cycles, passing 91 cycles of the test without being broken down (Figure 5.19 and Figure 5.22). When the weight began to reduce due to deterioration, the reduction was rapid for both fly ash and snow-added fly ash samples. However, the number of cycles at which breaking of the specimens began was significantly affected by the presence of snow in the specimens as can be seen from Figure 5.23. Images representing different freeze-thaw cycles are represented through Figures 5.17 to 5.22.

(a) FA 90 after 33 cycles (b) FI 90 after 33 cycles

Figure 5.17. 90 days cured samples after 33 freeze thaw cycles

(a) FA 90 after 65 cycles (b) FI 90 after 65 cycles

Figure 5.18. 90 days cured samples after 65 freeze thaw cycles

(a) FA 90 after 91 cycles (b) FI 90 after 91 cycles

Figure 5.19. 90 days cured samples after 91 freeze thaw cycles

(a) FA 180 after 33 cycles (b) FI 180 after 33 cycles

Figure 5.20. 180 days cured samples after 33 freeze thaw cycles

(a) FA 180 after 65 cycles (b) FI 180 after 65 cycles

Figure 5.21. 180 days cured samples after 65 freeze thaw cycles

(a) FA 180 after 91 cycles (b) FI 180 after 91 cycles

Figure 5.22. 180 days cured samples after 91 freeze-thaw cycles

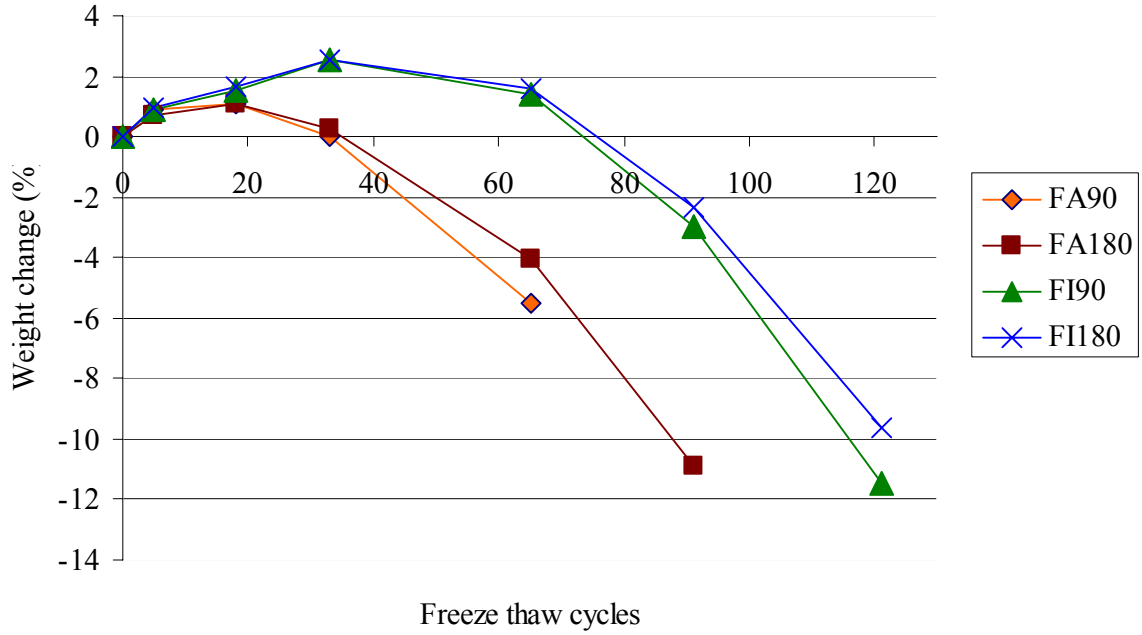

Figure 5.23. Deterioration pattern due to ASTM C666 test.

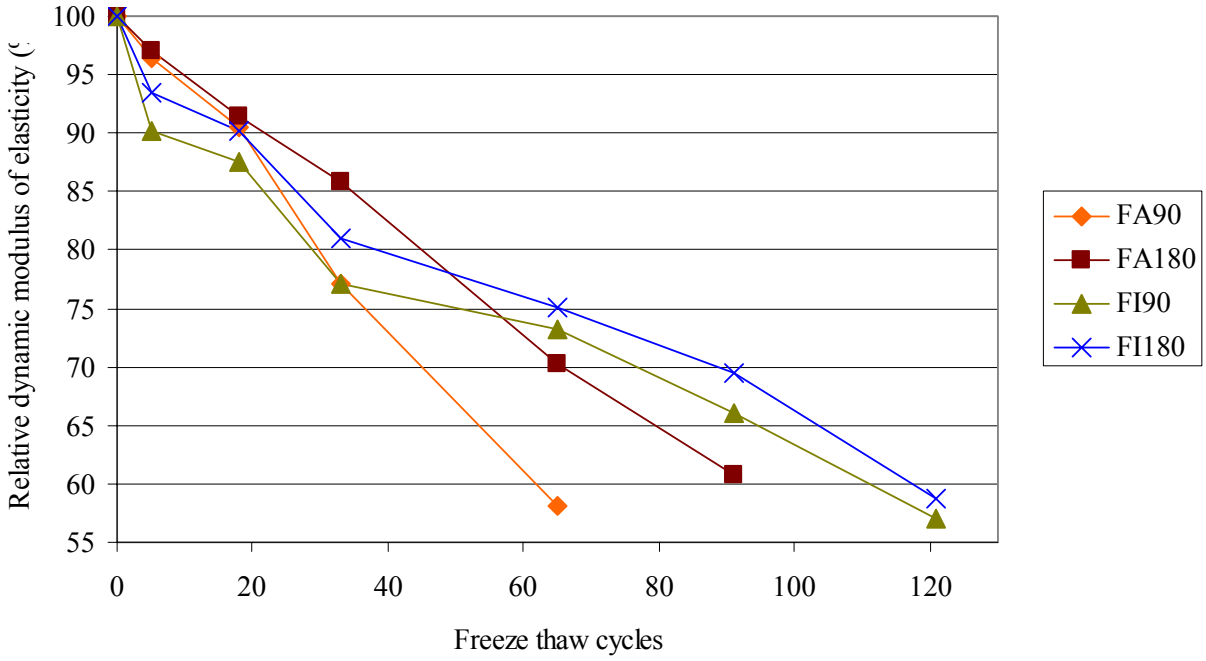

Figure 5.24. Durability factors of control compacted fly ash and snow-added fly ash samples

In this test natural snow was tested for its effectiveness in increasing the freeze-thaw property of the fly ash specimens. As can be seen from Table 5.7, it had a remarkable effect on improving the freeze-thaw property of the compacted fly ash blocks. Natural snow addition to the control specimens made the natural snow-added test specimens pass the freeze-thaw test with less damage to the test specimens. This appears to be the most effective and economical method to improve the freeze-thaw property of the compacted fly ash specimens. Also, natural snow addition does not add significant work or cost to the process.

This result is consistent with previously reported results from control fly ash and snow-added fly ash samples and it suggests that snow addition has positive impact on freezing and thawing behavior. The weight gain phenomena in this test might be attributed to water gain of samples in the freezing and thawing machine, which were sealed and cured for 90 to 180 days in the humid room. Figure 5.24 shows the durability factors of the control fly ash and snow-added fly ash samples, which correlated roughly with the weight

loss percentages in Figure 5.23. Snow addition substantially impacts the freezing and thawing behavior of the fly ash specimens with extra moisture supply and air entrainment.

By natural snow addition, controlled amount of microscopic snow crystals into fly ash specimens are entrained. Snow crystals preserved stability during mixing, transporting, placing compaction and hardening. Snow addition is done to improve the freeze-thaw resistance of fly ash specimens by 30 per cent increase in void ratio. In winter time, water in capillary pores expands on freezing resulting in disruptive internal stresses. Successive cycles of freezing and thawing may lead to progressive deterioration. By snow addition, voids uniformly dispersed in the matrix (created after melting of snow) provide a reservoir for water to expand. Snow addition amount of 10 per cent by weight of fly ash has provided protection to the test specimens.

5.10. Thermal Conductivity Analysis

The hot box apparatus, constructed to measure the heat transfer in the horizontal direction, is used for testing walls and other vertical structures. When constructed to measure heat transfer in the vertical direction, the hot box is used for testing roof, ceiling, floor, and other horizontal structures. The hot box apparatus constructed was able to measure the rate of heat flow through an element of known area for known test conditions while limiting extraneous heat flows. The hot box apparatus was required to establish and maintain a desired steady temperature difference across the test specimen for the period of time. The elapsed time required is that necessary to ensure constant heat flow and steady temperatures, and, for an additional period adequate to measure these quantities to the desired accuracy.

To determine the conductance, the transmittance, or the resistance, of the test specimens, it is necessary to know the area, the net heat flow, and the temperature differences, all of which shall be determined under such conditions that the flow of heat is steady.

In the hot box test setup the area and temperatures were measured directly. The heat flow Q, however, could not be directly measured. To determine the net heat flow through

the specimen, a five-sided metering box is placed with its open side against one face of the specimen.

The net heat transfer through the specimen was determined from the net measured heat input to the metering chamber. A need exists for accurate data on heat transfer through specimens at representative test conditions. The hot box test method is more suitable for providing such data for these specimens, which are exposed to temperature-controlled air on both sides.

The materials used in the construction of the hot box apparatus had a high thermal resistivity, low heat capacity and high air flow resistance. Polystyrene have been used since it combines high thermal resistivity, good mechanical properties, and ease of fabrication.

It is well known that the thermal behavior of the compacted fly ash specimens is related to their density. By lowering the density of fly ash specimens, a lower thermal conductivity can be achieved. Therefore, by creating air-bubble or voids in the fly ash specimens, lightweight samples with low thermal conductivity can be produced. The selection of lightweight compacted fly ash specimens are controlled by the properties required in the finished product: density, cost, strength, and thermal conductivity.

Research in recent projects in Boğaziçi University Karl Terzaghi Soil Mechanics and Geotechnics Laboratory has been focused on the potential uses of waste and by-product materials. Finding a useful and cost-effective utilization of such materials can help in protecting the environment as well as reducing the cost of construction. Although much work has been done on the effect of using natural snow on the mechanical properties of compacted fly ash specimens, very little research has been done on thermal conductivity.

The blocks were produced from fly ash (control samples) and natural snow-added fly ash which were used with different proportions in the mix as represented in Figure 5.27. The mechanical and thermal properties of the three types of compacted block specimens were compared with the control block specimens. In order to determine the thermal conductivity of the specimens, a guarded hot box was constructed in accordance with ASTM C1363. The specimens were located on the sixth side of the box. An electric heater

with a fan was used to heat the box from inside. Two thermocouples were stuck on the inside and outside of each face of the box.

Table 5.8. Properties of fly ash and snow-added compacted fly ash samples used for thermal insulation (cured for 90 days)

	Weight (grams)	Unit Weight (grams/cm^3)	K (W/m^0 C)	Change(%)
FA	411,14	13,29	0,301	-
FI10	379,02	12,62	0,342	13,6
FI20	340,01	11,26	0,369	22,5
FI30	264,97	9,15	0,359	19,2

A thermal imager was used for monitoring the temperature at the outside surface of the test specimens. Steady state conditions were reached in about 10 hours. The interior of the box was kept at about 52 ^{0}C.

By comparing three types of snow-added fly ash specimens for thermal insulation, it was found that 20 per cent snow-added fly ash specimen was a better mixture for making blocks having better thermal properties. 20 per cent snow-added fly ash block was found to be superior to 10 per cent, 30 per cent snow-added and control fly ash block in terms of thermal conductivity, K ranging from 0.369 to 0.301 W/m^{0}C as shown in Table 5.8. 30 per cent snow-added fly ash block was found to be superior to 20 per cent, 10 per cent snow-added and control fly ash block in terms of weight.

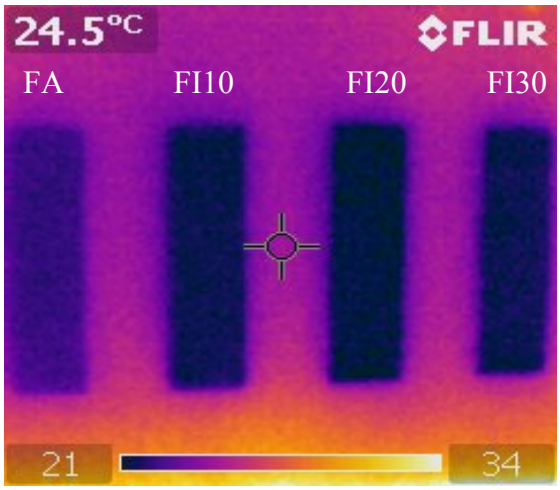

(a) Fly Ash samples after five minutes

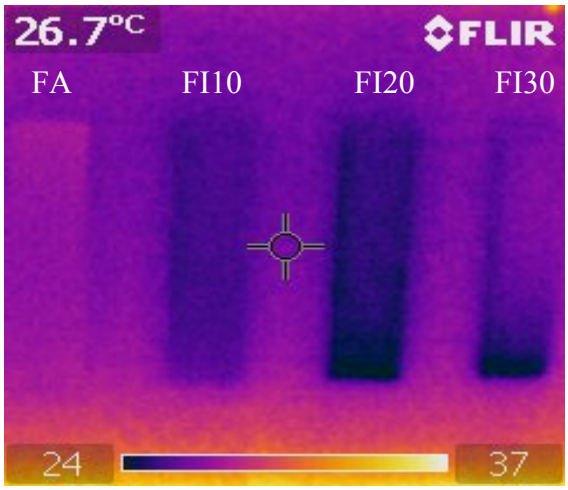

(b) Fly Ash samples after 60 minutes

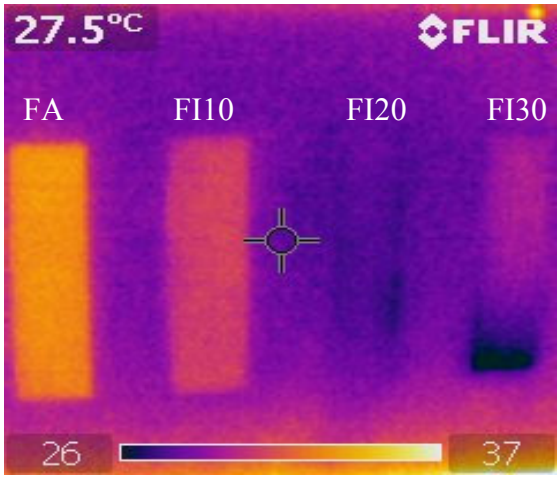

(c) Fly Ash samples after 240 minutes

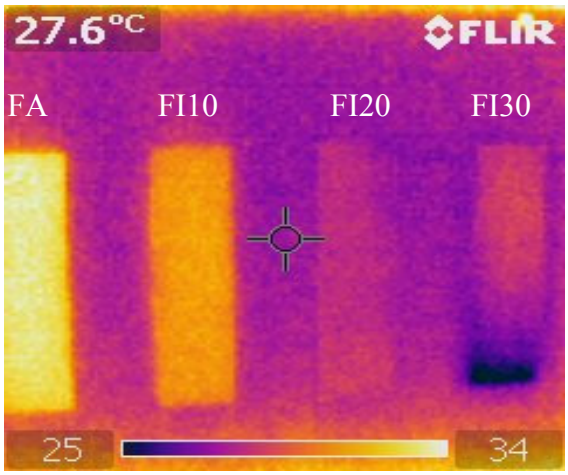

(d) Fly Ash samples after 380 minutes

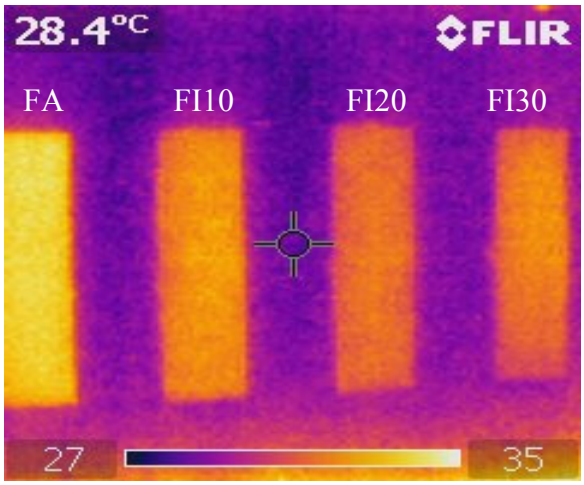

(e) Fly Ash samples after 1625 minutes

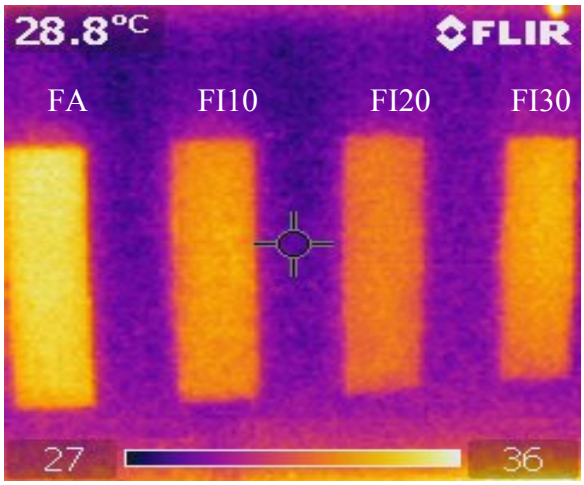

(f) Fly Ash samples after 2800 minutes

Figure 5.25. The thermal imager images taken at different time periods on the surface of the hotbox apparatus.(FA,FI10,FI20,FI30)

The efficiency of the compacted fly ash blocks was under investigation by monitoring the thermal variation during the test period. The thermal imager images taken at different time periods on the surface of the hotbox apparatus are presented in Figure 5.25. Heat transferred through the test specimens is continuously monitored by thermal imager from the outer sides of the specimen blocks and recorded to the storage area of the thermal imager. The surface temperatures of the specimens recorded at different time periods on the surface of the hotbox apparatus (FA, FI10, FI20, FI30) are represented in Figure 5.26. The outside and inside temperature of the hotbox apparatus are also recorded.

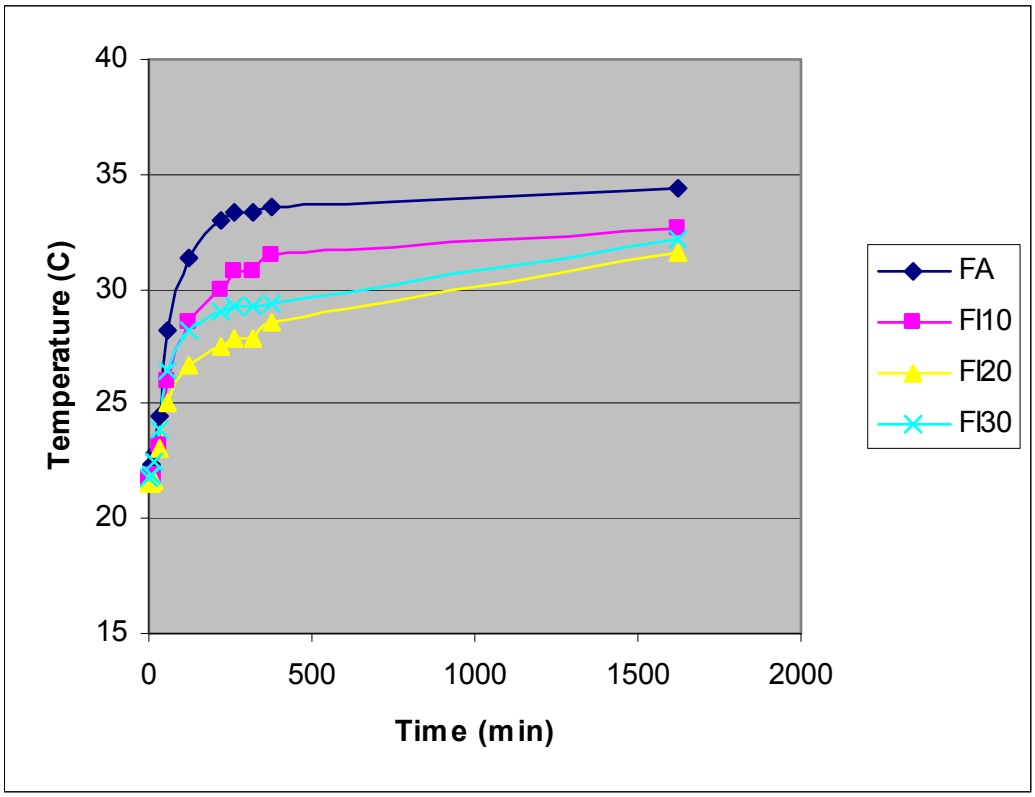

Figure 5.26. The surface temperatures of the specimens recorded at different time periods on the surface of the hotbox apparatus. (FA,FI10,FI20,FI30)

Table 5.9. The surface temperatures of the specimens recorded at different time periods on the surface of the hotbox apparatus. (FA,FI10,FI20,FI30)

Time (min)	inside temp (^{0}C)	FA surface temp	FI10 surface temp	FI20 surface temp	FI30 surface temp
0	20	22	21,7	21,5	21,8
5	52	22,2	21,8	21,6	21,9
10	52	22,4	21,8	21,6	21,9
15	52	22,8	21,9	21,7	22,5
30	52	24,5	23,2	23,1	23,9
60	52	28,2	26	25	26,5
120	52	31,4	28,5	26,7	28,2
220	52	33	30	27,5	29
260	52	33,3	30,8	27,8	29,3
320	52	33,3	30,8	27,8	29,3
380	52	33,6	31,5	28,6	29,4
1625	52	34,4	32,6	31,6	32,2
2803	52	34,7	33,4	32,5	33,5
3260	52	35	33,8	32,8	33,8
7220	52	35,6	34,4	34,2	35,6

(a) FA

(b) FI10

(c) FI20

(d) FI30

Figure 5.27. Cross sections of the control and snow-added fly ash specimens (FA, FI10, FI20, FI30)

The variation of thermal conductivity of fly ash with snow addition is shown in Table 5.8. As it can be seen from Table 5.8 that the highest value of K constant of fly ash specimens is obtained for specimens produced with 20 per cent snow addition. The values increase with increasing snow per cent except the FI30 sample. For 10, 20 and 30 per cent snow addition, the increase percentages were 13,6, 22,5 and 19,2 respectively, compared to the corresponding control test specimens (FA). The maximum increase in the K constant of the fly ash specimens occurred at 20 per cent snow addition. The 20 per cent snow-added compacted fly ash specimen blocks gave the lowest surface temperature compared with the other three specimen blocks as seen in the thermal images in Figure 5.25 and in the surface temperature data in Table 5.9. This is because of the unconnected voids in the fly ash matrix. On the other hand FI30 samples have interconnected voids as can be seen in the cross sections in Figure 5.27. These interconnected voids reduced the thermal conductivity performance of the snow-added fly ash specimens.

The increase in the K values were partly due to the decreasing unit weight and increasing void ratio of the test specimens. Unit weight decreased and void ratio increased with increasing snow content in the matrix. Experimentally obtained thermal conductivity values are in well agreement with the previous test results.

5.11. Erosion Analysis (Pinhole Tests)

The test is started with distilled water flowing horizontally under a hydraulic head of 50mm. through a one mm. diameter hole punched in the soil specimen. The solution emerging from the specimen under the initial 50mm. head provided the principle differentiation between dispersive and nondispersive behavior. Flow from the snow-added fly ash and control specimens were completely clear with no measurable increase in the hole size, with a constant value in the flow rate.

Table 5.10. Evaluation of the pinhole test results for the cured fly ash and fly ash + snow specimens (Method A)

	Dispersive classification	Cloudiness of flow at end of test	Hole size after test, mm.
FA1	ND1	Perfectly clear	1,0
FI1	ND1	Perfectly clear	1,0
FA28	ND1	Perfectly clear	1,0
FI28	ND1	Perfectly clear	1,0
FA90	ND1	Perfectly clear	1,0
FI90	ND1	Perfectly clear	1,0

*ND1: Nondispersive clay with very slight to no colloidal erosion under 380mm or 1020mm head.

Test results are evaluated from the appearance of the flowing solution emerging from all of the specimens (FA1, FI1, FA28, FI28, FA90, and FI90) the rate of flow, and the final size of the hole through the specimen as presented in Table 5.10. These observations provided that all of the samples tested are identified as non erodable (non dispersive). Even in one day curing condition the samples are classified as non dispersive. The cementitious minerals formed during one day curing period stiffened the matrix and the test results arose to be non dispersive for both the control fly ash and the snow-added fly ash samples. The snow-added fly ash specimens had 12 per cent less dry unit weight and 30 per cent rise in the void ratio values. Nevertheless the stronger structure didn't permit the pinhole to enlarge and classify the test samples as dispersive. This test method models the action of water flowing along a crack in an embankment.

5.12. Leachate Analysis

Water leach tests were conducted on control fly ash, and natural snow-added fly ash samples. The purpose of these tests was to estimate the leaching potential from control fly ash specimens as well as from natural snow-added fly ash specimens.

Table 5.11. Atomic absorption spectrometer test results of the leaching fluids

Species in (mg/L)	FA28	FI28	FA90	FI90	EPA Drinking water standards (MCL-max contaminant level)	Potential health effects
Arsenic	0.0012	0.0043	0.004	0.0036	0.001	Skin damage, problems with circulatory systems, increased risk of getting cancer
Cadmium	<0.001	<0.001	0.008	<0.001	0.005	Kidney damage
Chromium	4.09	0.074	0.693	0.084	0.1	Allergic dermatitis
Copper	0.028	<0.01	1.023	0.03	1.3	Gastrointestinal distress, Liver or kidney damage
Lead	0.142	<0.01	1.178	<0.01	0.015	Delays in physical, mental development, kidney problems
Nickel	0.009	0.033	0.031	0.027	-	-
Mercury	0.0045	0.0027	0.0037	0.0069	0.002	Kidney damage

Aqueous phase concentrations of Arsenic, Cadmium, Chromium, Copper, Lead, Nickel, and Mercury from the leaching tests are summarized in Table 5.11. Aqueous concentrations from the tests on natural snow-added fly ash samples are lower than the control fly ash specimens for 28 and 90 days cured samples in general. Aqueous concentrations from the tests on both natural snow-added and control specimens are also lower than the EPA Drinking water standards (MCL-max contaminant level) as described in Table 5.11.

Natural snow-added fly ash specimens' aqueous concentrations of cadmium, copper, lead and chromium are lower than the control fly ash samples for 28 days cured samples. The aqueous concentration of arsenic was 0,0012 mg/L for 28 days cured control fly ash specimens(FA28) and 0,0043 mg/L for snow-added fly ash specimens(FI28); 0,004 mg/L for 90 days cured control fly ash specimens(FA90) and 0,0036 mg/L for the natural snow-added fly ash specimens (FI90). The aqueous concentration of nickel from control fly ash specimens is even slightly lower than those from natural snow-added fly ash specimens for 28 days cured specimens, except for 90 days cured specimens. The aqueous concentrations of mercury from the leaching tests are higher in the control fly ash specimens in 28 days curing period than the natural snow-added fly ash test samples. In contrast, the aqueous concentrations of 90 days cured control fly ash samples from the leaching tests are higher

than the natural snow-added fly ash specimens. EPA drinking water standards are significantly higher than the test results achieved.

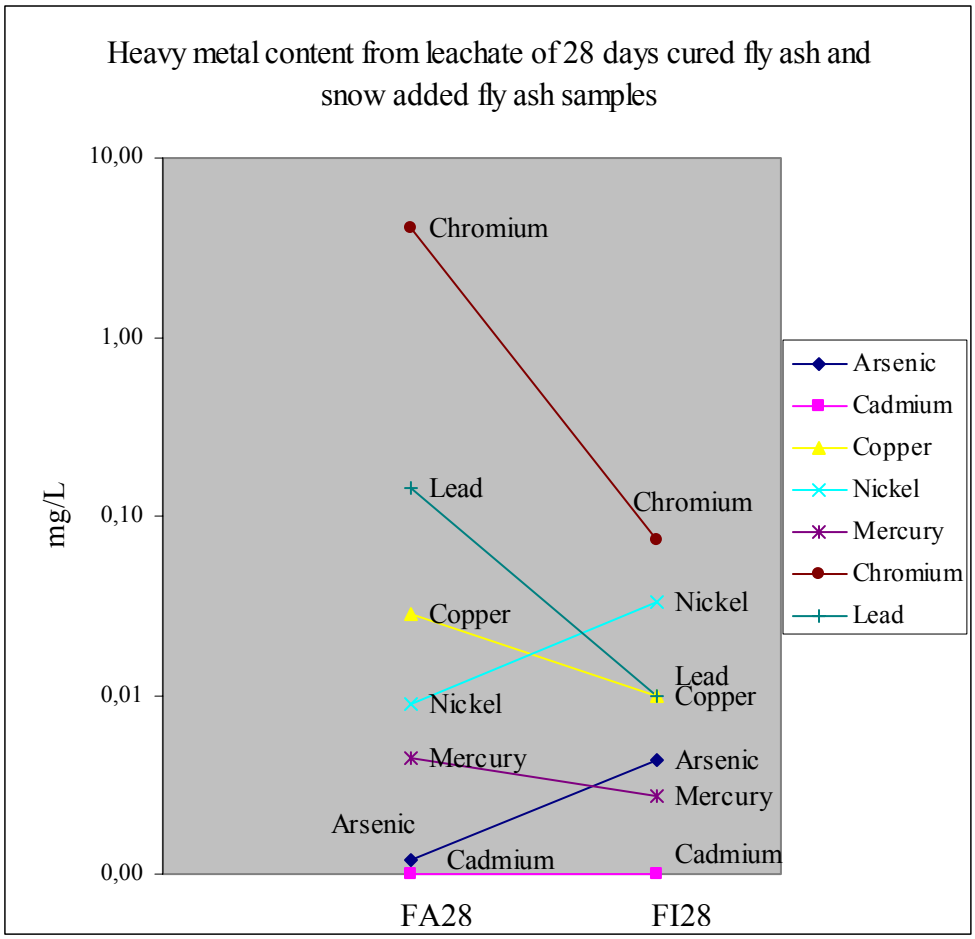

Figure 5.28. Heavy metal content from leachate of 28 days cured fly ash and snow-added fly ash samples

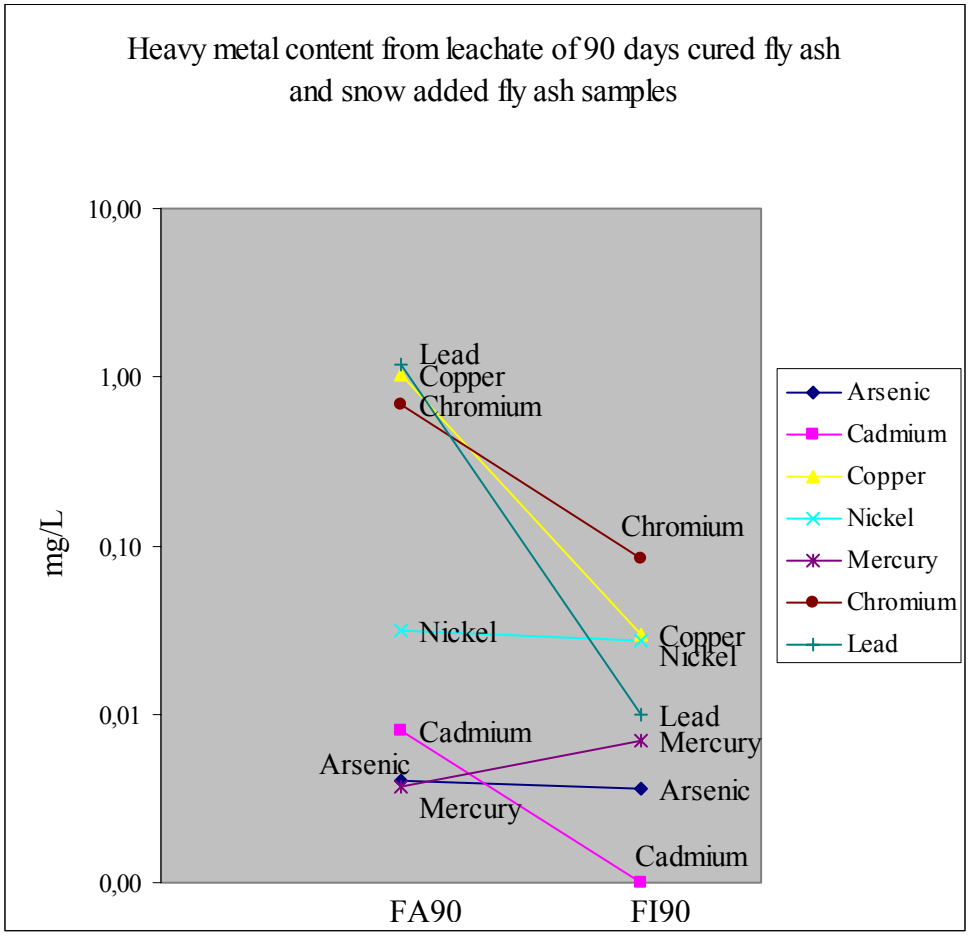

Figure 5.29. Heavy metal content from leachate of 90 days cured fly ash and snow-added fly ash samples

Aqueous concentrations of Arsenic, Cadmium, Copper, Nickel, Chromium, Lead and Mercury from the leaching tests are shown in Figure 5.28 as a function of natural snow content for samples cured for 28 days. For Mercury, Arsenic, Lead and Cadmium, the aqueous concentrations are very low regardless of the natural snow content and are comparable to those for the control fly ash samples alone.

Adding natural snow to the fly ash samples, caused the concentrations of Copper, Mercury, Cadmium, Lead and Chromium to decrease because of the decrease in the pH level of the leachate, which leads to greater adsorption of metals on the solid surface of the specimens. Because of the leaching potential of Copper, Mercury, Cadmium, Lead and Chromium from natural snow-added fly ash samples are lower than that of control fly ash

samples alone, leaching of Copper, Mercury, Cadmium, Lead and Chromium from the natural snow-added fly ash specimens should not be an issue of environmental concern.

Typical graphs showing how aqueous concentrations of Arsenic, Cadmium, Copper, Nickel, Chromium, Lead and Mercury vary with natural snow content cured for 90 days are presented in Figure 5.29. The aqueous concentrations of Arsenic, Cadmium, Copper, Nickel, Chromium and Lead are much lower for the natural snow-added fly ash samples than the control fly ash samples, and thus the concentrations from the natural snow-added fly ash samples decrease with increasing natural snow content. However, the decrease in concentration is not linear with the natural snow content, even though the mass of metals in natural snow-fly ash mixture decreases approximately linearly with increasing natural snow content. The concentration of heavy metals in the leachate from the control fly ash samples also depend on the metal content of the fly ash itself (coal source).

Fly Ash is the major component (90-100 per cent) of the natural snow-added fly ash and control fly ash test specimens, and the amount of metals in fly ash has significant contribution to the metal concentration in the leachate. To understand the effect of adding natural snow on the aqueous concentration of metals in leachate from natural snow-fly ash mixtures, the decrease in metal concentration due to natural snow addition was estimated by subtracting the metal concentration from the natural snow-added sample from the metal concentration obtained from the control fly ash sample.

Finally concentrations of heavy metals in leachate from the natural snow-added fly ash specimens prepared with natural snow and fly ash at different natural snow percentages tend to be lower than those from the control fly ash samples. The concentrations of metals in the leachate from the natural snow-fly ash mixtures varies non-linearly with natural snow content and cannot be estimated based on a simple calculation. The non-linear behavior is attributed to the variation in pH with fly ash content. Leaching potential of a metal from a natural snow-fly ash mixture depends on the metal concentration in the fly ash, pH of the leachate, and the type of fly ash. The pH of the leachate increases as the natural snow content of the mixture increases for 90 days curing period.

The key findings of the water quality monitoring of the test samples are:

- The water quality values indicate that the potential for leachate to form in the control and snow-added fly ash is being realized, nevertheless the majority of the fly ash used in the embankment will be covered with impermeable pavement.
- The leachate constituents, including chromium, lead, copper, mercury and cadmium, are being attenuated with natural snow addition, due to the stiffer matrix.
- The leaching fluid quality data indicate that the leachate from the control fly ash and snow-added fly ash has no discernable impact on ground water quality.

5.13. Length Change Determination

Figure 5.30 shows the expansion of the control fly ash and natural snow-added fly ash test specimens respectively. Each value is the average of axial readings on three samples. Expansion levels were different due to the natural snow content of the compacted specimens.

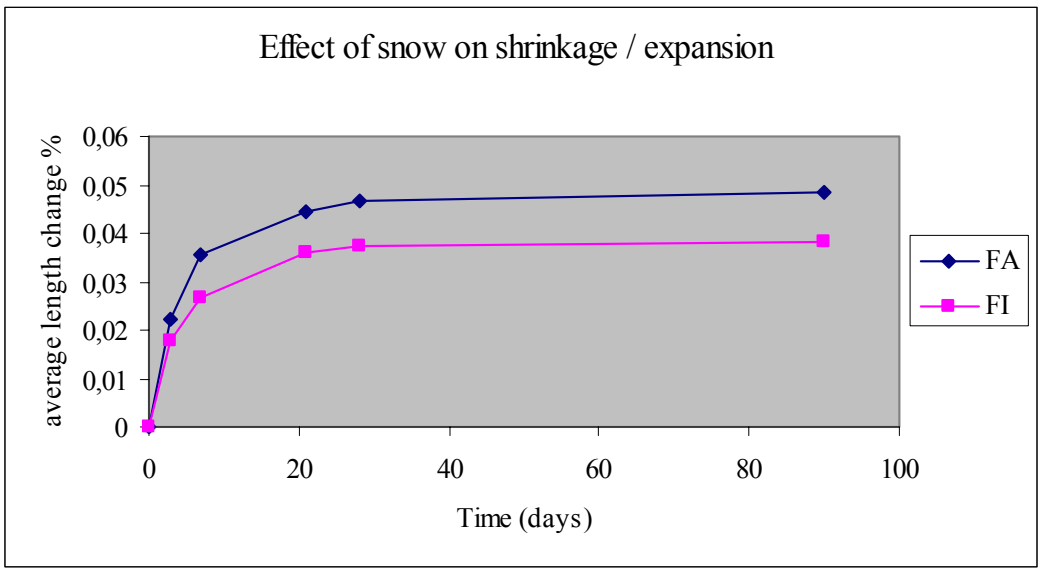

Figure 5.30. Average length change of the cured fly ash and fly ash + snow specimens

Control fly ash specimens showed larger expansion for the whole curing period. The expansion levels of the specimens reached at about 28 days were 0.046 per cent for the

control fly ash specimens and 0.037 per cent for snow-added fly ash specimens. The maximum expansion levels of the test specimens, reached at 90 days were 0.048 per cent for control fly ash test specimens and 0.038 per cent for natural snow-added fly ash test specimens. This indicates that the higher expansion percentages of the control test specimens may be attributed to the 30 per cent increase in the void ratio of the natural snow-added fly ash specimens. The cementitious minerals have more space to grow in the natural snow-added fly ash specimens. Pozzolanic reactions produce hydrates involving volume changes. The use of natural snow significantly reduced the expansion percentages of the test specimens. For comparison, the addition of natural snow to the control fly ash specimens yielded an expansion reduction of 19.23 per cent at 28 days and 21.19 per cent at 90 days. The efficiency of natural snow addition in reducing expansion was found to be quite favorable under these conditions, but the ability of natural snow to reduce expansion is further improved as the amount of curing is increased. The addition of natural snow reduces the expansion of the test samples at humid conditions because the void ratio of the snow-added fly ash test specimen is higher. The addition of natural snow increases the total porosity and the volume of the coarse pores in the matrix. These results are in accordance with the other tests results conducted on the test samples as described in the previous sections.

5.14. Summary of the Test Results

Unconfined compressive strength, splitting tensile strength, hydraulic conductivity testing, pH measurements, temperature measurement of fresh specimens, radioisotope activity comparison, X-Ray diffraction analysis, environmental scanning electron microscope analysis, resistance of samples to rapid freezing and thawing, thermal conductivity analysis, erosion analysis, leachate analysis and length change determination of fly ash and natural snow mixtures have been investigated in this work. Natural snow has been used to improve the engineering properties mentioned above. Natural snow has been used to provide additional water for the pozzolanic reaction after the compaction of the samples and to introduce air voids to increase the freeze-thaw resistance and thermal conductivity properties.

The unconfined compressive strength of samples with 10 per cent natural snow have increased by 70 per cent after 90 days of curing, which will lead to higher embankment stability and the possibility of steeper side slopes. The higher strength gain after 28 and 90 days is due to the excess water provided by the added snow which causes more crystal formation, and the slower hydration rate which causes larger size crystal development. The cementation reactions continue in the presence of free water. The excess 10 per cent water, added in the form of natural snow, provided a satisfactory environment for development of cementitious minerals, leading to higher strength. The snow-added fly ash samples have 30 per cent more voids than that of the control samples, this leads to more space for CSH crystals to develop which explains the higher unconfined compressive strength values.

The splitting tensile strength of samples with 10 per cent natural snow have increased by 85 per cent after 90 days of curing. The tensile strength values are approximately 10 per cent of unconfined compressive strength values. A similar trend to the one observed for unconfined compressive strength values is observed.

The higher void ratio of snow-added fly ash caused two to three orders of magnitude increase in hydraulic conductivity values. The values of k_{av} varied from $3.49x10^{-7}$ to $8.65x10^{-7}$ cm/s for control fly ash samples, which are typically in the range of the hydraulic conductivity coefficient of clay. The compacted control fly ash, therefore, would be practically impermeable. The values of k_{av} varied from $1.01x10^{-4}$ to $1.83x10^{-4}$ cm/s for snow-added fly ash samples, which are typically in the range of the hydraulic conductivity coefficient of silty sand. The compacted snow-added fly ash samples, therefore, would be summarized as low permeable. In embankments and retaining walls the snow-added fly ash would show higher performance than that of the compacted fly ash control samples, because it possesses better drainage characteristics and no tension cracks would develop. Since most strength gain and pozzolanic reaction occurs within the first 28 days of hydration, it is unlikely that k would change significantly beyond 90 days. Although self-hardening nature of the class C fly ash is appreciable, its hydraulic conductivity does not vary significantly with time. Therefore, embankments and backfills constructed of snow-added fly ash may continue to remain moderately permeable after construction as well.

pH values of the leachate decreased with increasing curing period for control fly ash samples, however the pH value increased with increasing curing period for snow-added fly ash samples. Within the 28 days curing period the total amount of voids in the fly ash mixtures increased with 10 per cent natural snow addition, which is primarily responsible for higher pH at higher fly ash content. As the curing period reached 90 days, the voids were more occupied with the hydration products and the pH values of natural snow-fly ash mixtures showed an increasing trend. The decreasing trend in the snow-added fly ash samples gave rise to less leaching of metals and the increasing trend in the control fly ash samples caused an increase in heavy metal leaching. The general observation for these pH determinations is that all of the mixtures were potentially capable of ettringite formation.

The temperature change of the compacted samples during the initial phase of hydration is observed with an infrared camera. The minimum temperature recorded in snow-added fly ash is 8^0 C after five minutes of curing in the laboratory conditions and is -1.0^0C after five minutes of curing in the field conditions (+2.0^0C curing temperature). After 240 minutes the recorded temperatures at the surface of the samples are similar for fly ash and snow-added fly ash. Natural snow addition to fly ash samples lead to lower hydration degrees for the first four hours curing. The thermal images of samples FA and FI described the effect of natural snow addition in delaying the hydration stage. The hydration rate is slowed by snow addition both in laboratory and field conditions.

The activities of ^{235}U, ^{226}Ra, ^{238}U, and ^{232}Th of the fly ash and snow-added fly ash samples compacted at optimum moisture content are determined using gamma spectrometry. The snow-added fly ash samples compacted at optimum moisture content represented a 31 to 42 per cent decrease in radiation amounts in Bq/kg. The decrease in radioisotope activities for snow-added fly ash samples can be directly linked with the extra moisture obtained by snow melting in the superficial pores, the radon atoms are trapped inside superficial pores by moisture. The results showed that the snow-added fly ash samples pose less radiation than the control fly ash samples and indicated that the snow-added fly ash samples examined in this work could be used in embankment construction without exceeding the proposed radioactivity criterion level.

The X-ray diffraction spectra of the fly ash, and samples compacted at optimum moisture content, and cured for one, 28, 90 days and five years are investigated. There were several crystalline phases as determined by the X-ray diffractometer. With increasing curing time, the formations of thaumasite and ettringite minerals were observed. Ettringite peak intensity increased with increasing curing time. Due to smaller amount of water in its atomic structure, thaumasite is seen in samples compacted at optimum water content. The peaks of the ettringite and thaumasite minerals are sharper and showed a rapid increase in the one, 28, 90 days and five years-cured snow-added fly ash samples.

ESEM examinations verified the results reported in the previous sections and provided an image of the microstructural development of the tested specimens. The numerous voids visible in the structure of the control and snow-added fly ash specimens at one day decreased substantially after 28 days, leading to a more compact morphology. The formation of this network is to a large extent ascribed to the extra water (10 per cent) supplied by snow addition over optimum moisture content of fly ash. The dense structure formed by the addition of snow reinforced the already present ettringite, providing an explanation for the early age strengths. There are abundant sulfate and aluminum ions available in the system to form ettringite. The availability of calcium ions in solution is critical in determining the ettringite formation. For the formation of thaumasite, carbonate ions must also be available in the system. Obviously these phases continued to develop and needle crystals crossed each other to form an improved and frame microstructure. This is consistent with the improved engineering properties of the snow-added fly ash specimens as stated in the previous sections.

An automatic environmental freeze-thaw cabinet was used to carry out the accelerated freeze-thaw test. The fundamental resonant frequencies were determined using the forced resonance method. As the test proceeded, samples developed cracks along the sides about mid depth and the lower and upper part of the samples started to break off. These cracks became more prominent and widespread as the test progressed, resulting in spalling and eventual breaking down of the samples. Damage to the fly ash structure due to freeze-thaw occurred because of the hydraulic pressure developed when water in the saturated pores freezed and increased its volume and certain amount of water forced out of the pores. Test was continued for up to 121 cycles for snow-added samples and at 91 cycles

still the visual rating was only three for the snow-added fly ash samples. Natural snow addition had a remarkable effect on improving the freeze-thaw property of the compacted fly ash blocks. By snow addition, voids uniformly dispersed in the matrix (created after melting of snow) provided a reservoir for water to expand. This appears to be the most effective and economical method to improve the freeze-thaw property of the compacted fly ash specimens.

The hot box apparatus constructed was able to measure the rate of heat flow through an element of known area for known test conditions while limiting extraneous heat flows. A thermal imager was used for monitoring the temperature at the outer surface of the test specimens. Steady state conditions were reached in about 10 hours. The interior of the box was kept at about 52 ^{0}C. By comparing three types of snow-added fly ash specimens for thermal insulation, it was found that 20 per cent snow-added fly ash specimen was a better mixture for making blocks having better thermal properties. 20 per cent snow-added fly ash blocks were found to be superior to 10 per cent, 30 per cent snow-added and control fly ash blocks in terms of thermal conductivity, K ranging from 0.369 to 0.301 W/m^{0}C. This is because of the unconnected voids in the fly ash matrix. The increase in the K values were partly due to the decreasing unit weight and increasing void ratio of the test specimens. Unit weight decreased and void ratio increased with increasing snow amount in the matrix. Experimentally obtained thermal conductivity values are in well agreement with the previous test results.

Flow from the pinhole test setup of snow-added fly ash and control specimens were completely clear with no measurable increase in the hole size, with a constant value in the flow rate. These observations provided that all of the samples tested are identified as non-erodable (non-dispersive). Even in one day curing condition the samples are classified as non dispersive. The cementitious minerals formed during one day curing period stiffened the matrix and the test results arose to be non dispersive for both the control fly ash and the snow-added fly ash samples. Nevertheless the stronger structure didn’t permit the pinhole to enlarge and classify the test samples as dispersive. This test method modelled the action of water flowing along a crack in an embankment.

Leachate analysis were conducted on control fly ash, and natural snow-added fly ash samples. Aqueous phase concentrations of arsenic, cadmium, chromium, copper, lead, nickel, and mercury from the leaching tests are investigated. Aqueous concentrations from the tests on natural snow-added fly ash samples are lower than the control fly ash specimens for 28 and 90 days cured samples in general. Aqueous concentrations from the tests on both natural snow-added and control specimens are also lower than the EPA drinking water standards (MCL-max contaminant level). However, the decrease in concentration is not linear with the natural snow content, even though the mass of metals in natural snow-fly ash mixture decreases approximately linearly with increasing natural snow content. The non-linear behavior is attributed to the variation in pH with fly ash content. Leaching potential of a metal from a natural snow-fly ash mixture depends on the metal concentration in the fly ash, pH of the leachate, and the type of fly ash. The leaching fluid quality data indicated that the leachate from the control fly ash and snow-added fly ash has no discernable impact on ground water quality.

The length change levels of the specimens reached at about 28 days were 0.046 per cent for the control fly ash specimens and 0.037 per cent for snow-added fly ash specimens (expansion). The maximum expansion levels of the test specimens, reached at 90 days were 0.048 per cent for control fly ash test specimens and 0.038 per cent for natural snow-added fly ash test specimens. The use of natural snow significantly reduced the expansion percentages of the test specimens. For comparison, the addition of natural snow to the control fly ash specimens yielded an expansion reduction of 19.23 per cent at 28 days and 21.19 per cent at 90 days. The addition of natural snow increased the total porosity and the volume of the coarse pores in the matrix. Pozzolanic reactions produced hydrates involving volume changes. The cementitious minerals had more space to grow in the natural snow-added fly ash specimens.

6. CONCLUSIONS

- The study demonstrates that snow may be successfully used to introduce extra water during the compaction of fly ash without causing any workability problem. The snow addition caused 30 per cent increase in void ratio; 12 per cent decrease in unit weight and 70 per cent increase in shear strength. Embankment constructed using snow added fly ash will be more environment friendly, have lighter weight, higher stability and due to increased void ratio the insulation property will be better.

- The decrease in radioisotope activities for snow added fly ash samples can be directly linked with the extra moisture obtained by snow melting in the superficial pores, the radon atoms are trapped inside superficial pores by moisture. The results showed that the snow-added fly ash samples pose less radiation than the control fly ash samples and indicated that the snow-added fly ash samples examined in this work could be used in embankment construction without exceeding the proposed radioactivity criterion level.

- Natural snow addition had a remarkable effect on improving the freeze-thaw property of the compacted fly ash blocks. By snow addition, voids uniformly dispersed in the matrix (created after melting of snow) provided a reservoir for water to expand. This appears to be the most effective and economical method to improve the freeze-thaw property of the compacted fly ash specimens.

- In embankments the snow added fly ash would show higher performance than that of the compacted control fly ash samples, because it possesses better drainage characteristics and no tension cracks would develop, therefore embankments constructed with snow added fly ash samples will be more resistant to frost action.

- The observed increase in tensile strength for snow-added fly ash is beneficial for potential use as base and sub base material for highway construction.

- A 30 per cent increase in void ratio means extra savings from transportation costs of fly ash, which will allow construction more economically. With the developed technique embankment construction activity will be continued even during wintertime.

For further study, in winter season in cold regions, test embankments are planning to be constructed and tested. This site work will prove the effectiveness of the developed technique. Test pads will be constructed and tests will be conducted at the site to observe the improvement in the environmental and engineering properties investigated in this thesis.

REFERENCES

1. Wang, J., H. Ban, X. Teng, H. Wang, and K. Ladwig, "Impacts of pH and ammonia on the leaching of Cu and Cd from coal fly ash", *Chemosphere,* Vol 64, pp.1892-1898, 2006.

2. Petropoulos, N.P., M.J.Anagnostakis, and S.E. Simopoulos, "Photon attenuation, natural radioactivity content and radon exhalation rate of building materials", *Journal of Environmental Radioactivity*, Vol 61, pp. 257–269, 2002.

3. Reed, M.A., C.W. Lovell, A.G. Altschaeffl and L.E. Wood, "Frost Heaving Rate Predicted from Pore Size Distribution," *Canadian Geotechnical Journal*, Vol.16, No.3, pp.453-472, 1979.

4. Hansbo, S., *Jordmateriallara,* Almqvist & Wiksell Forlag AB, Stockholm, 1975.

5. American Concrete Institute, *Guide to Residential Cast-in-Place Concrete Construction*, Report No. ACI 332R-84, American Concrete Institute, Detroit, USA, 1989.

6. Monahan, E.J., *Construction Of and On Compacted Fills,* John Wiley & Sons, New York, USA, 1986.

7. Baykal, G., "Strength improvement of fly ash using ice", *11th International Symposium on Coal Ash Use and Management*, American Coal Association & Energy Production Research Institute, Orlando, USA, pp. 67-72, 1995.

8. Baykal, G., **"**Compacted fly ash-ice for low cost housing projects", *International Journal for Housing Science and Its Applications.*, Vol 22, 1996.

9. Baykal, G., "Utilization of fly ash as highway safety barriers", *12th International Symposium on Management & Use of Coal Combustion Byproducts (CCBs)*, Orlando, USA, 1997.

10. UKQAA, *Annual PFA utilization statistics*, UK Quality Ash Association, Wolverhampton, UK,2000.

11. McManis, K. L., *Laboratory Evaluation of Fly Ash Treated Embankment and Base Material*, TRB Record No:1031, Nov. 1987.

12. Meyers, R.A., *Coal Structure*, New York: Academic Press, 1982.

13. Damberger, H.H., R.D. Harvey, R.R. Ruch and J.Jr. Thomas, "Coal Characterization", *The Science and Technology of Coal and Coal Utilization,* pp. 7-45, New York: Plenum Press, 1984.

14. Smoot, L. and P.J. Smith, "*Coal combustion and Gasification",* New York: Plenum Press, 1985.

15. Mehta, P.K., "Pozzolanic and Cementitious Byproducts as Mineral Admixtures for Concrete - A Critical Review", in American Concrete Institute Publication SP-79, *Fly Ash, Silica Fume, Slag and Other Mineral By-products in Concrete,* Vol. 1, pp. 1-46, ACI, 1983.

16. Tokyay, M. and K. Erdogdu, "*Characterization of Fly Ash Obtained from a Turkish Thermal Power Plant*", TÇMB / ARGE / Y98.3, Ankara, Turkey, 1998.

17. Chu, S.C and H. S. Kao, "A Study of Engineering Properties of a Clay Modified by Fly Ash and Slag." *Fly Ash for Soil Improvement-Geotechnical Special Publication*, Vol. 36, pp 89-99, 1993.

18. Cockrell, C. F. and J. W. Leonard, "Characterization and Utilization Studies of Limestone Modified Fly Ash" *Coal Research Bureau*, Vol. 60, 1970.

19. ASTM C618-92a. "Standard Specification for Fly Ash and Raw or Calcined Natural Pozzolan for Use as Mineral Admixture in Portland Cement Concrete", American Society for Testing and Materials, *Annual Book of ASTM Standards*, Volume 04.02, West Conshohocken, Pennsylvania, 1994.

20. Meyers, J.F., R. Pichumani and B.S. Kapples. *Fly Ash: A Highway Construction Material,* Federal Highway Administration, Report No. FHWA-IP-76-16, Washington, DC, 1976.

21. ASTM C204. "Test Method for Fineness of Portland Cement by Air Permeability Apparatus", American Society for Testing and Materials, *Annual Book of ASTM Standards*, Volume 04.02, West Conshohocken, Pennsylvania, 1994.

22. McKerall, W.C., W.B. Ledbetter and D.J. Teague, *Analysis of Fly Ashes Produced in Texas,* Texas Transportation Institute, Research Report No. 240-1, Texas A&M University, College Station, Texas, 1982.

23. Haque, M.N., H. Al-Khaiyat and O. Kayali, "Structural Lightweight Concrete-An Environmentally Responsible Material of Construction", *Proceedings of the International Conference on Challenges of Concrete- Sustainable Concrete Construction*, Dundee-Scotland, 9-11 September 2002, pp. 305-312, Thomas Telford, London, 2002.

24. Baykal, G., A.G. Doven, M.A. Savas, T. Ozturan and Z. Atay, *Uçucu Külden Pelet Agrega Üretimi için Laboratuvarda Model Tesis Kurulması ve Peletleme Işleminin Optimizasyonu*, The Scientific and Technical Research Council of Turkey, Construction Technologies Research Grant Committee, Project No: INTAG 627, Ankara, 1997.

25. Clarke, J.L., *Structural Lightweight Aggregate Concrete*, Blackie Academic and Professional, Berkshire, 1993.

26. Bradbury, H.W., "The Use of Fly Ash in Pre-Blended Cement", *Silicates Industrials,* No.12, pp. 283-288, 1982.

27. Berry, E.E., *Fly Ash for Use in Concrete-Part 1: A Critical Review of the Chemical, Physical and Pozzolanic Properties of Fly Ash,* CANMET Report No. 76-25,1976.

28. Raask, E., "Cenospheres in Pulverized Fuel Ash", *Journal of the Institute of Fuel,* No. 13, pp. 339-344, 1968.

29. Naik, T.R. and S.S. Singh, "Fly Ash Generation and Utilization- An Overview", *Proceedings of Workshop on Flowable Slurry Containing Fly Ash, Silica Fume,Slag and Natural Pozzolans in Concrete,* Vol. 1, pp. 1-32, Milwaukee, Wisconsin, 1995.

30. TRB, *Lime Stabilization: Reactions, Properties, Design, and Construction,* State of the Art Report 5. Transportation Research Board, National Research Council, Washington, D.C., 1987.

31. USGS, *Radioactive Elements in Coal and Fly Ash: Abundance, Forms, and Environmental Significance*, US Geological Survey Fact Sheet FS-163-97, October, 1997.

32. Collins, R.J. and S.K. Ciesielski, *Recycling and Use of Waste Materials and By-Products in Highway Construction, Volume 2 – Technical Appendix*, National Cooperative Highway Research Program Synthesis of Highway Practice No. 199, Transportation Research Board, Washington, DC, 1994.

33. FHWA, *Fly Ash Facts for Highway Engineers,* FHWA–IF–03–019, 81 pp., 2003.

34. RCRA Orientation Manual, *Resource Conservation and Recovery Act, Environmental Protection Agency ,Solid Waste and Emergency Response*, EPA-530-R-06-003 , March 2006, 254pp.

35. American Coal Ash Association, *Soil and Pavement Base Stabilization with Self-Cementing Coal Fly Ash*, Alexandria, Virginia, May 1999.

36. American Society of Civil Engineers, *Fly Ash for Soil Improvement*, Geotechnical Special Publication No. 36, , New York, New York, 1993.

37. *Guidelines and Guide Specifications for Using Pozzolanic Stabilized Mixture (Base Course or Subbase) and Fly Ash for In-Place Subgrade Soil Modifications*, AASHTO Task Force Report 28, Washington, DC.

38. Collins, R.J. and S.S. Tyson, "Utilization of Coal Ash in Flowable Fill Applications", *Proceedings of the Symposium on Recovery and Effective Reuse of Discarded Materials and By-Products for Construction of Highway Facilities*, Federal Highway Administration, Denver, Colorado, October, 1993.

39. Hennis, K.W. and C.W. Frishette, "A New Era in Control Density Fill", *Proceedings of the Tenth International Ash Utilization Symposium*, Electric Power Research Institute, Report No. TR-101774, Volume 2, Palo Alto, California, January, 1993.

40. Newman, F. B., L.F. Rojas-Gonzales, D.L. Knott, *Current Practice in Design and Use of Flowable Backfills for Highway and Bridge Construction,* GAI Consultants, Final Report, Research Project 90-12 for Pennsylvania Department of Transportation, Harrisburg, Pennsylvania, September, 1992.

41. Hobbs, P.V., *The physics of ice*, Clarendon Press, Oxford, 1974.

42. Mason B.J., *The Physics of Clouds,* Oxford, Clarendon Press, 1971.

43. Hausmann, M.R., 1990, *Engineering principles of Ground Modification*, McGraw-Hill, New York.

44. Andersland, O.B. and D.M. Anderson, 1978, *Geotechnical Engineering for Cold Regions*, Mc-Graw Hill, New York.

45. Gerdel, R.W., *Cold Regions Science and Engineering Monograph 1-A: Characteristics of the Cold Regions*, Cold Regions Research and Engineering Laboratory, U.S. Army Corps of Engineers, Hanover, New Hampshire, p. 51., 1969.

46. Pewe, T.L., 1975, *Quaternary geology of Alaska*., U.S. Department of Interior, Geological Survey Professional Paper 835. U.S. Gov.Print. Ofc., Washington, D.C. 145pp.

47. Aitken, G.W. and C.W. Fulwider, *Ground temperature observations, Aniak, Hanover*, U.S. Army Cold Regions Research and Engineering Laboratory, Technical Report 101, 1962.

48. Ezzaine K., A. Bougara, A. Kadri, H. Khelafi and E. Kadri, "Compressive strength of mortar containing natural pozzolan under various curing temperature", *Cement & Concrete Composites*, Vol.29, pp.587–93, Elsevier, 2007.

49. Ghrici, M., S. Kenai, and M. Said-Mansour, "Mechanical properties and durability of mortar and concrete containing natural pozzolana and limestone blended cements", *Cement & Concrete Composites*, Vol.29,pp.542–549, Elsevier, 2007.

50. Mouli, M. and H. Khelafi, "Performance characteristics of lightweight aggregate concrete containing natural pozzolan", *Building and Environment*, Vol.43, pp.31-36, Elsevier, 2008.

51. Sahu, S., S.A. Brown and R.J. Lee, "Thaumasite formation in stabilized coal combustion by-products", *Cement & Concrete Composites*, Vol.24, pp.385–91, Elsevier, 2002.

52. Nisnevich, M., G. Sirotin, T. Schlesinger and Y. Eshel, “Radiological safety aspects of utilizing coal ashes for production of lightweight concrete”, *Fuel*, Vol. 87, pp.1610-16, Elsevier, 2008.

53. Yu, K.N., E.C.M. Young, M.J. Stokes, M.K. Kwan and R.V. Balendran, “Radon Emanation from Concrete Surfaces and the Effect of the Curing Period, Pulverized Fuel Ash (PFA) Substitution and Age”, *Appl. Radiaion and lsotopes,* Vol. 48, pp.1003-07, Elsevier, 1997.

54. Kovler, K., A. Perevalov, V. Steiner and L.A. Metzger, “Radon exhalation of cementitious materials made with coal fly ash: Part 1 e scientific background and testing of the cement and fly ash emanation”, *Journal of Environmental Radioactivity*, Vol.82, pp.321-34, Elsevier, 2005.

55. Wang, S., E. Llazamos, L. Baxter and F. Fonseca, “Durability of biomass fly ash concrete: Freezing and thawing and rapid chloride permeability tests”, *Fuel*, Vol.87, pp.359–64, Elsevier, 2008.

56. Liu, H., W. Burkett and K. Haynes, *Improving Freezing and Thawing Properties of Fly Ash Bricks*, National Science Foundation (NSF), Small Business Innovation Research (SBIR) Phase-1 project, Grant No.NSF-DMI-0419311, 2004.

57. Yazıcı, H., “The effect of silica fume and high-volume Class C fly ash on mechanical properties, chloride penetration and freeze–thaw resistance of self-compacting concrete”, *Construction and Building Materials*, Vol.22, pp.456-62, Elsevier, 2008.

58. Heebink, L.V.,and D.J. Hassett, “Coal fly ash trace element mobility in soil stabilization”, *International Ash Utilization Symposium*, Kentucky, October 22-24, 2001.

59. Sushil, S. and V.S. Batra, “Analysis of fly ash heavy metal content and disposal in three thermal power plants in India” *Fuel*, Elsevier, 2006.

60. Erbe, M.W., R.W. Keating and W.K. Hodges, "Evaluation of water quality conditions associated with the use of coal combustion products for highway embankments", *International Ash Utilization Symposium*, Kentucky, Oct 18-20, 1999.

61. Kaniraj, S.R.and V. Gayathri, "Permeability and Consolidation Characteristics of Compacted Fly Ash", the *Journal of Energy Engineering*, Vol. 130, No. 1, ASCE, 2004.

62. Kalinski, M.E. and P.K. Yerra, "Hydraulic conductivity of compacted cement–stabilized fly ash" *Fuel*, Vol.85, pp.2330–36, Elsevier, 2006.

63. Kim, B., M. Prezzi and R. Saldago, "Geotechnical Properties of Fly and Bottom Ash Mixtures for Use in Highway Embankments", *Journal of Geotechnical and Geoenvironmental Engineering*, Vol. 131, No. 7, 1 July, 2005.

64. Wang, S., L. Baxter and F. Fonseca, "Biomass fly ash in concrete: SEM, EDX and ESEM analysis", *Fuel*, Vol.87, pp.372–79, Elsevier, 2008.

65. Antiohos, S. and S. Tsimas, "Investigating the role of reactive silica in the hydration mechanisms of high-calcium fly ash/cement systems", *Cement & Concrete Composites*, Vol.27, pp.171–81, Elsevier, 2005.

66. Döven, A.G., *Lightweight Fly Ash Aggregate Production Using Cold Bonding Agglomeration Process*, Ph.D.Thesis, Boğaziçi University, 1998.

67. ASTM D698, "Standard Test Methods for Laboratory Compaction Characteristics of Soil Using Standard Effort",American Society for Testing and Materials, *Annual Book of ASTM Standards*, Volume 04.08, West Conshohocken, Pennsylvania, 2000.

68. ASTM C39, "Standard Test Method for Compressive Strength of Cylindrical Concrete Specimens", American Society for Testing and Materials, *Annual Book of ASTM Standards*, Volume 04.02, West Conshohocken, Pennsylvania, 2005.

69. Bowles, J.E., *Engineering Properties of soils and their measurement*, McGRAW-HILL, Singapore, 1992.

70. ASTM D3967, "Standard Test Method for Splitting Tensile Strength of Intact Rock Core Specimens", American Society for Testing and Materials, *Annual Book of ASTM Standards*, Volume 04.08, West Conshohocken, Pennsylvania, 2005.

71. Tavenas, F., "The Permeability of Natural Soft Clays. Part I: Methods of Laboratory Measurement", *Canadian Geotechnical Journal,* Vol. 20, No. 4, Nov., pp. 629-644, 1983.

72. Bardet, J.P. *Experimental soil mechanics*, Prentice-Hall, Englewood Cliffs, N.J., pp.202–206, 1997.

73. Peirce, J.J., "Parameter Sensitivity of Hydraulic Conductivity Testing Procedure", *Geotechnical Testing Journal, ASTM,* Vol. 10, No. 4, Dec, pp. 223-228, 1987.

74. ASTM D1293, "Standard Test Methods for pH of Water", American Society for Testing and Materials, *Annual Book of ASTM Standards*, Volume 11.01, West Conshohocken, Pennsylvania, 2005.

75. ASTM C1064, "Standard Test Methods for Temperature of Freshly Mixed Hydraulic-Cement Concrete", American Society for Testing and Materials, *Annual Book of ASTM Standards*, Volume 04.02, West Conshohocken, Pennsylvania, 2005.

76. ASTM C666, "Standard Test Method for Resistance of Concrete to Rapid Freezing and Thawing", American Society for Testing and Materials, *Annual Book of ASTM Standards*, Volume 04.02, West Conshohocken, Pennsylvania, 2003.

77. ASTM C1363, "Standard Test Method for Thermal Performance of Building Materials and Envelope Assemblies by Means of a Hot Box Apparatus ", American Society for Testing and Materials, *Annual Book of ASTM Standards*, Volume 04.06, West Conshohocken, Pennsylvania, 2005.

78. ASTM D4647, “Standard Test Method for Identification and Classification of Dispersive Clay Soils by the Pinhole Test”, American Society for Testing and Materials, *Annual Book of ASTM Standards*, Volume 04.08, West Conshohocken, Pennsylvania, 2006.

79. ASTM D4874, “Standard Test Method for Leaching Solid Material in a Column Apparatus”, American Society for Testing and Materials, *Annual Book of ASTM Standards*, Volume 11.04, West Conshohocken, Pennsylvania, 2006.

80. Das, H.A., H.A. Van Der Sloot, and J. Wijkstra, “Measurement of the Leaching Behavior of Granular Solid Waste,” *Toxicological and Environmental Chemistry,* Vol. 19, pp. 109-118, 1989.

81.Creek, D.N. and C.D. Shackelford, “Permeability and Leaching Characteristics of Fly Ash Liner Materials,” *Transportation Research Record* 1345, 1992.

82. ASTM C490, “Standard Practice for Use of Apparatus for the Determination of Length Change of Hardened Cement Paste, Mortar, and Concrete”, American Society for Testing and Materials, *Annual Book of ASTM Standards*, Volume 04.02, West Conshohocken, Pennsylvania, 2004.

83. Hassett, D.J., D.F. Pflughoet-Hassett and G.J. McCarthy, “The Synthesis of Substituted Ettringites: Implications for Disposal of Hazardous Materials”, *FACSS XVIII and Pacific Conference Proceedings*, Anaheim, CA, 1991.

84. UNIPEDE, *Coal Ash Reference report*, Thermal Generation Study Committee Report, *20.05,* THERRES, 1997.

85. Papadakis, V.G. “Effect of fly ash on Portland cement systems. Part II: High calcium fly ash”. *Cement & Concrete Research,* pp 1647-54, Elsevier, 2000.

86. Taylor, H.F.W., *Cement chemistry*, Thomas Telford, London, 1997.

87. Srivastava, L. and R.J. Collins, *Ash Utilization in Highways: Delaware Demonstration Project,* EPRI, GS-6481, Research Project 2422-3, Interim Report, Palo Alto, CA, 1989.

88. Budhu, M., *Soil Mechanics and Foundations*, Wiley, New York, 2006.

REFERENCES NOT CITED

Brough, A.R., A. Katz, G.K. Sun, L.J. Struble, R.J. Kirkpatrick and J.F. Young, 2001, "Adiabatically cured, alkali-activated cement-based wasteforms containing high levels of fly ash :Formation of zeolites and Al-substituted C-S-H", *Cement and Concrete Research* pp 1437–47, Elsevier.

Lav, A.H., M.A. Lav and B. Göktepe, 2005, *Analyses and design of a stabilized fly ash as pavement base material*, World of Coal Ash Syposium, Kentucky, April 11-15, 2005.

Sear, L.K.A, 2001, *Fly ash standards, market strategy and UK practice*, International Ash Utilization Symposium, Kentucky, October 22-24, 2001.

Bergeson, K.L. and A.G. Barnes, 1998, "Iowa Thickness Design Guide for Low Volume Roads Using Reclaimed Hydrated Class C Fly Ash Bases", *Transportation Conference Proceedings.*

Ural, S., 2005, "Comparison of fly ash properties from Afsin–Elbistan coal basin, Turkey", *Journal of Hazardous Materials,* pp 85–92.

Mohanty, S. and Y. Chugh, 2006, "Postconstruction Environmental Monitoring of a Fly Ash-Based Road Subbase", *Practice Periodical on Structural Design and Construction*, Vol. 11, No. 4, 1 November.

Kumar, S. and C.B. Patil, 2006, "Estimation of resource savings due to fly ash utilization in road construction", *Resources, Conservation and Recycling,* Vol. 48, pp 125–140.

Pandian, N.S., 2004, "Fly ash characterization with reference to geotechnical applications" *J. Indian Inst. Sci.*, ,Vol 84., pp 189–216 ,November-December 2004.

Türkel, S., 2006, "Long-term compressive strength and some other properties of controlled low strength materials made with pozzolanic cement and Class C fly ash", *Journal of Hazardous Materials,* B137, pp 261–266.

Sheng, Y., Z. Wen, W. Ma, Y. Liu, J. Qi and J. Wu, 2006, "Long-term evaluations of insulated road in the Qinghai-Tibetan plateau", *Cold Regions Science and Technology,* Vol.45, pp 23-30.

Baykal, G., A. Edinçliler and A. Saygılı, 2004, "Highway embankment construction using fly ash in cold regions", *Resources, Conservation and Recycling,*Vol. 42, pp 209–222.

Liu, Z., Y. Lai, X. Zhang and M. Zhang, 2006, "Random temperature fields of embankment in cold regions", *Cold Regions Science and Technology*, Vol.45, pp 76–82.

Aruntaş H.Y., 2006, "Uçucu küllerin inşaat sektöründe kullanım potansiyeli", *J. Fac. Eng. Arch. Gazi Univ*., Vol 21, No 1, pp.193-203, 2006.

Şenol, A., B. Shafique, T.B. Edil and C.H. Benson, 2002, "Use of Class C Fly Ash For Stabilization of Soft Subgrade", *Proceedings of the Fifth International Congress on Advances in Civil Engineering*, 25-27 September 2002 ITU, Istanbul, Turkey.

Chugh, Y.P., C. Hance, S. Mohanty and R. Carty, 2003, "Development and Demonstration of Coal Combustion Byproducts Based Road Subbase", *Final Technical Report*, 31 July, ICCI Project Number: 00-48205.

Al-Jabri, K.S., A.W. Hago, A.S. Al-Nuaimi and A.H. Al-Saidy, 2005, "Concrete blocks for thermal insulation in hot climate", *Cement and Concrete Research*, Vol.35, pp.1472–1479, Elsevier.

Neto, L.P.C., M.C.G. Silva and J.J. Costa, 2006, "On the use of infrared thermography in studies with air curtain devices" , *Energy and Buildings*, Vol.38., pp.1194–1199, Elsevier.

Lin, K.L. and D.F. Lin, 2006, "Hydration characteristics of municipal solid waste incinerator bottom ash slag as a pozzolanic material for use in cement" *Cement & Concrete Composites*, pp.817-23, Elsevier.

Antiohos, S., A. Papageorgiou and S. Tsimas, 2006, "Activation of fly ash cementitious systems in the presence of quicklime.Part II: Nature of hydration products, porosity and microstructure development", *Cement and Concrete Research*, Vol.36, pp.2123–31, Elsevier.

Jordan, R.E., J.P. Hardy, F.E. Perron and D.J. Fisk, 1999, "Air permeability and capillary rise as measures of the pore structure of snow: an experimental and theoretical study", *Hydrological Processes*.,Vol. 13, pp.1733-53, Wiley.

Liu, X., S.J. Rees and J.D. Spitler, 2007, "Modeling snow melting on heated pavement surfaces. Part I: Model development", *Applied Thermal Engineering*, Vol.27, pp. 1115–24, Elsevier.

Rosenthal, W., J. Saleta and J. Dozier, 2007, "Scanning electron microscopy of impurity structures in snow", *Cold Regions Science and Technology*, Vol.47, pp.80–89, Elsevier.

Knapen, A., J. Poesen, G. Govers, G. Gyssels and J. Nachtergaele, 2007, "Resistance of soils to concentrated flow erosion: A review", *Earth-Science Reviews,* Vol.80, pp.75–109, Elsevier.

Sear, L.K.A, J.M. Garcia-Ruiz, T. Lasanta and F. Alberto, 1997, "Soil erosion by piping in irrigated fields" *Geomorphology*, Vol.20, pp.269-78, Elsevier.

Sear, L.K.A, A.J. Weatherley and A. Dawson, 2003, "The environmental impacts of using fly ash-the UK producers' perspective", *International Ash Utilization Symposium*, Kentucky, USA, 20-22 october 2003.

Bayat, B., 2002, "Comparative study of adsorption properties of Turkish fly ashes: I. The case of nickel(II), copper(II) and zinc(II)", *Journal of Hazardous Materials*, Vol.B95, pp.251–73, Elsevier.

Bayat, B., 2002, “Comparative study of adsorption properties of Turkish fly ashes: II. The case of chromium (VI) and cadmium (II)”, *Journal of Hazardous Materials*, Vol.B95, pp.275–90, Elsevier.

Pelleg, S.S. and H. Cohen, 1999, “Evaluation of the Leaching Potential of Trace Elements from Coal Ash to the Aquifer”, *International Ash Utilization Symposium*, Kentucky, Oct 18-20, 1999.

Otero-Rey, J.R., M.J.M, Fernandez, J.M. Pineiro, E.A. Rodriguez, S.M. Lorenzo, P.L. Mahia and D.P. Rodriguez, 2005, “Influence of several experimental parameters on As and Se leaching from coal fly ash samples”, *Analytica Chimica Acta,* Vol.531, pp.299–305, Elsevier.

Flyhammar, P. and D. Bendz, 2006, “Leaching of different elements from subbase layers of alternative aggregates in pavement constructions”, *Journal of Hazardous Materials*, Elsevier.

Palmer, B.G., T.B. Edil and C.H. Benson, 2000, “Liners for waste containment constructed with class F and C fly ashes”, *Journal of Hazardous Materials*, Vol.76, pp.193–216, Elsevier.

Sauer, J.J., C.H. Benson and T.B. Edil, 2005, *Metals Leaching from Highway Test Sections Constructed with Industrial Byproducts*, Geo Engineering Report No. 05-21.

Shafique, S.B., C.H. Benson and T.B. Edil, 2002, *Leaching of heavy metals from fly ash stabilized soils used in highway pavements*, Geo Engineering Report No. 02-14.

Bennazouk, A., O. Douzane and M. Queneudec, 2004, “Transport of fluids in cement–rubber composites”, *Cement & Concrete Composites*, Vol.26, pp.21–29, Elsevier.

Wolfe, W.E. and T.S. Butalia, 1999, “Effect of freeze-thaw cycling on the mechanical properties of FGD by-products”, *International Ash Utilization Symposium*, Kentucky, Oct 18-20.

Basheer, L. and D.J. Cleland, 2006, “Freeze-thaw resistance of concretes treated with pore liners”, *Construction and Building Materials*, Vol.20, pp.990-98, Elsevier.

Cho, T., 2007, “Prediction of cyclic freeze–thaw damage in concrete structures based on response surface method”, *Construction and Building Materials*, Vol.21, pp. 2031-40, Elsevier.

Hossain, K.M.A. and M. Lachemi, 2007, “Strength, durability and micro-structural aspects of high performance volcanic ash concrete”, *Cement and Concrete Research,* Vol.37, pp.759–66, Elsevier.

Schmidt, T., B. Lothenbach, M. Romer, K. Scrivener, D. Rentsch and R. Figi, 2008, “A thermodynamic and experimental study of the conditions of thaumasite formation”, *Cement and Concrete Research*, Vol.38, pp.337-49, Elsevier.

Wang, S., A. Miller, E. Llamazos, F. Fonseca and L. Baxter, 2008, “Biomass fly ash in concrete: Mixture proportioning and mechanical properties”, *Fuel*, Vol.87, pp.365–71, Elsevier.

Taylar, H.F.W, C. Famy and K.L. Scrivener, 2001, “Delayed ettringite formation”, *Cement and Concrete Research,* Vol.31, pp.683-693, Elsevier.

Xiao, L. and Z. Li, 2008, “Early-age hydration of fresh concrete monitored by non-contact electrical resistivity measurement”, *Cement and Concrete Research*, Vol.38, pp.312-319, Elsevier.

Clark, S.M, B. Colas, M. Kunz, S. Speziale and P.J.M. Monteiro, 2008, “Effect of pressure on the crystal structure of ettringite”, *Cement and Concrete Research*, Vol.38, pp.19–26, Elsevier.

Montagnaro, F., M. Nobili, P. Salatino, A. Telesca and G.L. Valenti, 2008, "Hydration products of FBC wastes as SO_2 sorbents: comparison between ettringite and calcium hydroxide", *Fuel Processing Technology,* Vol.89, pp.47-54, Elsevier.

Scrivener, K.L. and R.J. Kirkpatrick, 2008, "Innovation in use and research on cementitious material", *Cement and Concrete Research*, Vol.38, pp.128–36, Elsevier.

Antczak, E., D. Defer, M. Elaoami, A. Chauchois and B. Duthoit, 2007, "Monitoring and thermal characterisation of cement matrix materials using non-destructive testing", *NDT&E International*, Vol.40, pp.428–38, Elsevier.

Svinning, K., A. Hoskuldsson and H. Justnes, 2008, "Prediction of compressive strength up to 28 days from microstructure of Portland cement", *Cement & Concrete Composites*, Vol.30, pp.138–51, Elsevier.

Perkins, R.B. and C.D. Palmer, 1999, "Solubility of ettringite ($Ca_6[Al(OH)_6]2(SO_4)_3$. $26H_2O$) at 5–75°C", *Geochimica et Cosmochimica Acta*, Vol. 63, pp.1969–80, Elsevier.

Richardson, I.G., 2008, "The calcium silicate hydrates", *Cement and Concrete Research*, Vol.38, pp.137–158, Elsevier.

Turhan, Ş., 2008, "Assessment of the natural radioactivity and radiological hazards in Turkish cement and its raw materials", *Journal of Environmental Radioactivity*, Vol.99, pp.404-14, Elsevier.

Zaidi, J.H., M. Arif, S. Ahmad, I. Fatima and I.H. Qureshi, 1999, "Determination of natural radioactivity in building materials used in the Rawalpindi/Islamabad area by γ-ray spectrometry and instrumental neutron activation analysis", *Applied Radiation and Isotopes*, Vol.51,pp.559-64, Elsevier.

Kumar, V., T.V. Ramachandran and R. Prasad, 1999, "Natural radioactivity of Indian building materials and by-products", *Applied Radiation and Isotopes*, Vol.51, pp.93-96, Elsevier.

Zielinski, R.A., J.R. Budahn, 1998, "Radionuclides in fly ash and bottom ash: improved characterization based on radiography and low energy gamma-ray spectrometry", *Fuel*, Vol. 77, pp.259-61, Elsevier.

Srivastava, S., R. Chaudhary and D. Khale, 2007, "Influence of pH, curing time and environmental stress on the immobilization of hazardous waste using activated fly ash", *Journal of Hazardous Materials*, Elsevier.

Hale, W.M., S.F. Freyne, T.D. Bush and B.W. Russell, 2007, "Properties of concrete mixtures containing slag cement and fly ash for use in transportation structures", *Construction and Building Materials*, Elsevier.

Guo, M.B., W.X. Dong, W.M. Yuan, Y.J. Jia and G.X. Jian, 2007, "Drying Shrinkage of Cement-Based Materials Under Conditions of Constant Temperature and Varying Humidity", *Journal of China University of Mining & Technology*, Vol.17, pp.428–31, Elsevier.

Haha, M.B., E. Gallucci, A. Guidom and K.L. Scrivener, 2007, "Relation of expansion due to alkali silica reaction to the degree of reaction measured by SEM image analysis", *Cement and Concrete Research*, Vol. 37, pp.1206–14, Elsevier.

Maierhofer, C., R. Arndt, M. Röllig, C. Rieck, A. Walther, H. Scheel and B. Hillemeir, 2006, "Application of impulse-thermography for non-destructive assessment of concrete structures", *Cement & Concrete Composites*, Vol.28, pp.393–401, Elsevier.

Demirboğa, R., 2007, "Thermal conductivity and compressive strength of concrete incorporation with mineral admixtures", *Building and Environment*, Vol.42, pp.2467–71, Elsevier.

Williams, P.J.and M.W. Smith, 1989, *The frozen earth-Fundamentals of geocryology*, Cambridge University Press, Cambridge, UK, pp.113-114.

Keller, W.D., 1963, “The origin of high alumina clay minerals-a review, Clay and Clay Minerals”, *Proceedings of the Twelfth National Conference*, Monograph No.19, Earth Science Series, Pergamon Press, New York, pp.129-151.

APPENDIX A: STRESS-STRAIN CURVES FOR SAMPLES CURED AT DIFFERENT TIME PERIODS

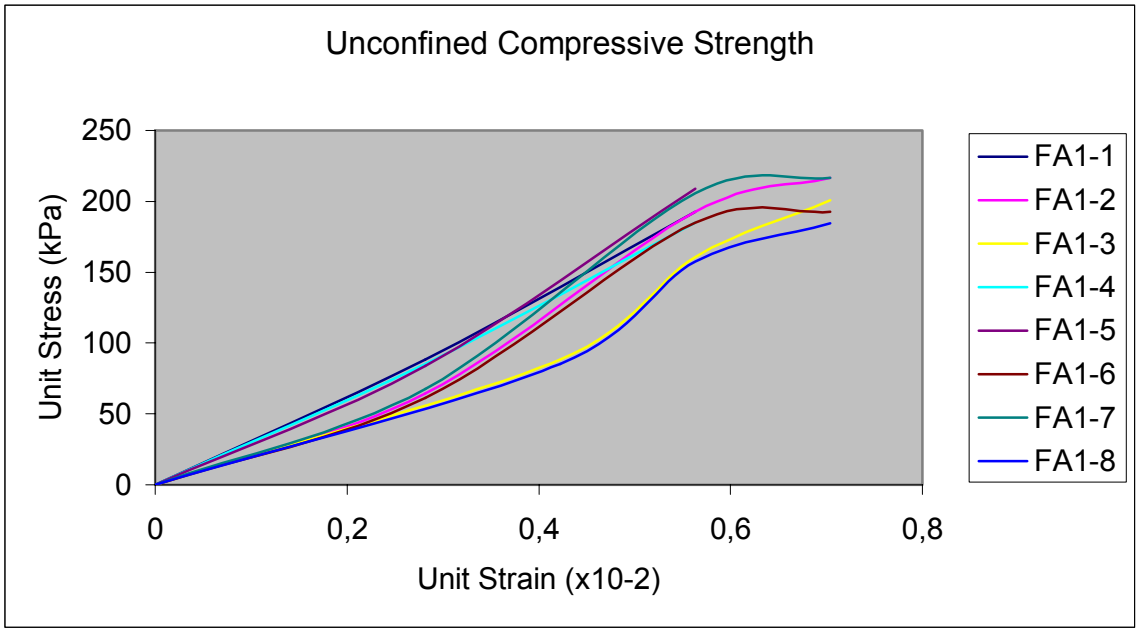

Figure A.1. Stress-strain curves for fly ash only samples cured for one day

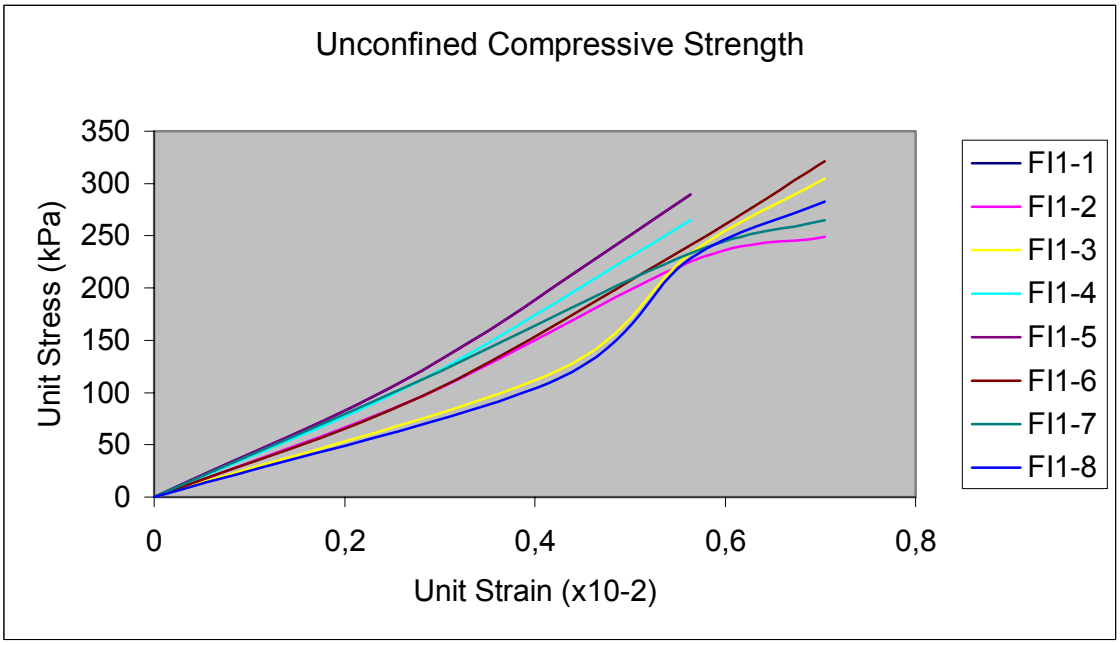

Figure A.2. Stress-strain curves for snow added fly ash samples cured for one day

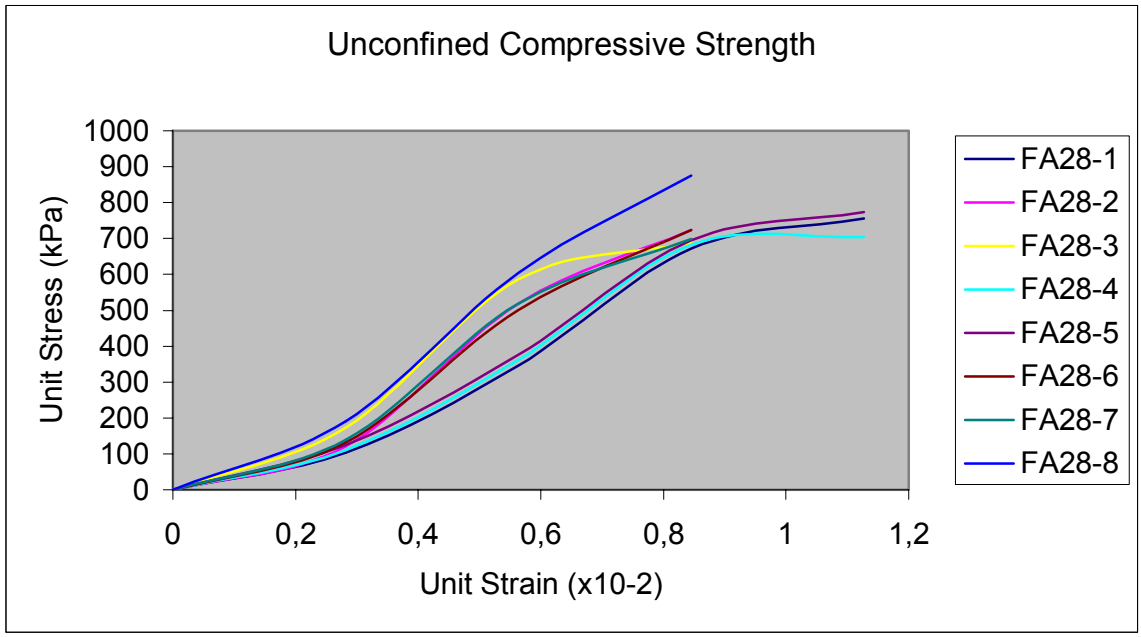

Figure A.3. Stress-strain curves for fly ash only samples cured for 28 days

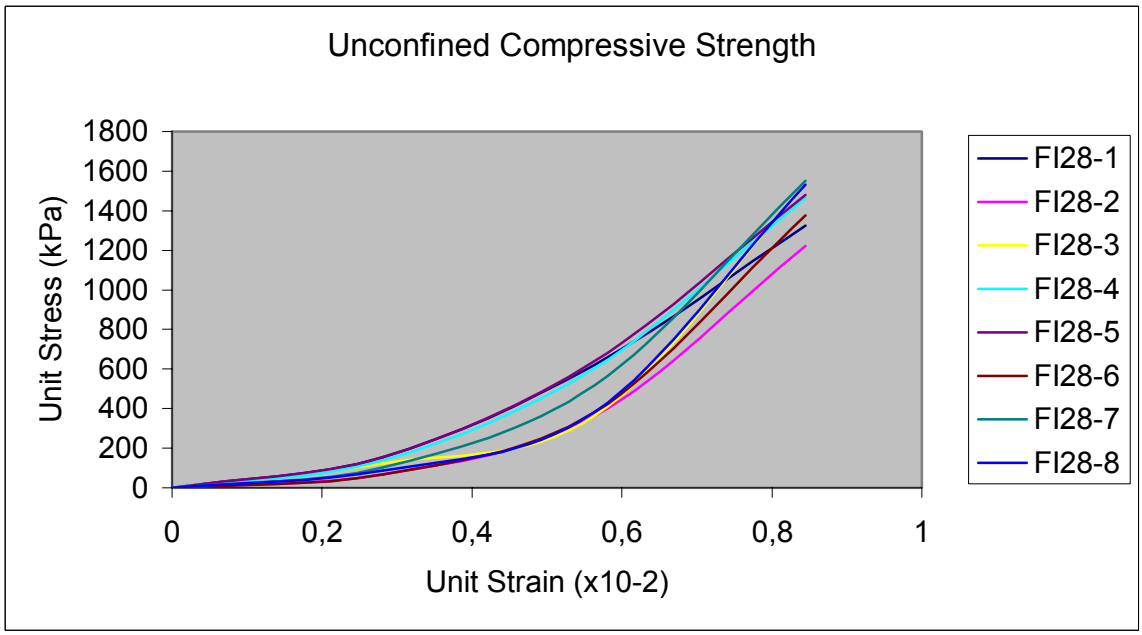

Figure A.4. Stress-strain curves for snow added fly ash samples cured for 28 days

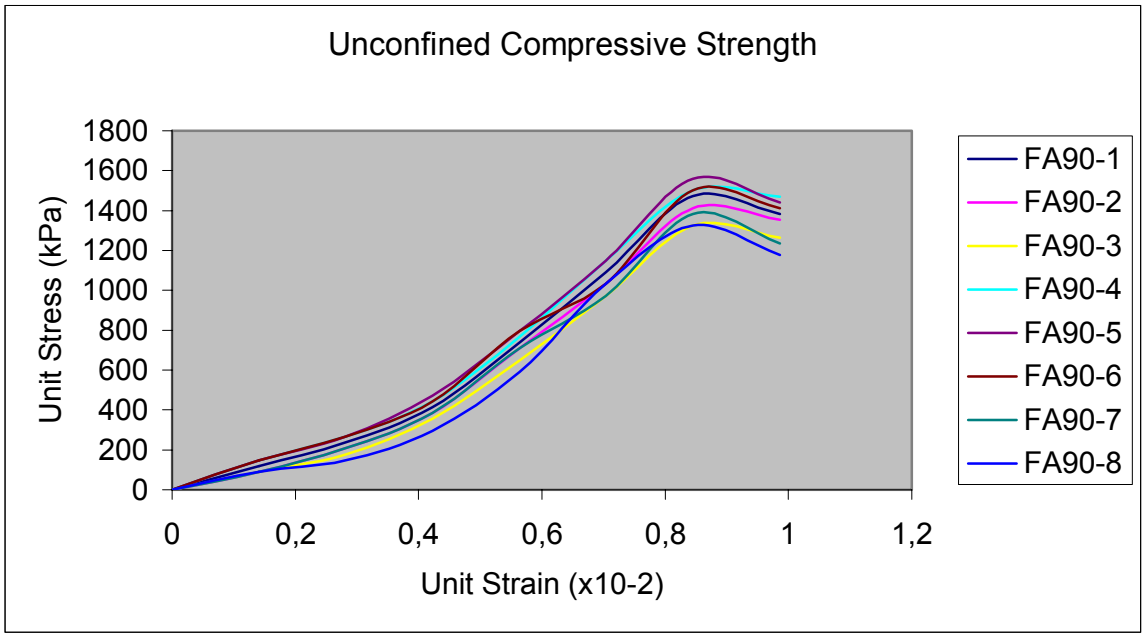

Figure A.5. Stress-strain curves for fly ash only samples cured for 90 days

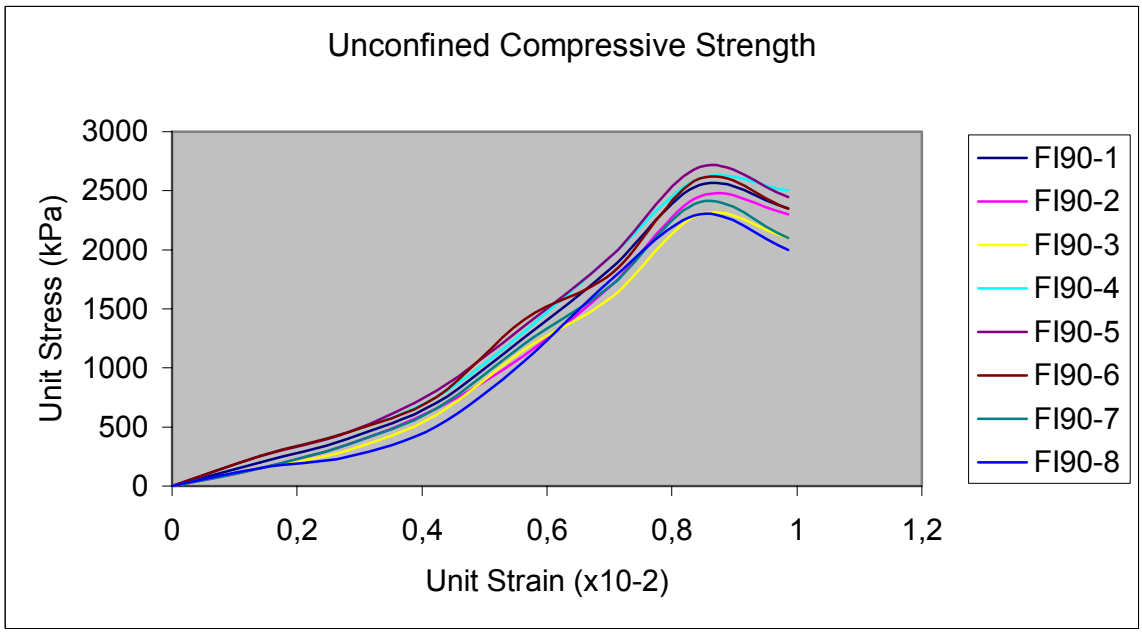

Figure A.6. Stress-strain curves for snow added fly ash samples cured for 90 days